

The *Kepler* characterization of the variability among A- and F-type stars

I. General overview

K. Uytterhoeven^{1,2,3}, A. Moya⁴, A. Grigahcène⁵, J.A. Guzik⁶, J. Gutiérrez-Soto^{7,8,9}, B. Smalley¹⁰, G. Handler^{11,12}, L.A. Balona¹³, E. Niemczura¹⁴, L. Fox Machado¹⁵, S. Benatti^{16,17}, E. Chapellier¹⁸, A. Tkachenko¹⁹, R. Szabó²⁰, J.C. Suárez⁷, V. Ripepi²¹, J. Pascual⁷, P. Mathias²², S. Martín-Ruiz⁷, H. Lehmann²³, J. Jackiewicz²⁴, S. Hekker^{25,26}, M. Gruberbauer^{27,11}, R.A. García¹, X. Dumusque^{5,28}, D. Díaz-Fraile⁷, P. Bradley²⁹, V. Antoci¹¹, M. Roth², B. Leroy⁸, S.J. Murphy³⁰, P. De Cat³¹, J. Cuypers³¹, H. Kjeldsen³², J. Christensen-Dalsgaard³², M. Breger^{11,33}, A. Pigulski¹⁴, L.L. Kiss^{20,34}, M. Still³⁵, S.E. Thompson³⁶, and J. Van Cleve³⁶

(Affiliations can be found after the references)

Received / Accepted

ABSTRACT

Context. The *Kepler* spacecraft is providing time series of photometric data with micromagnitude precision for hundreds of A-F type stars. **Aims.** We present a first general characterization of the pulsational behaviour of A-F type stars as observed in the *Kepler* light curves of a sample of 750 candidate A-F type stars, and observationally investigate the relation between γ Doradus (γ Dor), δ Scuti (δ Sct), and hybrid stars. **Methods.** We compile a database of physical parameters for the sample stars from the literature and new ground-based observations. We analyse the *Kepler* light curve of each star and extract the pulsational frequencies using different frequency analysis methods. We construct two new observables, 'energy' and 'efficiency', related to the driving energy of the pulsation mode and the convective efficiency of the outer convective zone, respectively. **Results.** We propose three main groups to describe the observed variety in pulsating A-F type stars: γ Dor, δ Sct, and hybrid stars. We assign 63% of our sample to one of the three groups, and identify the remaining part as rotationally modulated/active stars, binaries, stars of different spectral type, or stars that show no clear periodic variability. 23% of the stars (171 stars) are hybrid stars, which is a much higher fraction than what has been observed before. We characterize for the first time a large number of A-F type stars (475 stars) in terms of number of detected frequencies, frequency range, and typical pulsation amplitudes. The majority of hybrid stars show frequencies with all kinds of periodicities within the γ Dor and δ Sct range, also between 5 and $10 d^{-1}$, which is a challenge for the current models. We find indications for the existence of δ Sct and γ Dor stars beyond the edges of the current observational instability strips. The hybrid stars occupy the entire region within the δ Sct and γ Dor instability strips and beyond. Non-variable stars seem to exist within the instability strips. The location of γ Dor and δ Sct classes in the (T_{eff} , $\log g$)-diagram has been extended. We investigate two newly constructed variables, 'efficiency' and 'energy', as a means to explore the relation between γ Dor and δ Sct stars. **Conclusions.** Our results suggest a revision of the current observational instability strips of δ Sct and γ Dor stars and imply an investigation of pulsation mechanisms to supplement the κ mechanism and convective blocking effect to drive hybrid pulsations. Accurate physical parameters for all stars are needed to confirm these findings.

Key words. Asteroseismology - Stars: oscillations - Stars: variables: δ Scuti - Stars: fundamental parameters - binaries: general - Stars: statistics

1. Introduction

With the advent of the asteroseismic space missions MOST (Walker et al. 2003), CoRoT (Baglin et al. 2006), and *Kepler* (Borucki et al. 2010), a new window is opening towards the understanding of the seismic behaviour of A- and F-type pulsators. The main advantages of these space missions are (1) the long-term continuous monitoring of thousands of stars, which enables both the determination of long-period oscillations and the resolving of beat frequencies; and (2) the photometric precision at the level of milli- to micro-magnitudes, which will provide a more complete frequency spectrum and also allow the detection of low-amplitude variations that are unobservable from the ground and providing a more complete frequency spectrum. The availability of these long-term, very precise light curves makes possible the first comprehensive analysis of the variability of a

sample of several hundred candidate A-F type stars that is presented here.

The region of variable A- and F-type, including main sequence (MS), pre-MS, and post-MS stars, with masses between 1.2 and $2.5 M_{\odot}$ hosts the γ Doradus (γ Dor) and δ Scuti (δ Sct) pulsators. The γ Dor stars were recognized as a new class of pulsating stars less than 20 years ago (Balona, Krisciunas & Cousins 1994). Our current understanding is that they pulsate in high-order gravity (g) modes (Kaye et al. 1999a), excited by a flux modulation mechanism induced by the upper convective layer (Guzik et al. 2000; Dupret et al. 2004; Grigahcène 2005). Typical γ Dor periods are between 8 h and 3 d. From the ground, about 70 *bona fide* and 88 candidate γ Dor pulsators have been detected (Balona et al. 1994; Handler 1999; Henry, Fekel & Henry 2005; De Cat et al. 2006; Henry et al. 2011; among other papers).

Send offprint requests to: K. Uytterhoeven

The δ Sct variables, on the other hand, have been known for decades. They show low-order g and pressure (p) modes with periods between 15 min and 5 h that are self-excited through the κ -mechanism (see reviews by Breger 2000; Handler 2009a). Several hundreds of δ Sct stars have been observed from the ground (e.g. catalogue by Rodríguez & Breger 2001).

Because the instability strips of both classes overlap, the existence of hybrid stars, i.e. stars showing pulsations excited by different excitation mechanisms, is expected, and a few candidate hybrid stars have indeed been detected from the ground (Henry & Fekel 2005; Uytterhoeven et al. 2008; Handler 2009b).

The main open question in seismic studies of A- and F-type stars concerns the excitation and mode selection mechanism of p and g modes. The only way to understand and find out systematics in the mode-selection mechanism is a determination of pulsation frequencies and pulsation mode parameters for a large number of individual class members for each of the pulsation classes, and a comparison of the properties of the different case-studies. So far, a systematic study of a sufficiently substantial sample was hampered by two factors. First, the number of detected well-defined pulsation modes is too small to construct unique seismic models, which is caused by ground-based observational constraints, such as bad time-sampling and a high noise-level. Second, only a small number of well-studied cases exist, because a proper seismic study requires a long-term project, involving ground-based multi-site campaigns spanning several seasons, or a dedicated space mission.

First demonstrations of the strength and innovative character of space data with respect to seismic studies of A-F type stars are the detection of two hybrid γ Dor- δ Sct stars by the MOST satellite (HD 114839, King et al. 2006; BD+18-4914, Rowe et al. 2006), and the detection of an impressive number of frequencies at low amplitudes, including high-degree modes as confirmed by ground-based spectroscopy, in the precise space CoRoT photometry of the δ Sct stars HD 50844 (Poretti et al. 2009) and HD 174936 (García Hernández et al. 2009), and the γ Dor star HD 49434 (Chapellier et al. 2011). The first indications that hybrid behaviour might be common in A-F type stars were found from a pilot study of a larger sample of *Kepler* and CoRoT stars (Grigahcène et al. 2010; Hareter et al. 2010). Recently, Balona et al. (2011a) announced the detection of δ Sct and γ Dor type pulsations in the *Kepler* light curves of Ap stars. Hence, a breakthrough is expected in a currently poorly-understood field of seismic studies of A-F type pulsators through a systematic and careful investigation of the pulsational behaviour in a large sample of stars.

The goals of the current paper are (1) to present a first general characterization of the pulsational behaviour of main-sequence A-F type stars as observed in the *Kepler* light curves of a large sample; and (2) to observationally investigate the relation between γ Dor and δ Sct stars and the role of hybrids. In forthcoming papers, detailed seismic studies and modelling of selected stars will be presented.

2. The *Kepler* sample of A-F type stars

2.1. The *Kepler* data

The NASA space mission *Kepler* was launched in March 2009 and is designed to search for Earth-size planets in the extended solar neighbourhood (Borucki et al. 2010; Koch et al. 2010). To this end, the spacecraft continuously monitors the brightness of $\sim 150\,000$ stars in a fixed area of 105 deg^2 in the constellations Cygnus, Lyra, and Draco, at Galactic latitudes from 6 to 20 deg.

The nearly uninterrupted time series with micromagnitude precision also opens up opportunities for detailed and in-depth asteroseismic studies with unprecedented precision (Gilliland et al. 2010a). Of all *Kepler* targets, more than 5000 stars have been selected as potential targets for seismic studies by the *Kepler* Asteroseismic Science Consortium, KASC¹.

The *Kepler* Mission offers two observing modes: long cadence (LC) and short cadence (SC). The former monitors selected stars with a time resolution of ~ 30 min (Jenkins et al. 2010a), the latter provides a 1-minute sampling (Gilliland et al. 2010b). The LC data are well-suited to search for long-period g-mode variations in A-F type stars (periods from a few hours to a few days), while the SC data are needed to unravel the p-mode oscillations (periods of the order of minutes to hours).

The *Kepler* asteroseismic data are made available to the KASC quarterly. In this paper we consider data from the first year of *Kepler* operations: the 9.7 d Q0 commissioning period (1 May - 11 May 2009), the 33.5 d Q1 phase data (12 May - 14 June 2009), the 88.9 d Q2 phase data (19 June - 15 September 2009), the 89.3 d time string of Q3 (18 September - 16 December 2009), and 89.8 d of Q4 data (19 December 2009 - 19 March 2010). The SC data are subdivided into three-monthly cycles, labelled, for example, Q3.1, Q3.2 and Q3.3.

Not all quarters Q0–Q4 are available for all stars. The first year of *Kepler* operations was dedicated to the survey phase of the mission. During this phase as many different stars as possible were monitored with the aim to identify the best potential candidates for seismic studies. From the survey sample, the KASC working groups selected subsamples of the best seismic candidates for long-term follow-up with *Kepler*. From quarter Q5 onwards, only a limited number of selected KASC stars are being observed with *Kepler*. The results of the selection process of the most promising γ Dor, δ Sct, and hybrid candidates are presented in this work.

2.2. Selection of the A-F type star sample

We selected all stars in the *Kepler* Asteroseismic Science Operations Center (KASOC) database initially labelled as γ Dor or δ Sct candidates. The stars were sorted into these KASOC categories either because the *Kepler* Input Catalogue (KIC; Latham et al. 2005; Brown et al. 2011) value of their effective temperature T_{eff} and gravity $\log g$ suggested that they lie in or close to the instability strips of γ Dor and δ Sct stars, or because they were proposed as potential variable A-F type candidates in pre-launch asteroseismic *Kepler* observing proposals. To avoid sampling bias and to aim at completeness of the sample, we analysed all stars listed in the KASOC catalogue as δ Sct or γ Dor candidates. Our analysis results provide feedback on the initial guess on variable class assignment by KASOC. As will be seen (Sect. 6.2), several of these stars actually belong to other pulsation classes, many of which are cool stars. Because there are much fewer B-type stars in the *Kepler* field of view than cooler stars, there is a natural selection effect towards cooler stars. We also included stars initially assigned to other pulsation types that showed periodicities typical for δ Sct and/or γ Dor stars. We are aware that many more δ Sct and γ Dor candidate stars are being discovered among the KASC targets, but we cannot include all in this study.

The total sample we considered consists of 750 stars. For 517 stars both LC and SC data are available, while 65 and 168 stars were only observed in SC and LC mode, respectively. An

¹ <http://astro.phys.au.dk/KASC>

overview of the A-F type star sample is given in Table 1, available in the on-line version of the paper. The first three columns indicate the KIC identifier of the star (KIC ID), right ascension (RA), declination (DEC), and *Kepler* magnitude (Kp). The *Kepler* bandpass is wider than the typical broad-band filters that are commonly used in optical astronomy (e.g. Johnson *UBVRI*), and can be described as 'white' light. The next three columns provide information on the spectral type (Spectral Type), alternative name of the target (Name), and a comment on its variability (Variable). Information on binarity comes from the *The Washington Double Star Catalog* (Worley & Douglass 1997; Mason et al. 2001), unless mentioned otherwise. For binary stars labelled with '★', the double star was suspected by inspecting Digitized Sky Survey and 2MASS images by eye. The next set of columns provides information on the *Kepler* time series. For each star, the number of datapoints (N datapoints), the total time span of the dataset (ΔT) expressed in d, the longest time gap in the *Kepler* light curves (δT) expressed in d, and the available (range of) quarters in LC (Quarters LC) and SC (Quarters SC) mode are given.

2.3. Sample stars in the literature

Most of the 750 sample stars were previously unstudied. We searched the catalogue by Skiff (2007) and found information on spectral types for only 212 stars. Besides 198 confirmed A- or F-type stars, among which are fourteen chemically peculiar stars, we discovered that stars with a different spectral type also ended up in the sample. There are six known B stars, one M star, three K stars, and six G-type stars in the sample. The G star KIC 7548061 (V1154 Cyg) is a known and well-studied Cepheid (e.g. Pigulski et al. 2009) and is the subject of a dedicated paper based on *Kepler* data by Szabó et al. (2011). Sixty-two stars are known to belong to multiple systems, including at least fourteen eclipsing binaries (EB; KIC 1432149, Hartman et al. 2004; KIC 10206340, Malkov et al. 2006; catalogues by Prša et al. 2011 and Slawson et al. 2011). Seven stars are only known as '(pulsating) variable stars'. The star KIC 2987660 (HD 182634) is reported as a δ Sct star by Henry et al. (2001). Our sample also includes a candidate α^2 Canum Venaticorum star, namely KIC 9851142 or V2094 Cyg (Carrier et al. 2002; Otero 2007). The *Kepler* field hosts four open clusters. In our sample at least six known members of NGC 6819 are included. Also one, eight, and nine members of NGC 6791, NGC 6811, and NGC 6866, respectively, are in our sample. All 750 stars are included in the analysis.

3. Physical parameters of the sample stars

Seismic models require accurate values of physical parameters such as $\log g$, T_{eff} , metallicity $[M/H]$, and projected rotational velocity $v \sin i$. We compiled an overview of all T_{eff} , $\log g$, and $v \sin i$ values available for the sample stars in Table 2 in the on-line version of the paper. The different sources include literature and KIC, along with values derived from new ground-based data. A description of the different sources is given below. The columns of Table 2 are (1) KIC identifier (KIC ID); (2) T_{eff} value from KIC; (3)-(5) T_{eff} values taken from the literature or derived from new ground-based data (Literature); (6) adopted T_{eff} value (Adopted); (7) $\log g$ value from KIC; (8)-(9) $\log g$ values taken from the literature or derived from new ground-based data (Literature); (10) adopted $\log g$ value (Adopted); (11)-(12) $v \sin i$ values derived from spectroscopic data (Spectra). Stars that are known to be spectroscopic binaries

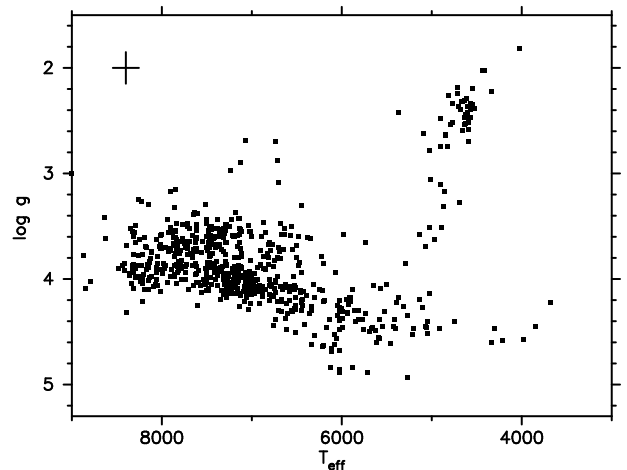


Fig. 1. 750 sample stars in the (T_{eff} , $\log g$)-diagram. The cross at the left top corner represents the typical error bars on the values: 290 K for T_{eff} and 0.3 dex for $\log g$.

are flagged ° behind its KIC identifier (KIC ID). The derived physical parameters of the binary stars have to be considered with caution because the contribution of the binary components might not have been correctly separated.

KIC-independent values of $\log g$ and T_{eff} are only available for 110 stars. The values used for the subsequent analysis are (in order of priority, depending on availability and accuracy) the spectroscopically derived values, or the most recent photometrically derived values. For all other stars we use the only source: the KIC values. The corresponding adopted T_{eff} (in K), and $\log g$ (in dex) values are given in boldface in the sixth and tenth column of Table 2, respectively (column 'Adopted'). For 65 and 71 stars no value of T_{eff} and $\log g$, respectively, is available. Figure 1 shows the sample of 750 stars in the (T_{eff} , $\log g$)-diagram. We estimated the error bars on the KIC values by comparing them with the adopted values taken from the literature or ground-based data. The average difference was 290 K for T_{eff} and 0.3 dex for $\log g$. $v \sin i$ values are only available for 52 of the sample stars.

3.1. Literature

Besides papers dedicated to specific targets of our sample, the on-line catalogues by Soubiran et al. (2010), Lafrasse et al. (2010), Kharchenko et al. (2009), Masana, Jordi, & Ribas (2006), Nordström et al. (2004), Glebocki & Stawikowski (2000), Allende Prieto & Lambert (1999), and Wright et al. (2003) were very helpful in the search for values of T_{eff} , $\log g$, and $v \sin i$. Also, photometric indices by Hauck & Mermilliod (1998) were used to estimate values of T_{eff} and $\log g$. We took care not to include T_{eff} values that are derived from the spectral type rather than directly from data. The literature values of T_{eff} and $\log g$ can be found in columns 3-5 and columns 8-9 of Table 2, respectively ('lit'). We note that the given errors on T_{eff} and $\log g$, which sometimes seem unrealistic small, are taken from the quoted paper and are not rounded to the number of significant digits. Values of $v \sin i$, expressed in km s^{-1} , are given in the last two columns of Table 2. The source of each value is indicated by the label.

3.2. *Kepler* Input Catalogue

The KIC provides an estimate of T_{eff} and $\log g$ for most *Kepler* targets derived from *Sloan* photometry (see the second and seventh column, 'KIC', of Table 2, respectively). Unfortunately, the KIC values of $\log g$ are known to have large error bars (Molenda-Żakowicz et al. 2011, Lehmann et al. 2011). Moreover, a comparison between KIC estimates of the stellar radius and the radius derived from evolutionary models indicate that the KIC values of $\log g$ might be shifted towards lower values by about 0.1 dex. The temperature values, on the other hand, are fairly good for A-F type stars, and become less reliable for more massive or peculiar stars, because for higher temperatures the interstellar reddening is apparently not properly taken into account. The stars in our sample are reddened up to 0.3 mag in $(B - V)$, with an average reddening of $E(B - V) = 0.04$ mag. The 85 stars for which no KIC T_{eff} value is available, which are generally faint stars ($K_p > 11$ mag), are not considered in any analysis related to temperature, unless values of T_{eff} exist in the literature or are available from the analysis of new ground-based observations (see below).

3.3. New ground-based observations of sample stars

In the framework of the ground-based observational project for the characterization of KASC targets (see Uytterhoeven et al. 2010a,b for an overview), targets of the A-F type sample are being observed using multi-colour photometry and/or high-to-mid-resolution spectroscopy. The goal is to obtain precise values of physical parameters that are needed for the seismic modelling of the stars. A detailed analysis of a first subsample of A-F type stars has been presented by Catanzaro et al. (2011). Several other papers are in preparation. We include the available results to date in this paper, because the precise values of T_{eff} and $\log g$ are needed for the interpretations in Sections 7 and 8.

3.3.1. Strömgren photometry from the Observatorio San Pedro Mártir

Multi-colour observations were obtained for 48 sample stars over the period 2010 June 13–17 with the six-channel *uvby- β* Strömgren spectrophotometer attached to the 1.5-m telescope at the Observatorio Astronómico Nacional-San Pedro Mártir (OAN-SPM), Baja California, Mexico. Each night, a set of standard stars was observed to transform instrumental observations into the standard system using the well known transformation relations given by Strömgren (1966), and to correct for atmospheric extinction. Next, the photometric data were dereddened using Moon's UVBYBETA programme (Moon 1985), and T_{eff} and $\log g$ values were obtained using the *uvby* grid presented by Smalley & Kupka (1997). A detailed description of the data will be given by Fox Machado et al. (in prep.). The resulting stellar atmospheric parameters are presented in Table 2 under label 'b'.

3.3.2. SOPHIE spectra from the Observatoire de Haute Provence

We also analysed spectra of two sample stars, KIC 11253226 and KIC 11447883, obtained during the nights of 2009 July 31, August 1, and August 5 with the high-resolution ($R \sim 70000$) spectrograph SOPHIE, which is attached to the 1.93-m telescope at the Observatoire de Haute Provence (OHP), France. The spectra were reduced using a software package directly adapted from

HARPS, subsequently corrected to the heliocentric frame, and manually normalized by fitting a cubic spline.

To derive stellar atmospheric parameters, the observed spectra, which covers the wavelength range 3870–6940 Å, were compared with synthetic spectra. The synthetic spectra were computed with the SYNTH code (Kurucz 1993), using atmospheric models computed with the line-blanketed LTE ATLAS9 code (Kurucz 1993). The parameters were derived using the methodology presented in Niemczura, Morel & Aerts (2009) which relies on an efficient spectral synthesis based on a least-squares optimisation algorithm. The resulting values of T_{eff} , $\log g$ and $v \sin i$ are presented in Table 2, under label 'h'. The detailed analysis results, including element abundances and microturbulence, will be presented in a dedicated paper (Niemczura et al. in prep.), including several other *Kepler* stars.

3.3.3. Spectra from the Tautenburg Observatory

Spectra of 26 sample stars were obtained from May to August 2010 with the Coude-Échelle spectrograph attached to the 2-m telescope of the Thüringer Landessternwarte Tautenburg (TLS), Germany. The spectra cover 4700 to 7400 Å in wavelength range, with a resolution of $R = 32\,000$. The spectra were reduced using standard ESO-MIDAS packages. We obtained between two and seven spectra per star, which were radial velocity corrected and co-added. The resulting signal-to-noise in the continua is between 150 and 250.

Stellar parameters such as T_{eff} , $\log g$, [M/H], and $v \sin i$ have been determined by a comparison of the observed spectra with synthetic ones, where we used the spectral range 4740 to 5800 Å, which is almost free of telluric contributions. The synthetic spectra have been computed with the SynthV programme (Tsymbal 1996) based on atmosphere models computed with LLmodels (Shulyak et al. 2004). Scaled solar abundances have been used for different values of [M/H]. A detailed description of the applied method can be found in Lehmann et al. (2011). The resulting values of T_{eff} , $\log g$ and $v \sin i$ are presented in Table 2, under label 'g'. Errors are determined from χ^2 statistics and represent a 1- σ confidence level. Detailed analysis results, including also values of [M/H] and microturbulent velocity, will be published in a dedicated paper (Tkachenko et al. in prep.).

4. Characterization of the sample

Figure 2 shows the distribution of the 750 sample stars in T_{eff} (top left), $\log g$ (top right), *Kepler* magnitude K_p (bottom left), and total length of the *Kepler* light curve ΔT , expressed in d (bottom right). For the analysis we used T_{eff} and $\log g$ values given in boldface in Table 2. Note that seven stars in our sample are hotter than $T_{\text{eff}} = 9000$ K, and fall off the diagram.

The following typical global parameters have been observed for δ Sct and γ Dor stars (e.g. Rodríguez & Breger 2001; Handler & Shobbrook 2002): $\log g = 3.2 - 4.3$ and $T_{\text{eff}} = 6300 - 8600$ K for δ Sct stars, and $\log g = 3.9 - 4.3$ and $T_{\text{eff}} = 6900 - 7500$ K for γ Dor stars. While γ Dor stars are generally MS stars, several more evolved δ Sct stars have been observed.

The distributions in Fig. 2 show that about 70% of the total sample does indeed have T_{eff} values between 6300 K and 8600 K. However, a significant number (about 20%) are cooler stars. The $\log g$ values of our sample are concentrated on 3.5 – 4.5, which represents about 76% of the total sample.

The sample consists of stars with magnitudes in the range $6 < K_p < 15$ mag. The majority (about 55%) is located in the

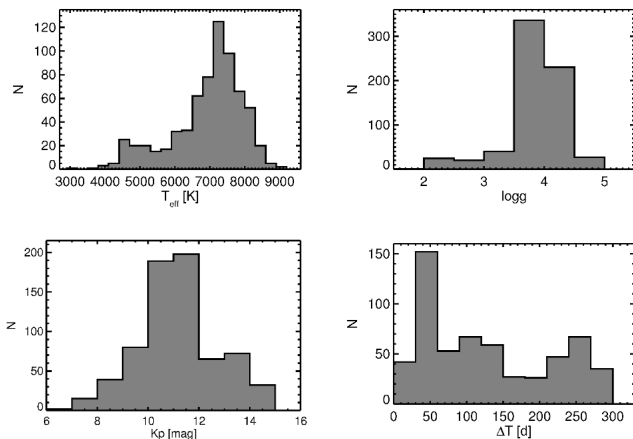


Fig. 2. Distribution in T_{eff} (top left), $\log g$ (top right), *Kepler* magnitude K_p (bottom left), and total time span ΔT of the *Kepler* light curves, expressed in d (bottom right) of the 750 sample stars. The number of stars belonging to each bin (N) is indicated on the Y-axis. We used the adopted values of T_{eff} and $\log g$, as given in boldface in Table 2.

interval $K_p = [10, 12]$ mag. Given that stars with magnitudes fainter than $V = 9$ are difficult to monitor spectroscopically from the ground with 2 m-class telescopes, the fact that about 92% of the stars are fainter than $V = 9$ has implications for the feasibility of possible spectroscopic ground-based follow-up observations (see Uytterhoeven et al. 2010a,b).

Finally, the total length of the *Kepler* dataset (not taking into account possible gaps of several tens of days) is spread between 9.5 and 322 d. For a considerable fraction (19%) of the sample only Q0 and Q1 data are available, with a total length of 44 d, implying a frequency resolution slightly worse than 0.02 d^{-1} . On the other hand, 351 stars, or 47% of the total sample, have a time span of more than 200 d (resulting in a frequency resolution better than 0.005 d^{-1}). Of these 351 stars, 46% have a maximum time gap in the light curve of less than 10 d, and 23% have a gap of over 200 d and up to 325 d.

In the following sections we will describe the variability analysis results of all 750 stars. At this stage we did not exclude any of the stars from the sample on grounds of non-compatibility of physical parameters with the current expectations for A- and F-type pulsators, to present a homogenous analysis and to investigate if *Kepler* confirms the current understanding of δ Sct and γ Dor stars.

5. Frequency analysis

5.1. Treatment of the *Kepler* light curves

In this paper we used the ‘non-corrected’ light curves available to KASC for asteroseismic investigations through the KASOC database. A description of the *Kepler* data reduction pipeline is given by Jenkins et al. (2010a,b). However, these raw time series suffer from some instrumental perturbations that need to be corrected for, e.g. perturbations caused by the heating and cooling down of the *Kepler* CCDs, variations caused by changes in the aperture size of the source mask, etc. Some of the effects are well known, and the corresponding non-stellar frequencies are tabulated by the *Kepler* team (e.g. frequencies near 32, 400, 430, and 690 d^{-1}). Other perturbations are not documented, and are harder to evaluate and correct for.

We subjected the light curves of all sample stars to an automated procedure that involves fitting a cubic spline to the time series, and correcting the residuals for discontinuities and outliers. To investigate if and to what extent artificial periodicities at the same timescale as the expected pulsations in γ Dor and δ Sct stars are introduced by the correction, we also corrected a subsample of stars by a different procedure that takes three types of effects into account, namely outliers, jumps, and drifts (see García et al. 2011). Both correction methods gave the same frequency analysis results within the accuracy of the dataset.

Next, the *Kepler* flux ($F_{Kp}(t)$) was converted to parts-per-million (ppm) ($F_{\text{ppm}}(t)$), using the following formula:

$$F_{\text{ppm}}(t) = 10^6 \times \left(\frac{F_{Kp}(t)}{f(t)} - 1 \right), \quad (1)$$

with $f(t)$ a polynomial fit to the light curve. A test on the effect of the use of different polynomial orders (2 to 10) on the detected frequencies in the time series showed that, in general, a third or fourth order polynomial fits the overall curvature better than a linear fit. The choice of the polynomial did not change periodicities with frequencies higher than 0.2 d^{-1} . The obtained error for frequencies between 0.01 and 0.2 d^{-1} was of the order of $1/\Delta T \text{ d}^{-1}$, with ΔT the total time span of the light curve expressed in d.

5.2. Frequency analysis

The *Kepler* time series of the 750 sample stars were analysed in a homogenous way, using a programme based on the Lomb-Scargle analysis method (Scargle 1982). Frequencies were extracted in an iterative way until the Scargle false alarm probability (fap; Scargle 1982), a measure for the significance of a peak with respect to the underlying noise level, reached 0.001. In view of the almost uninterrupted and equidistant sampling of the *Kepler* data, this estimate of the fap is a fast and reliable approximation of the true fap, because the number of independent frequencies can be estimated precisely (see also the discussion in Sect. 4 of Balona et al. 2011b). Frequencies were calculated with an oversampling factor of 10. Time series consisting of only LC data were not searched for periods shorter than 1 hour, because the corresponding Nyquist frequency is 24 d^{-1} . For SC data, with a time sampling of about 1 min, frequencies up to 720 d^{-1} could be detected.

As a comparison, subsamples of the stars were analysed using different analysis methods, such as SigSpec (Reegen, 2007, 2011), Period04 (Lenz & Breger 2005), the generalized Lomb-Scargle periodogram (Zechmeister & Kürster 2009), and the non-interactive code, *freqfind* (Leroy & Gutiérrez-Soto, in prep.). The latter code is based on the non-uniform fast Fourier transform by Keiner, Kunis & Potts (2009), and significantly decreases the computation time for unevenly spaced data. The results obtained with the different methods were consistent.

6. Classification

6.1. δ Sct, γ Dor, and hybrid stars

We performed a careful inspection (one-by-one, and by eye) of the 750 light curves, the extracted frequency spectra, and list of detected frequencies, and tried to identify candidate δ Sct, γ Dor, and hybrid stars. We used a conservative approach and omitted frequencies with amplitudes lower than 20 ppm for the classification. We also filtered out obvious combination frequencies

and harmonics² in an automatic way, and only considered apparent independent frequencies for the analysis. We suspect that the variable signal of a few stars is contaminated by the light variations of a brighter neighbouring star on the CCD. We flagged all stars with a high contamination factor (> 0.15), as given by the KIC. If the light curves of the neighbouring stars on the CCD were available through KASOC³, we carefully checked the light curves of these stars with their neighbours. Stars that show an obvious contamination effect were omitted from classification. We used information on T_{eff} (Table 2) to distinguish between δ Sct and γ Dor stars versus β Cep and SPB stars. To be conservative, low frequencies ($< 0.5 \text{ d}^{-1}$) (see, for instance, the frequency spectra in Fig. 4) are currently not taken into account in the analysis, because in this frequency range real stellar frequencies are contaminated with frequencies resulting from instrumental effects (see Sect. 5.1), and the separation of the different origins requires a dedicated study, which is beyond the scope of this paper.

We encountered a variety of light curve behaviour. Based on a small number of stars and using only the first quarter of *Kepler* data, Grigahcène et al. (2010) already proposed a subdivision of the AF-type pulsators into pure δ Sct stars, pure γ Dor stars, δ Sct/ γ Dor hybrids and γ Dor/ δ Sct hybrids, using the fact that frequencies are only detected in the δ Sct (i.e. $> 5 \text{ d}^{-1}$, or $> 58 \mu\text{Hz}$) or γ Dor (i.e. $< 5 \text{ d}^{-1}$ or $< 58 \mu\text{Hz}$) domain, or in both domains with dominant frequencies in either the δ Sct star or γ Dor star region, respectively. Among the 750 sample stars we see different manifestations of hybrid variability. There are stars that show frequencies with amplitudes of similar height in both regimes, and stars with dominant frequencies in the γ Dor (δ Sct) domain and low amplitude frequencies in the δ Sct (γ Dor) domain. The light curves show diversity as well. Balona et al. (2011d) already commented on the different shapes of light curves of pure γ Dor stars.

In this work, we focus on stars that show at least three independent frequencies. We classified the stars in three groups: δ Sct stars, γ Dor stars, and hybrid stars. Because the underlying physics that causes the different types of hybrid behaviour is currently not clear, all types of hybridity (both δ Sct/ γ Dor hybrids and γ Dor/ δ Sct hybrids) are included in the group of hybrids. A star was classified as a hybrid star only if it satisfied all of the following criteria:

- Frequencies are detected in the δ Sct (i.e. $> 5 \text{ d}^{-1}$ or $> 58 \mu\text{Hz}$) and γ Dor domain (i.e. $< 5 \text{ d}^{-1}$ or $< 58 \mu\text{Hz}$),
- The amplitudes in the two domains are either comparable, or the amplitudes do not differ more than a factor of 5–7 (case-to-case judgement),
- At least two independent frequencies are detected in both regimes with amplitudes higher than 100 ppm.

By using these criteria, we should reduce the number of false positive detections. In particular, we tried to avoid a hybrid star classification of ‘pure’ δ Sct stars that show a prominent long-term variability signal caused by rotation. We also tried to take care of more evolved δ Sct stars that are expected to pulsate with

² As obvious combination frequencies and harmonics we considered nf_i or $kf_i \pm lf_j$, with f_i and f_j different frequencies, $n \in [2, 3, 4, 5]$, and $k, l \in [1, 2, 3, 4, 5]$.

³ Unfortunately, only 40 stars of the sample could be checked in this way. We saw a clear contamination for the stars KIC 4048488 and KIC 4048494, KIC 5724810 and KIC 5724811, and KIC 3457431 and KIC 3457434. Less clear contamination is seen for KIC 4937255 and KIC 4937257, and KIC 10035772 and KIC 10035775, which are stars that show no obvious periodic variable signals.

frequencies lower than 5 d^{-1} . Stars that exhibited only or mainly frequencies in the δ Sct domain (i.e. $> 5 \text{ d}^{-1}$) and did not satisfy all of the above given criteria were assigned to the pure δ Sct group. Likewise, the group of pure γ Dor stars consists of stars that do not comply with the hybrid star criteria, and that have only or mainly frequencies lower than 5 d^{-1} . However, the classification of pure γ Dor stars is not as straightforward, because several other physical processes and phenomena can give rise to variability on similar timescales, such as binarity and rotational modulation caused by migrating star spots. We tried our best to select only γ Dor stars, but are aware that nonetheless, and most likely, our selection is contaminated with a few non-*bona fide* γ Dor stars. For stars that were observed in non-consecutive *Kepler* quarters, we tried to beware of frequencies introduced by the spectral window. For instance, frequently a peak near 48 d^{-1} ($555 \mu\text{Hz}$) is detected (e.g. KIC 2166218 and KIC 7798339), which for a γ Dor pulsator can result in an incorrect classification as hybrid star.

In Figs 3–5 a portion of the light curve with a time span of 2 d (δ Sct stars) or 5 d (γ Dor and hybrid stars) and a schematic overview of the detected independent frequencies (i.e. combination frequencies are filtered out in an automated way, see above) are given for a few representative stars of each group. The amplitudes and *Kepler* flux are expressed in ppm, and the frequencies are given in both d^{-1} (bottom X-axis) and μHz (top X-axis). The dotted grey line in the amplitude spectra separates the δ Sct and γ Dor regime. The dates are in the Heliocentric Julian Date (HJD) format $\text{HJD}_0 = 2\,454\,950.0$. The figures illustrate the variety of pulsational behaviour within the groups. The δ Sct stars (Fig. 3) display an impressive variety of amplitude heights. The variability of the stars in panels (d) and (e), KIC 9845907 and KIC 9306095, respectively, is dominated by one high-amplitude frequency. Several lower amplitude variations are also present. The chance of confusing a high amplitude δ Sct star (HADS) and binarity is high for KIC 9306095. The stars in panels (a), (b), and (c) show multiperiodic variations with frequency amplitudes of similar size. The rotational frequency near 1.2 d^{-1} and its first harmonic of the star KIC 10717871 (panel c) could be mistaken for γ Dor-like frequencies. Because there are no other longer-term periodicities, there is no evidence for the possible hybrid status of this star (panel c).

The light curves of γ Dor stars (Fig. 4) vary from obvious beat patterns to less recognizable variable signals. Balona et al. (2011d) already pointed out that there are symmetric (e.g. panel d) and asymmetric (e.g. panel e) light curves among the stars that show obvious beating, and that most likely in these cases the pulsation frequencies are comparable to the rotation frequency. Balona et al. (2011d) also suggested that the more irregular light curves likely stem from slowly rotating stars.

Examples of hybrid stars are given in Fig. 5. The grey dotted line in the right panels guide the eye to separate the δ Sct and γ Dor regimes. The stars KIC 3119604 and KIC 2853280 (panels a and b, respectively) are clearly dominated by δ Sct frequencies, while the γ Dor frequencies have lower amplitudes. The star KIC 9664869 (panel c) is an example of a star that exhibits frequencies with amplitudes of comparable height in the two regimes. The highest peak in the γ Dor region is most likely related to the stellar rotation period, however, because several harmonics are also observed. The bottom two panels are examples of hybrid stars dominated by γ Dor periodicities.

Table 3, available in the on-line version of the paper, presents an overview of the stars assigned to the three groups. For each star (KIC ID) we provide the classification (Class), the total number of independent frequencies (N) detected above the sig-

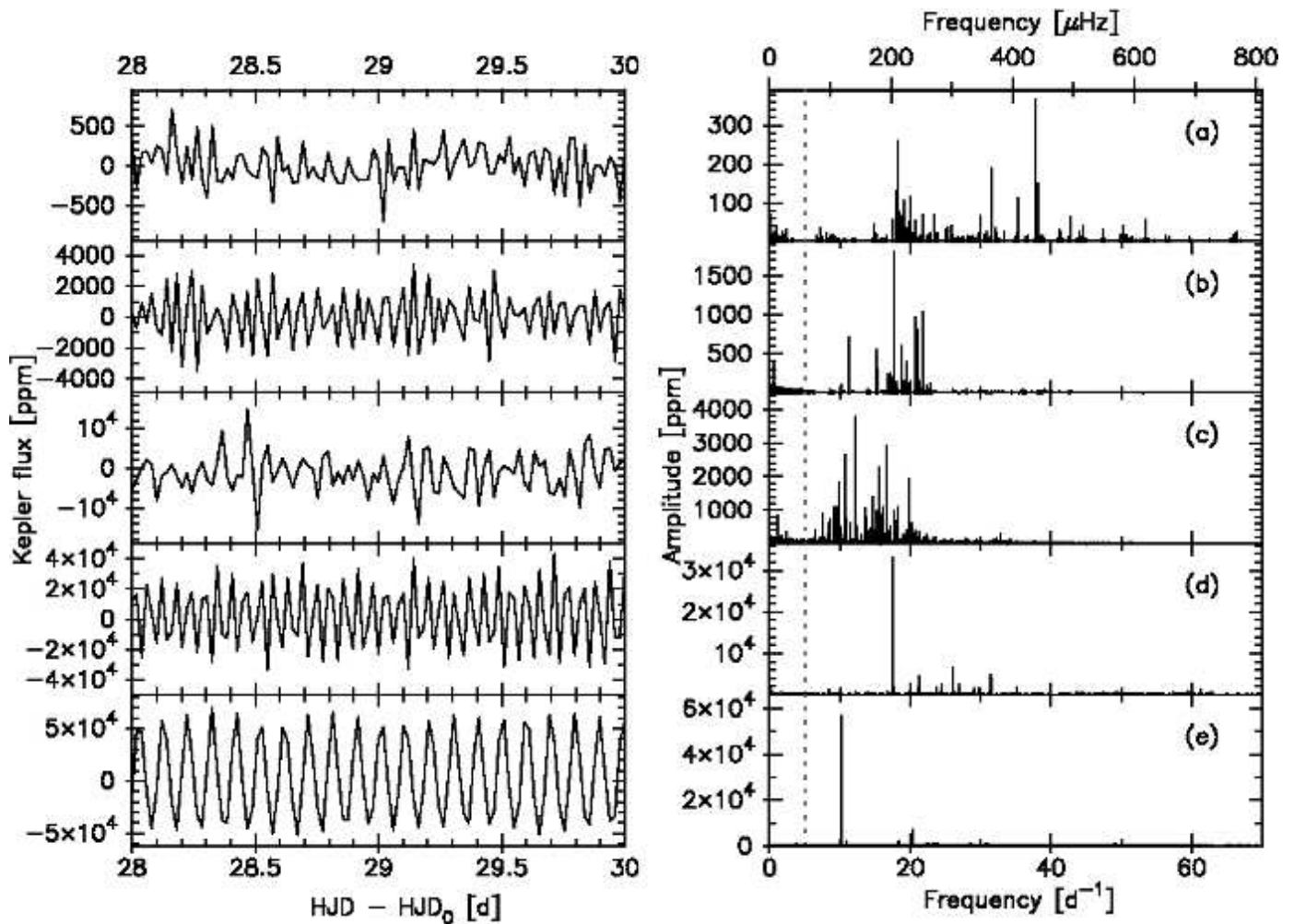


Fig. 3. Light curve and frequency spectrum of five stars assigned to the δ Sct group, illustrating the variety of pulsational behaviour within the group. The left panel shows a portion of the *Kepler* light curves. The *Kepler* flux is expressed in ppm, HJD is given in d with respect to $\text{HJD}_0 = 2454950.0$. The right panel gives a schematic representation of the detected independent frequencies, expressed in d^{-1} (bottom X-axis) or μHz (top X-axis). Amplitudes are given in ppm. The dotted grey line separates the δ Sct and γ Dor regime. Note the different Y-axis scales for each star. (a) KIC 8415752; (b) KIC 8103917; (c) KIC 10717871; (d) KIC 9845907; (e) KIC 9306095.

nificance level ($f_{\text{ap}} = 0.001$) and with amplitudes higher than 20 ppm, and the number of independent frequencies detected in the γ Dor and δ Sct regime ($N_{\gamma\text{Dor}}$ and $N_{\delta\text{Sct}}$, respectively). The next column gives as a reference the total number of frequencies detected above the significance level, including combination frequencies and harmonics (N_{total}). The next four columns denote the frequency range of peaks in the γ Dor and δ Sct regimes ($(\text{Freq Range})_{\gamma\text{Dor}}$ and $(\text{Freq Range})_{\delta\text{Sct}}$, expressed in d^{-1}), the highest amplitude ($\text{Amplitude}_{\text{high}}$, expressed in ppm) and associated frequency ($\text{Freq}_{\text{high}}$, in d^{-1}). In the last column a flag (●) indicates if the risk on light contamination with a neighbouring star on the CCD is high (contamination factor > 0.15). A typical error on the frequency associated with the highest amplitude is 0.0001 d^{-1} . The error on the amplitude ranges from a few ppm up to about 30 ppm. We note that for stars identified as γ Dor or δ Sct stars we report on frequencies up to 6 d^{-1} or from 4 d^{-1} , respectively, to account for, for instance, the frequency spectrum of more evolved stars.

We note that for several stars classified as γ Dor star only LC data are available. This may create a selection effect, because short-term δ Sct periods are more difficult to detect in the short

timstrung of LC data owing to sampling restrictions. Also, as mentioned above, even though we carefully checked the stars one by one, we expect to have a few false positive detections of hybrid and γ Dor stars because the typical γ Dor frequencies can be easily confused with variations of the order of a day caused by rotation or binarity. A more careful analysis and interpretation of the full frequency spectrum of all individual stars of the sample will clarify this matter, but this is beyond the scope of this paper.

We compared our classification with the automated supervised classification results presented by Deboscher et al. (2011). Because these authors studied public *Kepler* Q1 data, only 479 objects of our sample appear in their catalogue. We point out that the classifier by Deboscher et al. (2009) only takes three independent frequencies with the highest amplitudes into account. Hence, the recognition and classification of hybrid behaviour is currently not implemented. Moreover, because the classifier does not take external information into account that can distinguish between B-type stars and AF-type stars (e.g. colour information, spectral classification based on spectra), there is often a confusion between δ Sct and β Cep stars, and between γ Dor and SPB stars. In general, there is good agreement ($> 87\%$, clas-

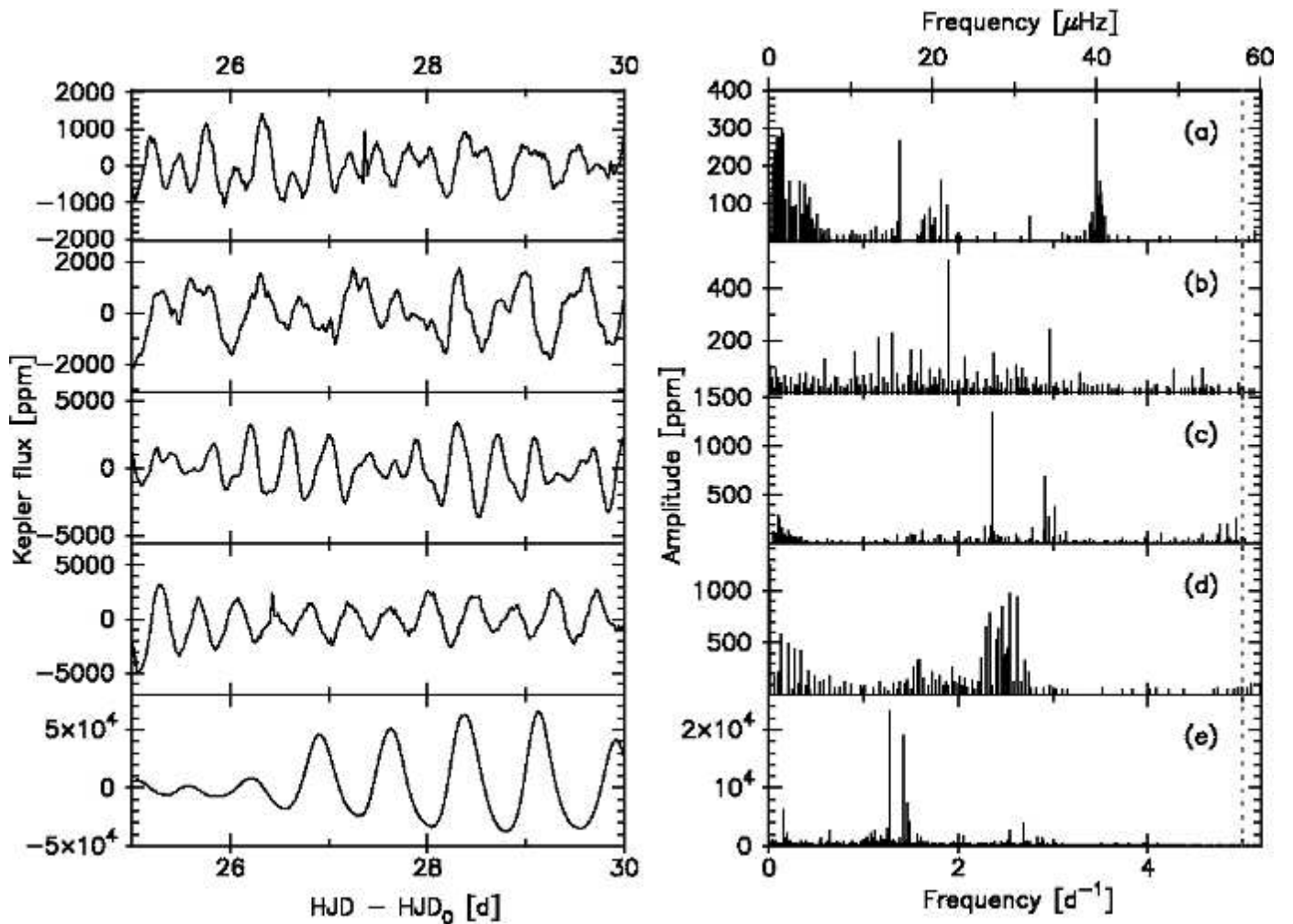


Fig. 4. Similar figure as Fig. 3, but for five candidate γ Dor stars. Note the different X-axis scale with respect to Fig. 3. (a) KIC 1432149; (b) KIC 5180796; (c) KIC 7106648; (d) KIC 8330056; (e) KIC 7304385.

sified in terms of δ Sct or β Cep stars) with the classification by Debosscher et al. (2011) for stars that we classified as δ Sct stars. The γ Dor stars, as we classified them, are in general less easily recognized by the automated classifier. Often they appear as ‘miscellaneous’ in their list. This is not surprising, because so far only a few high-quality light curves of well-recognized γ Dor stars were available that could be used as a template to feed the classifier. Stars that we identified as hybrid stars appear in the catalogue by Debosscher et al. (2011) as ‘miscellaneous’ or as δ Sct, γ Dor, β Cep, or SPB stars. The work presented in this paper will provide valuable feedback and information to refine the automated supervised classification procedure developed by Debosscher et al. (2009).

6.2. Other classes

About 63% of our sample is recognized as δ Sct, γ Dor, or hybrid star. Table 4, in the on-line version of the paper, gives an overview of the ‘classification’ of the remaining 37% of the stars. For each star (KIC ID) the associated classification (Class) and a flag (Flag) indicating a high risk on light contamination by a neighbouring star (\bullet if there is a contamination factor > 0.15), are given. Table 4 includes stars that show no clear periodic variability on timescales typical for δ Sct and γ Dor pulsators (‘...’, or ‘solar-like’), stars that exhibit stellar activity and show a rota-

tionally modulated signal (‘rotation/activity’), binaries (‘binary’ or eclipsing binary ‘EB’), B-type stars (‘Bstar’), candidate red giant stars (‘red giant’), Cepheids (‘Cepheid’), and stars whose light is contaminated by another star (‘contaminated’). Although the observed ranges in T_{eff} and $\log g$ include typical values for RR Lyr stars (see Fig. 2), we did not find any in our sample, but there are ~ 40 such stars observed by *Kepler*, which are studied separately (Kolenberg et al 2010; Benkő et al. 2010). Unclear cases mostly show a behaviour that might be related to rotation and are hence also labelled ‘rotation/activity’. We also assigned the candidate γ Dor stars for which less than three significant peaks were detected to this category. The light curve and frequency spectra of a few examples of these other classifications are given in Figs 6 and 7.

One hundred and twenty-one stars do not show an obvious periodicity in the expected range for γ Dor and δ Sct stars, or have an unresolved frequency spectrum within the available dataset. The star KIC 9386259 (Fig. 6, panel a) is an example of a star showing no clear periodicity. Furthermore, we used the label ‘...’ for some stars for which less than three significant frequencies were detected (e.g. KIC 11509728 and KIC 11910256). We investigated the stars for signatures of solar-like oscillations and identified 75 candidate solar-like oscillators (‘solar-like’, see Table 4).

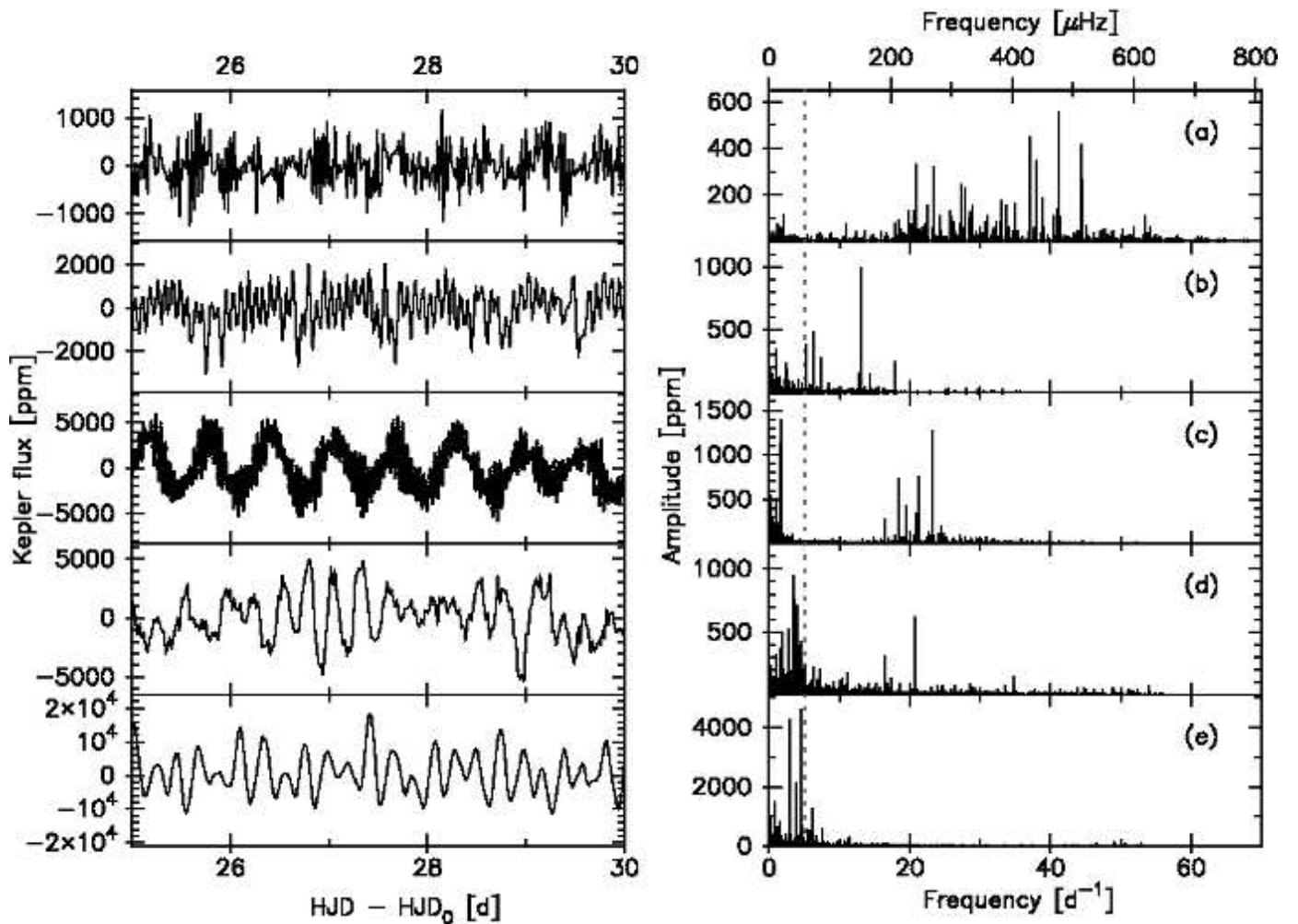


Fig. 5. Similar figure as Fig. 3, but for five candidate hybrid stars. (a) KIC 3119604; (b) KIC 2853280; (c) KIC 9664869; (d) KIC 9970568; (e) KIC 3337002. The two top panel (a)-(b) are δ Sct frequency-dominated stars, and the two bottom panels (d)-(e) are γ Dor frequency-dominated stars.

We identified seven B-type stars and 44 red giant stars in the sample. The giant stars show an envelope of frequencies with amplitudes up to 100–200 ppm in the region 0.5 – 5 d^{-1} , as illustrated by KIC 2584202 (Fig. 6, panel b). Among the B-type stars, we recognized five SPB stars and one candidate β Cep star.

Within the sample we identified at least 39 binaries, including 28 EBs. In Table 4 the binary stars are labelled ‘binary’, or ‘EB’ for an EB. If the variability of one of the components is identified as typical for one of the three groups outlined in Sect. 6.1, we also indicated this in Table 4. Panels (c), (d) and (e) of Fig. 6 show examples of EBs. An interesting target is KIC 11973705, because it most likely is a binary with a δ Sct and SPB component (see also Balona et al. 2011b). For three stars reported in the literature as EBs (Prša et al. 2011; Slawson et al. 2011; Hartman et al. 2004), KIC 2557115, KIC 5810113, and KIC 1432149, we find no clear evidence of their eclipsing nature in the *Kepler* lightcurves. In case of KIC 1432149, presented by Hartman et al. (2004) as an EB with period 9.3562 d, we cannot confirm its eclipsing nature or its orbital period, and we suspect that this target has been misidentified as an EB.

Several stars show an irregular light curve typical of stellar activity, or a clearly rotationally modified signal (panels (a)-(c) of Fig. 7). It is also not impossible that low-amplitude pulsating γ Dor star candidates are hidden among the stars labelled as

‘rotation/activity’ in Table 4. Namely, when only one or two of their pulsation frequencies reach the current detection threshold, they are not yet assigned to a pulsation group. A possible γ Dor candidate is given in panel (d) of Fig. 7.

In some cases the light curves look very peculiar, and the origin of the variability is not clear. This is the case for KIC 3348390 (panel (e) of Fig. 7) and KIC 4857678, for instance.

We discovered several interesting targets among the 750 stars of the sample. Dedicated studies of groups of individual stars will be presented in forthcoming papers. Below, we will sort the stars into different classes.

7. Characterization of the different classes

The classification described in the previous section results in the following distribution. A total of 63% of the sample can be identified as γ Dor, δ Sct or hybrid stars: 27% are classified as δ Sct stars (206 stars), 23% as hybrid stars (171 stars; of which 115 stars are δ Sct-dominated and 56 stars are γ Dor-dominated), and 13% as γ Dor stars (100 stars). A striking result is that almost a quarter of the sample, i.e. 171 stars, shows hybrid behaviour. This is in sharp contrast with the results obtained from ground-based observations, where so far only three candidate

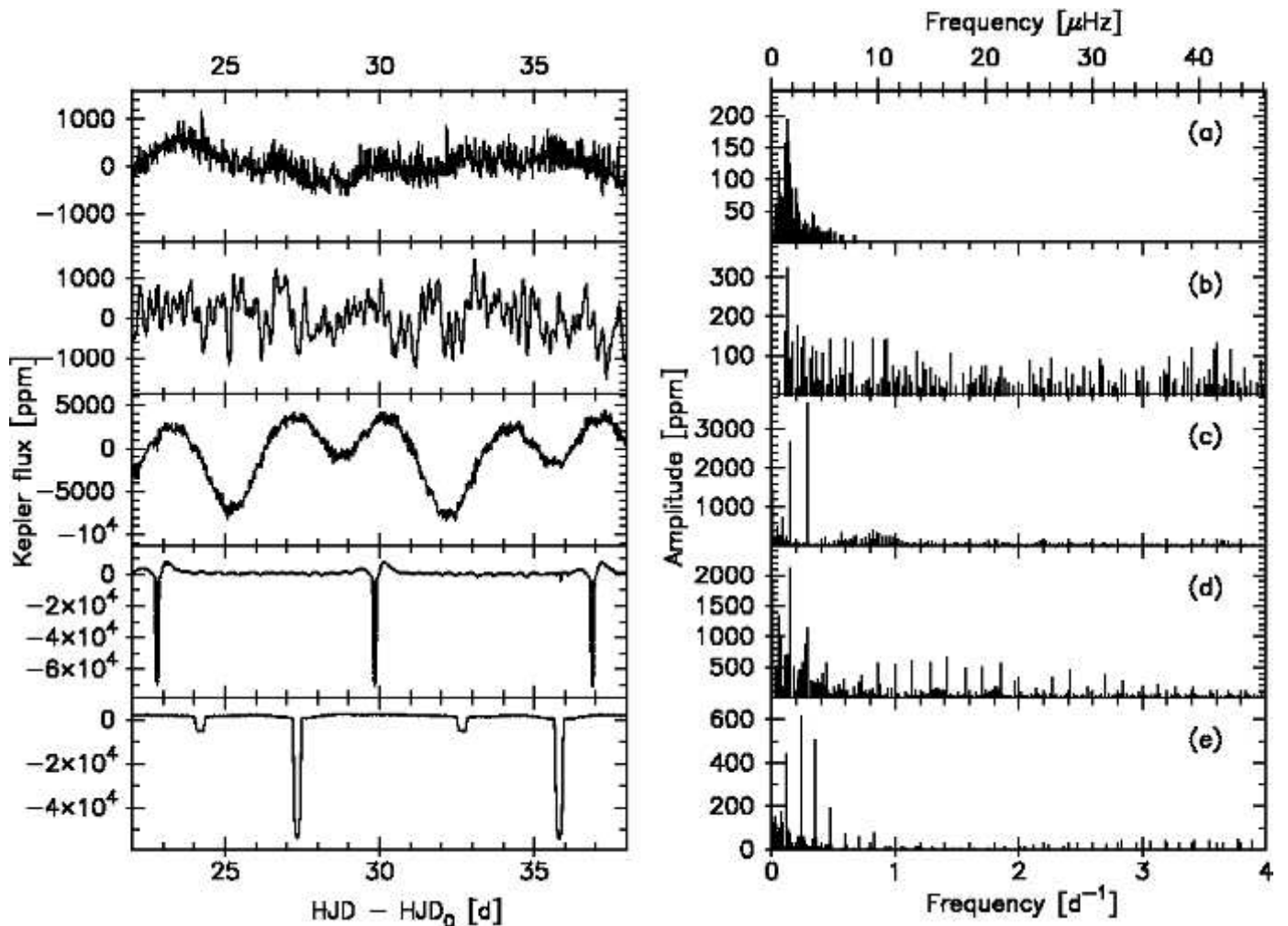


Fig. 6. Similar figure as Fig. 3, but for stars that were not assigned to the groups of δ Sct, γ Dor or hybrid stars. (a) KIC 9386259, no clear periodic signal detected; (b) KIC 2584202, red giant star; (c) KIC 5197256, EB or ellipsoidal variable with a δ Sct component; (d) KIC 3230227, EB with a γ Dor component; (e) KIC 9851142, EB with most likely a γ Dor component.

γ Dor- δ Sct hybrid stars have been discovered. The far superior precision of the space data opens a new window in detecting low amplitude variations. This result was already hinted at by Grigahcène et al. (2010) and Hareter et al. (2010), but the quantification by means of this sample is remarkable.

Of the remaining 37% of the sample, a considerable number (121 stars, 16%) do not show clear variability with periods in the expected range for γ Dor and δ Sct stars. Among this group are 75 candidate solar-like oscillators. Our sample has seven B-type stars (1%) and 44 stars (6%) are identified as red giant stars. One Cepheid turned out to be among the sample. About 8% of the sample shows stellar activity, often manifesting itself by a rotationally modulated signal.

At least 5% of the sample stars are identified through the analysis of their light curve as binary or multiple systems, of which 3.5% show eclipses. When we also consider the known binaries from the literature (Table 1), we arrive at a binary rate of 12% within the sample. The number of binary detections is only a fraction of what is expected. The binary rate among A-F type stars in general and δ Sct stars in particular is estimated to be at least 30% (Breger & Rodríguez 2000; Lampens & Boffin 2000). Several additional stars are expected to be part of multiple systems with possibly much longer periods than the available *Kepler* time span. The percentage of EBs in our sample is high.

Prša et al. (2011) reported a 1.2% occurrence rate of EBs among the *Kepler* targets.

Figure 8 shows the stars that are not assigned to one of the δ Sct, γ Dor or hybrid star groups in a (T_{eff} , $\log g$)-diagram. The solid thick black and light grey lines mark the blue and red edge of the observed instability strip of δ Sct and γ Dor stars, respectively (Rodríguez & Breger 2001; Handler & Shobbrook 2002). Owing to the possibly incorrect separation of the binary component's contribution, we considered the physical parameters of the binaries as insufficiently constrained and omitted them. The same holds for the B-type stars, which are much hotter than the T_{eff} region shown here. The stars that show no clear periodic variability on timescales typical for δ Sct and γ Dor pulsators (open triangles) and stars that exhibit stellar activity (bullets) are found along the MS and in more evolved stars. The location of the only Cepheid in our sample is marked by a cross. The candidate red giants (open squares) are all but one found in the expected region of the (T_{eff} , $\log g$)-diagram. This implies that the KIC photometry separates giant from MS stars well.

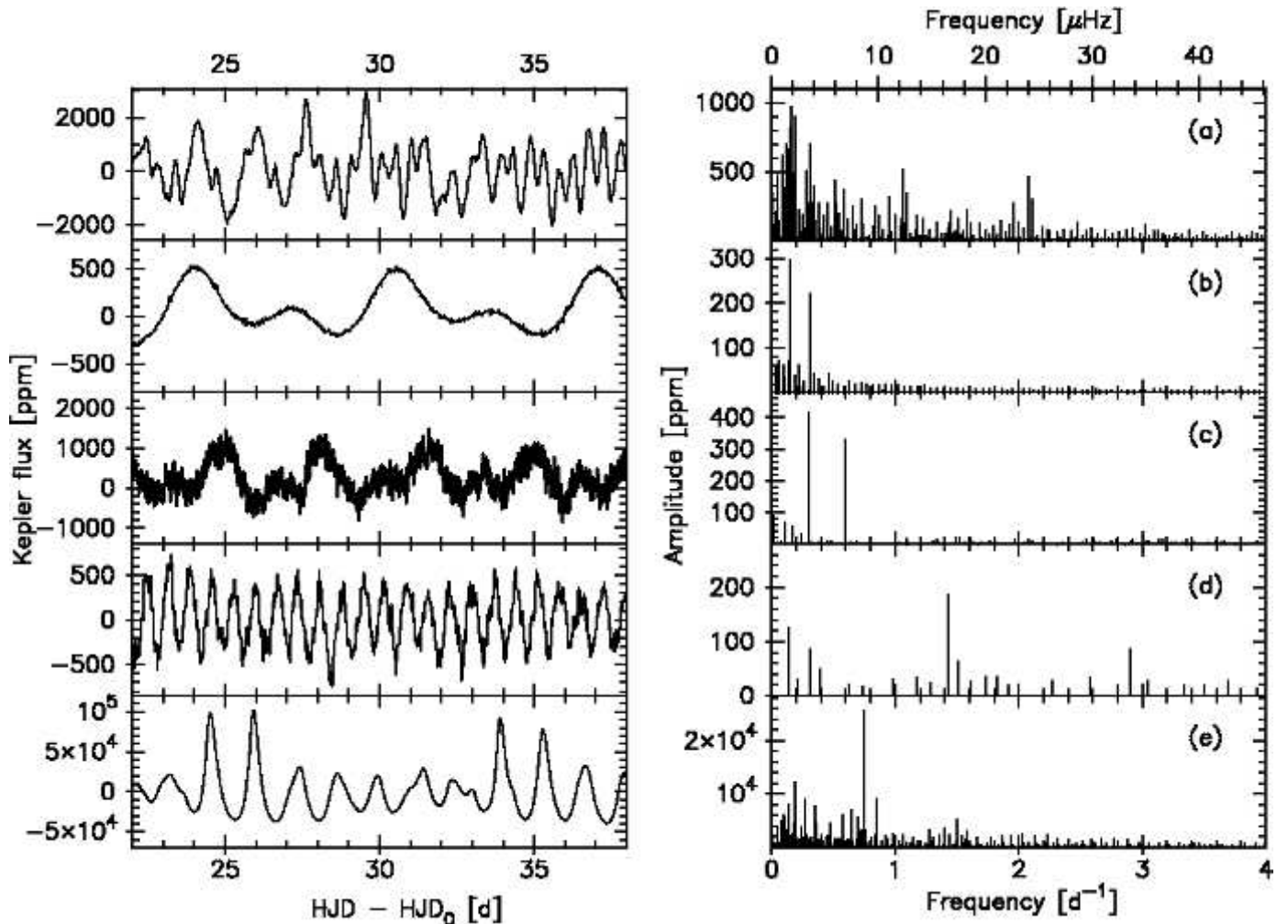


Fig. 7. Similar figure as Fig. 3, but for stars that were not assigned to the groups of δ Sct, γ Dor or hybrid stars. Stellar activity/rotational modulation: (a) KIC 8748251, (b) KIC 8703413 and (c) KIC 11498538; No clear classification: (d) KIC 12062443, and (e) KIC 3348390.

7.1. Characterization of stars that show no clear periodic variability

We now focus on the properties of the 121 stars that show no clear periodic variability in the γ Dor and δ Sct range of frequencies to understand why no oscillations are detected. Figure 9 presents the distribution in T_{eff} (top left), $\log g$ (top right), K_p (bottom left), and total time span ΔT , expressed in d, of the *Kepler* light curves (bottom right).

The cool boundary of the observational instability strip for γ Dor stars is located around $T_{\text{eff}} = 6900$ K. At least ⁴ 78% of the 121 stars have cooler temperatures, and hence no A-F type variability is expected. About 75 stars are identified as candidate solar-like oscillators. However, 10% of the 121 stars that show no clear periodicity are located inside the instability strip of γ Dor or δ Sct stars⁵ (see also Fig. 8). Additional investigation is needed to confirm that these stars do not show variability, which would imply that non-variable stars exist in the instability strip.

Sixty percent (71 stars) of our non-variable stars are fainter than $K_p = 12$ mag, and 18% are fainter than $K_p = 14$ mag. The

faintness of the star most likely has an impact on the (non-)detection of periodicities. To quantify this, we counted the fraction of apparently non-periodic stars per magnitude bin for the full sample of 750 stars. The number of stars that show no clear periodicity increases dramatically towards faint stars: the fraction is only 2% for magnitude $K_p = 9$ mag, 5% for $K_p = 10$ mag, 12% for $K_p = 11$ mag, 15% for $K_p = 12$ mag, 41% for $K_p = 13$ mag, and 68% for $K_p > 14$ mag. The fainter the star, the more difficult it becomes to detect periodicities. Our analysis results, which were obtained by only considering amplitudes above 20 ppm, lead us to suspect that the *Kepler* detection limit of A-F type low-amplitude oscillations (≤ 20 ppm) lies around $K_p = 14$ mag (see also Sect. 7.2).

We find no evidence for a selection effect towards stars with a short time span in the available *Kepler* time series. The right panel of Fig. 9 shows that also several time series with long time spans do not show clear variability. Also, the observing mode has no obvious influence on the (non-)detection of oscillations. Fifty-four percent of the 121 stars have only LC data, while 46% have only SC data.

To summarize, stars that show no clear periodic variations are generally the cooler and fainter stars of the sample. We do not find evidence for a bias towards the total time span of the

⁴ For 11% of the 121 stars we have no information on T_{eff} or $\log g$.

⁵ As demonstrated in Sect. 7.2, a revision of the current instability strip is required.

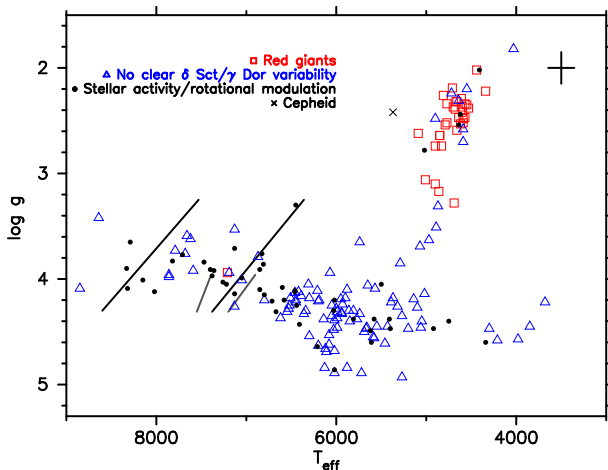


Fig. 8. (T_{eff} , $\log g$)-diagram with stars that show no clear periodic variability on timescales typical for δ Sct and γ Dor pulsators (open triangles), stars identified as red giants (open squares), stars that exhibit stellar activity (bullet), and a Cepheid (cross). The cross at the right top corner represents the typical error bars on the values: 290 K for T_{eff} and 0.3 dex for $\log g$. The solid thick black and light grey lines mark the blue and red edge of the observed instability strips of δ Sct and γ Dor stars, as described by Rodríguez & Breger (2001) and Handler & Shobbrook (2002), respectively. In the on-line version of the paper the open squares, open triangles, bullets, and crosses, are red, blue, black, and black, respectively.

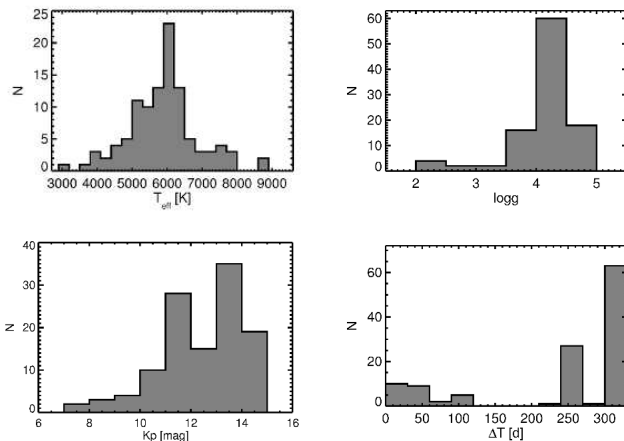


Fig. 9. Distribution in T_{eff} (top left), $\log g$ (top right), *Kepler* magnitude K_p (bottom left), and total time span ΔT of the *Kepler* light curves (bottom right) of the 121 stars that show no clear periodic variability. The number of stars belonging to each bin is given on the Y-axis.

available light curve or towards the observing mode (LC versus SC).

7.2. Characterization of δ Sct, γ Dor, and hybrid stars

7.2.1. The (T_{eff} , $\log g$)-diagram

The current ground-based (GB) view on the positions of the δ Sct and γ Dor classes in the (T_{eff} , $\log g$)-diagram (parameters

are taken from the literature⁶) is presented in panel (a) of Fig. 10. A comparison of $\log g$ values derived from Geneva photometry and from other sources (photometry and spectroscopy) indicates a systematic difference of about 0.4 dex for $\log g$ values above 4.35 dex as calculated from the Geneva photometry (Cuypers & Hendrix, private communication). Therefore we have corrected the values based on Geneva photometry. Evidently, the δ Sct and γ Dor stars occupy distinct locations in the (T_{eff} , $\log g$)-diagram, with a small overlap region.

Panel (b) of Fig. 10 shows a different picture. Here the δ Sct, γ Dor, and hybrid stars from the *Kepler* sample are plotted. We used the adopted values of T_{eff} and $\log g$, as given in Table 2. The cross in the top right corner of the figure shows typical errors on the values. The stars are scattered in the (T_{eff} , $\log g$)-diagram: the δ Sct and γ Dor stars are not confined anymore to the two regions that were clearly seen for the ground-based stars. Even when considering the large error bars on the values, the scatter is present. *Kepler* δ Sct stars exist beyond the red edge of the instability strip, while *Kepler* γ Dor pulsations appear in both hotter and cooler stars than previously observed from the ground. The *Kepler* hybrid stars occupy the entire region between the blue edge of the δ Sct instability strip and the red edge of the γ Dor instability strip, and beyond. The position of the *Kepler* δ Sct and γ Dor stars suggests that the edges of the so far accepted observational instability strips need to be revised. However, we need accurate values of T_{eff} and $\log g$ for all stars to confirm this finding.

Because for most stars in our sample only KIC-based estimates of T_{eff} and $\log g$ are available, we selected the stars that have reliable estimates of these parameters derived from ground-based spectra or multi-colour photometry (see Sect. 3). From this selection, 69 are classified as belonging to one of the three groups. The subsample of 69 stars is plotted in panel (c) of Fig. 10. The position of the stars in the (T_{eff} , $\log g$)-diagram confirms the general findings described for the full sample. However, the scatter across the diagram of γ Dor stars is less present, but almost all γ Dor candidates lie outside the observational instability strip for γ Dor stars. Ground-based observations for the derivation of more precise values of T_{eff} and $\log g$ are needed for all other stars to confirm the exact locations of the stars.

Panel (d) of Fig. 10 shows the *Kepler* stars assigned to the three groups that have amplitudes higher than 1000 ppm (see Table 3), which approximately corresponds to amplitudes higher than 1 mmag and hence might be observable from the ground. We notice that the *Kepler* stars with ground-based observable amplitudes also do not fit within the observational instability strips.

The left column of Fig. 11 presents an overview of the distribution in T_{eff} for the three groups of A-F type stars. The histograms related to δ Sct, hybrid, and γ Dor stars are coloured in dark grey, middle grey, and light grey respectively. The distribution in T_{eff} peaks around 7400 K, 7200 K, and 7000 K for δ Sct, hybrid, and γ Dor pulsators, respectively. Comparing these values with the center of the observed instability strips by Rodríguez & Breger (2001) and Handler & Shobbrook (2002), we find that a large part of the *Kepler* stars are concentrated near

⁶ Rodríguez & Breger 2001; Rodríguez et al. 2000; Henry & Fekel (2005); Poretti et al. (1997); Breger et al. (1997); Zerbi et al. (1997, 1999); Aerts et al. (1998); Kaye et al. (1999b); Gray & Kaye (1999); Eyer & Aerts (2000); Guinan et al. (2001); Aerts (2001); Martín et al. (2003); Mathias et al. (2004); Rowe et al. (2006); Bruntt et al. (2008); Cuypers et al. (2009); Uytterhoeven et al. (2008); Catanzaro et al. (2010, 2011)

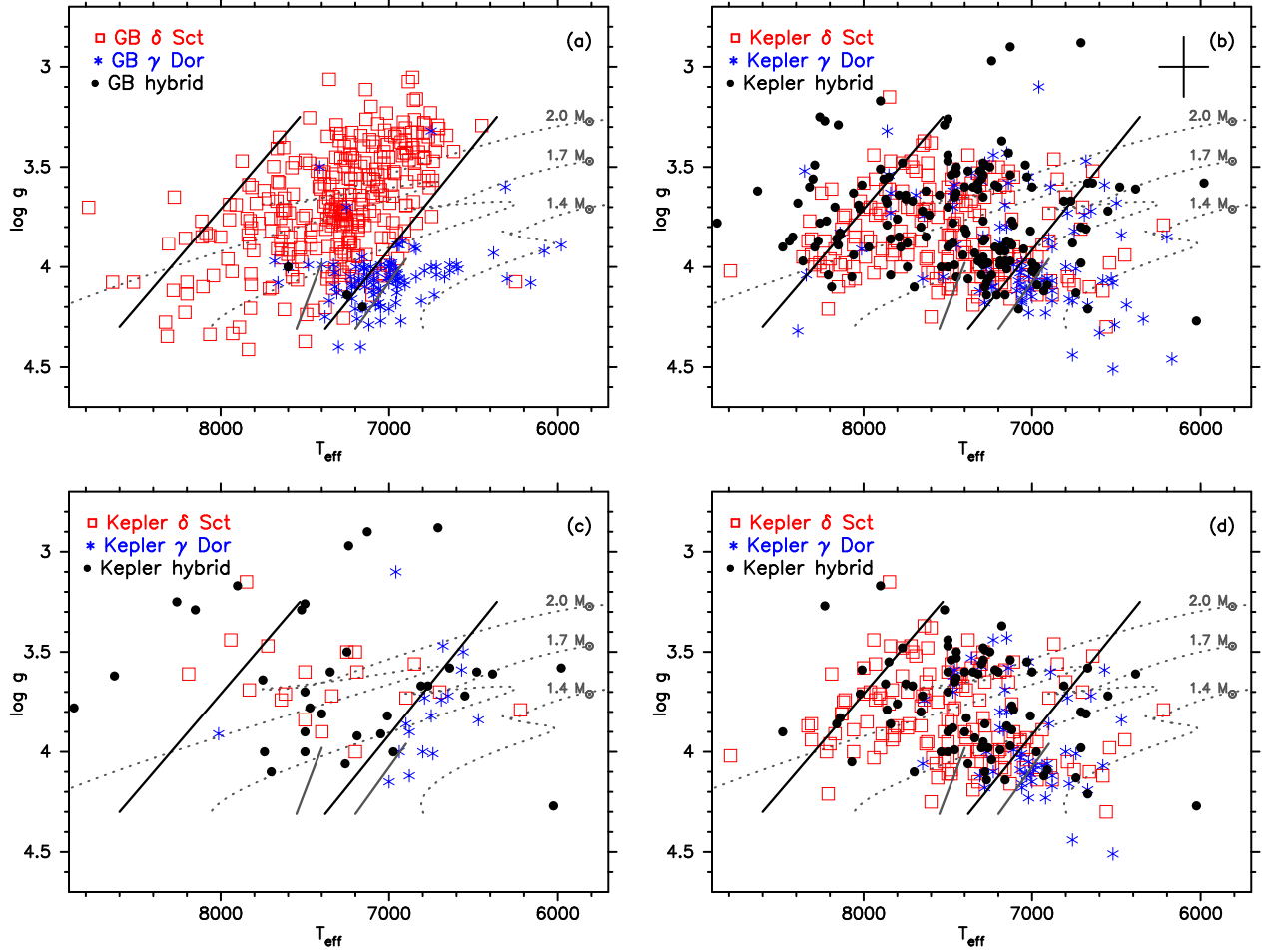


Fig. 10. (a): $(T_{\text{eff}}, \log g)$ -diagram of the δ Sct, γ Dor, and hybrid stars detected from the ground (parameters taken from the literature). (b): $(T_{\text{eff}}, \log g)$ -diagram of the *Kepler* stars we classified as δ Sct, γ Dor, and hybrid stars in this paper. Open squares represent δ Sct stars, asterisks indicate γ Dor stars, and hybrid stars are marked by bullets. The black cross in the right top corner shows typical errors on the values. (c): $(T_{\text{eff}}, \log g)$ -diagram of the subsample of 69 *Kepler* stars for which accurate T_{eff} and $\log g$ values are available. The colour-codes are the same as for panel (b). (d) $(T_{\text{eff}}, \log g)$ -diagram of the subsample of *Kepler* stars that show pulsations with amplitudes higher than 1000 ppm (> 1 mmag). Evolutionary tracks for MS stars with masses $1.4 M_{\odot}$, $1.7 M_{\odot}$, and $2.0 M_{\odot}$ are plotted with grey dotted lines. The evolutionary tracks have been computed using the Code Liégeois d'Évolution Stellaire (CLES, Scuflaire et al. 2008). The input physics included is similar to the one used in Dupret et al. (2005) with the following values for the modelling parameters $\alpha_{\text{MLT}} = 1.8$, $\alpha_{\text{ov}} = 0.2$ and $Z = 0.02$. The solid thick black and light grey lines mark the blue and red edge of the observed instability strips of δ Sct and γ Dor stars, as described by Rodríguez & Breger (2001) and Handler & Shobbrook (2002), respectively. In the on-line version of the paper the symbols representing the δ Sct, γ Dor, and hybrid stars are red, blue, and black, respectively.

the overlap of the two instability strips, and that many members of the three groups coincide in the same region in the $(T_{\text{eff}}, \log g)$ -diagram. It will be interesting to investigate why stars with similar values of T_{eff} and $\log g$ in some cases pulsate as a δ Sct star, and in others as a γ Dor star, or as both. Another interesting and puzzling result is that γ Dor and δ Sct pulsations seem to be excited in a far wider range of temperatures than previously expected.

The distribution in $\log g$ is similar for all classes. Most stars have $\log g$ values between 3.5 dex and 4.3 dex, with a peak around $\log g = 3.9$ dex. We point out that the $\log g$ values derived from the KIC for A-F type stars are known to have large uncertainties, and only few stars have measurements from other sources. Without more stars with accurate values derived from ground-based observations we cannot draw any conclusions.

The distribution in *Kepler* magnitude K_p (bottom left, Fig. 2) is representative for the distribution in K_p for γ Dor and δ Sct stars. It illustrates that the cut-off magnitude for the detection of γ Dor and δ Sct type of variations with *Kepler* lies around $K_p = 14$ mag. The majority of the sample stars have magnitudes in the range $K_p = 10 - 12$ mag.

$v \sin i$ values are available for 41 stars of the subsample consisting of δ Sct, γ Dor and hybrid stars (see Table 2). Of the five γ Dor stars, four have $v \sin i$ values above 90 km s^{-1} , and one has $v \sin i = 15 \text{ km s}^{-1}$. Of the sixteen δ Sct stars, eight stars have high $v \sin i$ values, six have moderate values ($40 < v \sin i < 90 \text{ km s}^{-1}$), and two low values ($v \sin i < 40 \text{ km s}^{-1}$). Of the 20 hybrid stars almost all have high $v \sin i$ values, with six stars having $v \sin i$ values above 200 km s^{-1} . Extrapolating these numbers to the full sample, we expect that many stars in the sample are moderate-to-fast rotators.

7.2.2. Frequencies and amplitudes

Up to 500 non-combination frequencies are detected in the *Kepler* time series of a single star (see Table 3). These large numbers of frequencies are in sharp contrast with the small number of frequencies observed from the ground, e.g. up to 79 pulsation and combination frequencies for the δ Sct star FG Vir (e.g. Breger et al. 2005) and up to 10 frequencies in the γ Dor hybrid candidate HD 49434 (Uytterhoeven et al. 2008), but are commonly seen in space observations because of their higher precision and sensitivity to low-amplitude variations (e.g. Poretti et al. 2009, García Hernández et al. 2009, Chapellier et al. 2011). However, it needs to be carefully checked whether all of the apparent individual frequencies are of pulsational origin.

For the majority of stars (66%), less than 100 frequencies were found, and 10% of the stars show variations with more than 200 frequencies. If we look at the extreme cases we find that for 29 stars (6%) fewer than 10 frequencies were detected, while for 5 stars (1%) more than 400 frequencies were found. The middle panel of Fig. 11 shows the distribution of the number of detected frequencies for the δ Sct (top, dark grey), hybrid (middle, middle grey), and γ Dor (bottom, light grey) stars. The highest number of frequencies are found for hybrid stars. It is worth mentioning that the number of detected frequencies versus T_{eff} follows a distribution that peaks near 7700 K, 7500 K, and 7000 K for δ Sct, hybrid, and γ Dor stars, respectively. More modes are excited near the centre of the δ Sct instability strip. For the hybrid and γ Dor stars most detected frequencies are found towards the red edge of the (overlap in the) instability strip.

The right panel of Fig. 11 shows the distribution of the highest measured amplitude in ppm logarithmic scale ($\log(\text{Amplitude})$) for the different groups using the same colour-code as before. The range in highest amplitude measured is 40 to 155 000 ppm. For about 59% of the stars the highest amplitude is lower than 2000 ppm. Only 16 stars (3.5%) show variability with highest amplitudes below 100 ppm, while 26 stars (5%) have amplitudes above 10 000 ppm. In general, higher amplitudes are detected in δ Sct pulsators than in γ Dor stars. We point out that the origin of high peaks detected in γ Dor stars, e.g. the amplitude of 23 000 ppm in the star KIC 7304385, is most likely related to the rotation of the star. It is worth mentioning that amplitudes above 10 000 ppm are also detected in faint targets. The highest amplitudes are found for stars within the temperature range $T_{\text{eff}} = 6600 - 7100$ K, which is the cool part of the instability strips.

We detected δ Sct frequencies between 4 and 80 d⁻¹. We found indications that a handful of stars vary with even shorter periods. However, these short periods need to be confirmed by means of a careful investigation of the specific frequency spectra, which is beyond the scope of this paper.

When considering the δ Sct stars and hybrid classes, which amount to a total of 375 stars, we find that 56% shows an upper frequency limit between 40 and 70 d⁻¹. Only 10% of the δ Sct and hybrid stars have frequencies up to 80 d⁻¹, and 9% only show variations with frequencies lower than 20 d⁻¹. We note that γ Dor-dominated hybrids that show variations with frequencies higher than 60 d⁻¹ are rare (three stars in our sample).

The majority of the hybrid stars detected in the *Kepler* data show all kinds of periodicities within the γ Dor and δ Sct range (see columns 6 and 7 in Table 3 which give the frequency range of the detected frequencies in the γ Dor and δ Sct domains). This observational fact is interesting because from a theoretical point of view no excited modes are expected between about 5 and 10 d⁻¹, i.e. the so-called 'frequency gap' (see, e.g. Grigahcène

et al. 2010). Only for five hybrid stars a 'frequency gap' is observed⁷. Possible explanations for the absence of gaps, within the present non-adiabatic theories, are that the frequencies within the gap are high-degree and/or rotationally split modes (Bouabid et al. 2009).

8. A first step towards understanding the relation between δ Sct, γ Dor, and hybrid stars

As presented in the previous section, it is not trivial to distinguish between the three groups of variable A-F type stars defined in Section 6.1. The relation between the three groups is currently unclear as well because δ Sct, γ Dor, and hybrid stars coincide in the (T_{eff} , $\log g$)-diagram (Fig. 10). Driven by the idea to find observables based on physical concepts that allow insight in the different internal physics of the three types of stars, we constructed two new observables that can provide an alternative way to improve our understanding of the relation between the three groups. We point out that several observational parameters can be found that reflect the different inherent properties of the three groups in one way or another. For instance, δ Sct stars pulsate with shorter periods, and are generally hotter than γ Dor stars. A combination of these parameters will lead to a differentiation of the groups, such as for instance a (T_{eff} , f_{max})-diagram, with f_{max} the frequency associated to the highest amplitude mode. However, we emphasize that our aim is to find observables that can be directly related to the internal physics of the stars.

According to the current instability theories, which need to be revised following the results presented in this work, the main driving process of the oscillations in δ Sct stars is related to the opacity variations in the ionization zones (Unno et al. 1989). These zones are located in the region where the main energy transport mechanism is convection and where a small quantity of energy is transported by radiation. The total amount of driving energy going into the mode is directly related to the radiative luminosity in this zone, and this latter quantity is a function of the convective efficiency. Therefore, we expect a relation between the energy of the observed modes and the convective efficiency of the outer convective zone. We searched for this relation and constructed two observables, *energy* and *efficiency*, that are estimates of the energy and the convective efficiency, using the available observational data.

8.1. Energy

The kinetic energy of a wave is given by

$$E_{\text{kin}} = \frac{1}{2} f(\rho_*) (A\zeta)^2, \quad (2)$$

where f is a function of the stellar density ρ_* , A is the amplitude of the oscillation, and ζ is the pulsation frequency. Using the available observational data, we construct the following observable that we call *energy*, which is a first approximation and estimate of the kinetic energy of the wave:

$$\text{energy} \equiv (A_{\text{max}} \zeta_{\text{max}})^2, \quad (3)$$

where A_{max} and ζ_{max} refer to the highest amplitude mode of the star (in ppm), and associated frequency (in d⁻¹). The pulsation

⁷ The six hybrid stars that show a 'frequency gap' are: KIC 3851151, KIC 4556345, KIC 7770282, KIC 9052363, and KIC 9775454.

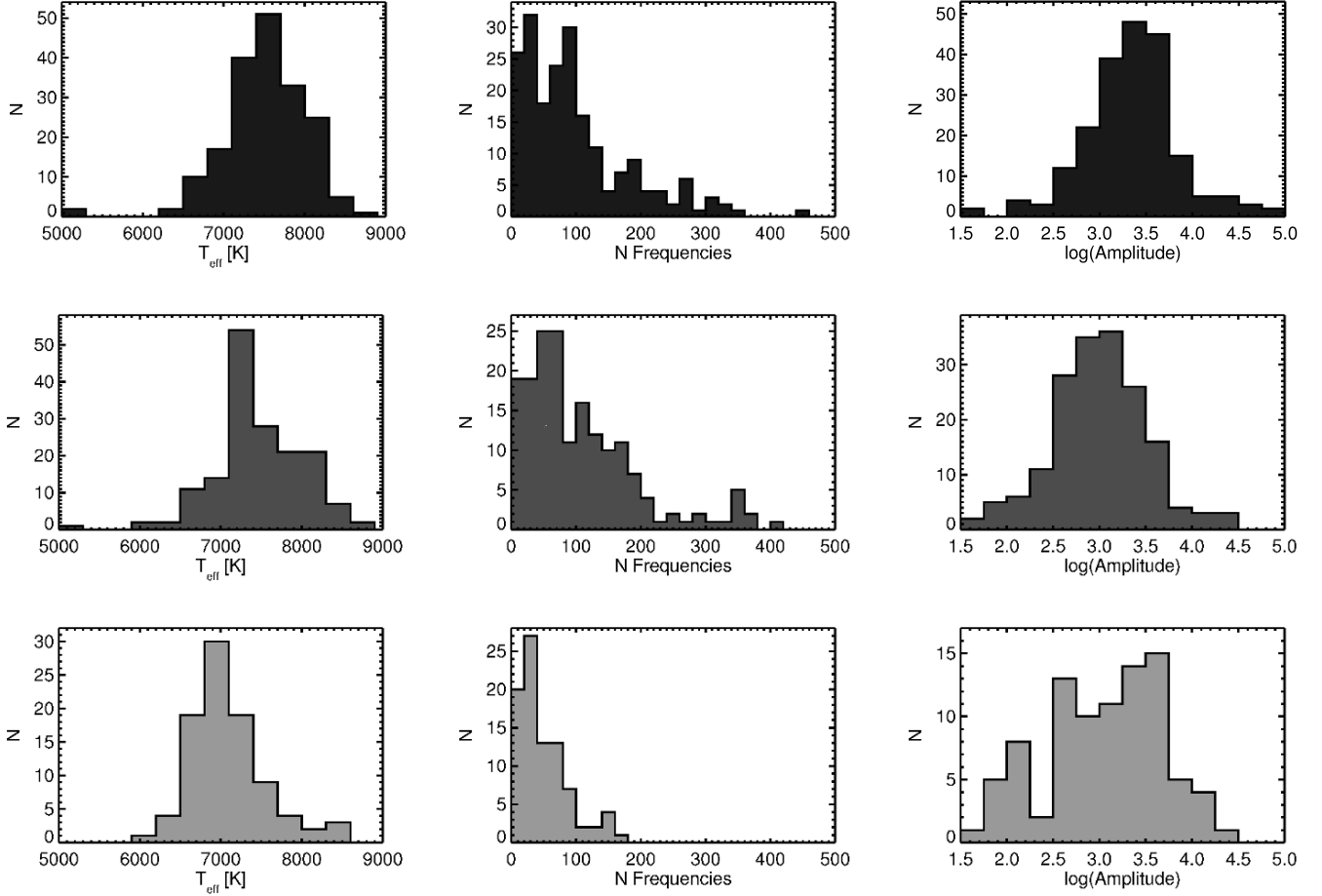


Fig. 11. Distribution in T_{eff} (left column), number of detected (independent) frequencies (middle column) and highest amplitude (ppm, in logarithmic scale) (right column), for the three groups of A-F type stars: δ Sct stars (top; dark grey), hybrid stars (middle; middle grey), and γ Dor stars (bottom; light grey). The number of stars belonging to each bin (N) is indicated on the Y-axis.

amplitude is a function of the observed amplitude and the relative variation of the flux, and is given by the expression (Moya & Rodríguez-López 2010):

$$\Delta R/R = -\frac{\Delta m}{\ln(5 + 10dT)}, \quad (4)$$

where $\frac{\Delta R}{R}$ is the relative pulsational amplitude, Δm the observed magnitude variation of the mode, and dT is given by

$$dT = \frac{\delta T_{\text{eff}}}{T_{\text{eff}}} \frac{\xi_r}{r}, \quad (r = R), \quad (5)$$

with ξ_r the variation in radius of the mode, and dT is evaluated at the surface of the star ($r = R$).

Non-adiabatic calculations of a representative model of a hybrid pulsating AF-type star including time dependent convection (Grigahcène et al. 2005) show that the difference between the predicted dT value of asymptotic g-modes (γ Dor stars) and low-order p-modes (δ Sct stars) is around one order of magnitude or less, where the δ Sct stars have higher values. Therefore, we can directly use the observed magnitude variation as a measurement of the radial amplitude variation. That we are using an approximation does not change the conclusions of the present study, because the observed differences are larger than two orders of magnitude (see Figs 12 and 13).

The right column of Fig. 12 shows the distribution in $\log(\text{energy})$ for the δ Sct (top, dark grey), hybrid (middle, middle grey), and γ Dor (bottom, light grey) stars. Clearly, the weight of the distribution is located in the region $\log(\text{energy}) > 8$ for stars dominated by frequencies in the δ Sct domain, and in the region $\log(\text{energy}) < 8$ for stars with dominant γ Dor pulsations.

8.2. Efficiency

In the introduction of this section we pointed out that a relation between the convective efficiency and mode excitation can exist. Recent studies on convective efficiency of the outer convective zone of F-G-K stars using 3D models show that the convective efficiency is related to the position of the star in the Hertzsprung-Russell (HR-) diagram (Trampedach & Stein 2011). To construct an observable related to the convective efficiency that can be described with only variables related with the position in the HR-diagram, we found inspiration in the analytic description of the

convective energy given by the mixing length theory⁸ (Böhm-Vitense 1958). There, the convective efficiency, Γ , is defined as

$$\Gamma = \left[\frac{A^2}{a_0 (\nabla_{\text{rad}} - \nabla)} \right]^{1/3}, \quad (6)$$

with a_0 a constant, ∇_{rad} and ∇ the radiative and real temperature gradient, respectively, and

$$A \sim \frac{c_p \kappa p \rho c_s \alpha^2}{9 \sigma T^3 g \sqrt{2 \Gamma_1}} \quad (7)$$

(see Cox & Giuli 1968).

This quantity, which measures the ratio between the convective and radiative conductivity, depends on a large number of physical variables: the specific heat capacity at constant pressure c_p , the opacity κ , the pressure p , the stellar density ρ , the sound velocity c_s , the mixing length parameter α , the Stephan-Boltzmann constant σ , the temperature T , the gravity g , and the first adiabatic coefficient Γ_1 . Because we only have information on a limited number of observational variables, our estimate of the quantity is only an approximation. Inspired by these equations, we searched for the combination of temperature and gravity that empirically provided the best means to separate between γ Dor and δ Sct stars (see statistical test below), and define the observable *efficiency* as

$$\text{efficiency} \equiv (T_{\text{eff}}^3 \log g)^{-2/3} \sim \Gamma. \quad (8)$$

Because the efficiency of the convective zone is expected to be higher for γ Dor stars than for δ Sct stars, the observable *efficiency* should have a higher value for γ Dor stars than δ Sct stars. This behaviour is indeed observed, as illustrated in the left panel of Fig. 12, where the distribution in $\log(\text{efficiency})$ is given. The majority of δ Sct stars have values $\log(\text{efficiency}) < -8.1$ dex, while the histograms for γ Dor pulsators peak in the region $\log(\text{efficiency}) > -8.1$ dex.

8.3. Efficiency versus energy

When we plot the two new observables, $\log(\text{energy})$ versus $\log(\text{efficiency})$, the groups of δ Sct and γ Dor stars are fairly well separated (see top panels Fig. 13). A $\log(\text{energy})$ value of 8 leaves 90% of the δ Sct and γ Dor stars separated. The bottom panel of Fig. 13 shows the same diagram with values for the hybrid stars included, using the same colours and symbols as before. Typical errors on the values are 0.04 dex and 0.12 dex for $\log(\text{energy})$ and $\log(\text{efficiency})$, respectively. The hybrid stars are placed in the intermediate region. We observed that δ Sct (γ Dor) dominated hybrids fall in the same region as the δ Sct (γ Dor) stars.

We performed a Mann-Whitney U test with an adapted p-value ($p = 0.0166$) according to the closed-test principle described in Horn & Vollandt (1995), to statistically investigate if the mean of the distribution in $\log(\text{energy})$ and $\log(\text{efficiency})$ is different for the three different groups. The test shows that the difference in the mean of the distributions in both $\log(\text{energy})$ and $\log(\text{efficiency})$ is statistically significant for all groups. However, the apparent separation in $\log(\text{efficiency})$ becomes less

⁸ In analogy to the mean free parameter in gas kinetic theory, the mixing length is defined as the mean distance over which a fluid bulb conserves its properties. Generally, the mixing-length is assumed to be proportional to the pressure-scale height by a factor α that is usually called mixing-length parameter.

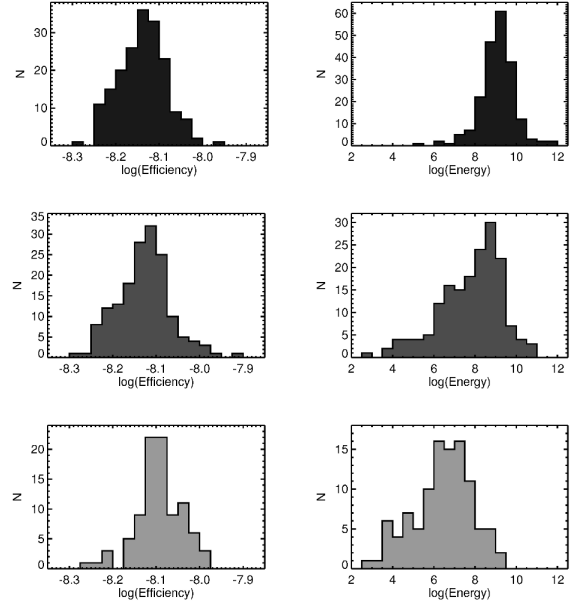


Fig. 12. Distribution in $\log(\text{energy})$ (right), and $\log(\text{efficiency})$ (left) for the δ Sct (top, dark grey), hybrid (middle, middle grey), and γ Dor (bottom, light grey) stars. The number of stars belonging to each bin (N) is indicated on the Y-axis.

evident when we take the considerable error bars into account. We also performed a χ^2 test (as described by Press et al. 1992) to determine if the distributions themselves were different. All distributions are statistically significant, save for the γ Dor versus hybrid star *efficiencies*, where they are marginally similar. This conclusion holds even if we vary the T_{eff} and $\log g$ values within the error ranges and recompute the *efficiencies* or vary the inputs into the *energies*. We point out once again that the definition of *efficiency* is only a rough estimate of the theoretical expression for the convective efficiency, and might - at this stage - not be refined enough to display the separating power between the groups we expect the convective efficiency to have. In a follow-up investigation we will assess the goodness of approximation of our definition of *efficiency* by comparison with values of the convective efficiency as given by Eq. (6), calculated for several model stars, and finetune its definition.

The two new approximate observables *energy* and *efficiency* reflect the different internal physics of oscillators with dominant δ Sct pulsations and oscillators dominated by γ Dor pulsations, and seem to allow us to distinguish between them. However, it needs to be further investigated if the two observables can be considered as independent parameters. This, together with an exploration of the physical mechanisms behind the instability of these stars, is the topic of a forthcoming paper. The observables *energy* and *efficiency* are promising starting points to explore the relation between δ Sct, γ Dor and hybrid stars, but need to be refined.

9. Summary, discussion, and future prospects

We analysed the *Kepler* light curves based on survey phase data with time spans between 9 d and 322 d available through KASOC and associated frequency spectra of 750 candidate A-F type stars in search for δ Sct, γ Dor, and hybrid pulsators. The main results are:

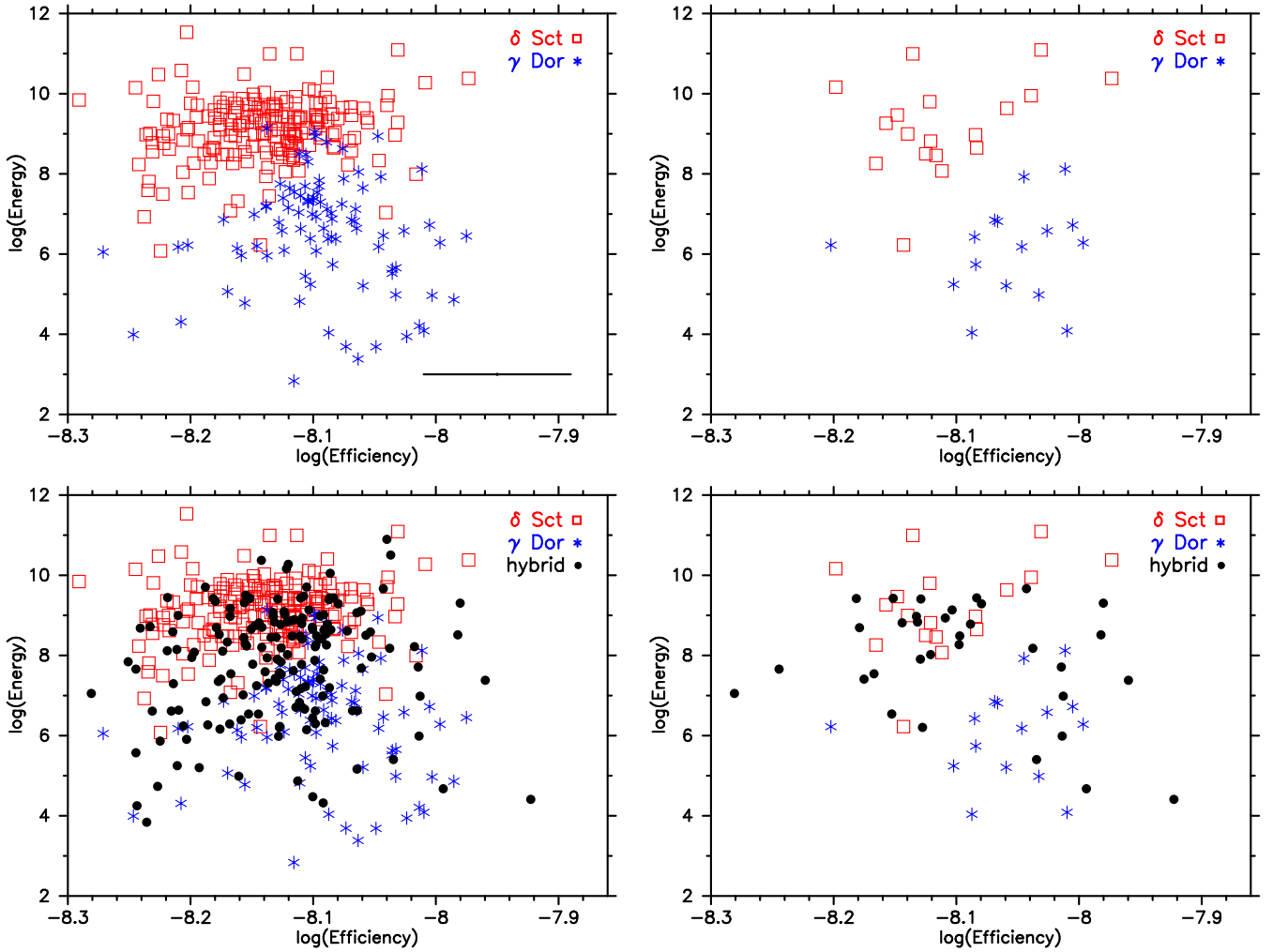


Fig. 13. Observable $\log(\text{energy})$ plotted versus $\log(\text{efficiency})$ for δ Sct (open squares) and γ Dor (asterisks) stars only (top), and for hybrid stars as well (bullets) (bottom). The left panels include all 480 *Kepler* stars that are assigned to one of the three groups. The right panels show the 49 stars for which reliable values of T_{eff} and $\log g$ are available. In the on-line version of the paper the symbols representing the δ Sct, γ Dor and hybrid stars are red, blue, and black, respectively. The cross in the right bottom corner of the top left panel represents the typical error bars on the values: 0.04 dex and 0.12 dex for $\log(\text{energy})$ and $\log(\text{efficiency})$, respectively.

- The *Kepler* light curves of the sample of 750 candidate A-F type stars show a variety in variability behaviour.
- Observationally, we propose three main groups to describe the observed variety: γ Dor, δ Sct, and hybrid stars. The latter group includes both δ Sct-dominated and γ Dor-dominated hybrid stars. About 63% of the sample are unambiguously assigned to one of the three groups.
- About 23% of the sample are hybrid candidates (171 stars, or 36% of the stars assigned to the three groups). This is in strong contrast with the number of hybrid candidates so far observed from the ground, but compatible with the first *Kepler* study of γ Dor and δ Sct variables by Grigahcène et al. (2010). The far superior precision of the *Kepler* space data opens a new window in detecting low-amplitude variations. *Kepler* will be ideal to study hybrid behaviour in different types of stars, such as roAp stars (Balona et al. 2011a), sdB stars (Østensen et al. 2010), and B stars (Balona et al. 2011b).
- We presented a characterization of the stars in terms of number of detected frequencies, frequency range, and typical pulsation amplitudes, which provides valuable feedback for

models and instability studies. This is the first time that this kind of information is available for a substantial sample of stars. Up to 500 non-combination frequencies are detected in the *Kepler* time series of a single star. The highest pulsation amplitude measured is 58 000 ppm. The shortest detected δ Sct periods are about 18 min. We find that hybrid stars show all kinds of periodicities within the γ Dor and δ Sct range. In particular, the majority of hybrid stars shows frequencies between 5 and 10 d^{-1} . From a theoretical point of view, this result presents a number of challenges, because the currently accepted over-stability mechanisms cannot explain the presence of pulsational modes in the wide frequency ranges observed with *Kepler*. It needs to be investigated if and to what extent the presence of stochastic modes, high-degree, and/or rotationally split modes with high amplitudes, granulation and effects of convection can explain part of the unexpected observed modes.

- The location of γ Dor and δ Sct classes in the $(T_{\text{eff}}, \log g)$ -diagram has been extended (Fig. 10). We find indications that *Kepler* δ Sct stars exist beyond the red edge of the observational instability strip, while *Kepler* γ Dor pulsations seem to

appear in both hotter and cooler stars than observed so far. The *Kepler* hybrid stars occupy the entire region between the blue edge of the δ Sct instability strip and the red edge of the γ Dor instability strip and beyond. These results, if confirmed by verification of the temperature and $\log g$ values in a more comprehensive sample, imply that the observational instability strips need to be extended to accommodate the *Kepler* δ Sct and γ Dor stars. From a theoretical point of view, the overall presence of hybrid stars implies an investigation of other pulsation mechanisms to supplement the κ mechanism and convective blocking effect to drive hybrid pulsations.

- Two new ‘observables’ that reflect the different internal physics of δ Sct and γ Dor pulsators are introduced to investigate the relation between the two types of pulsations (Fig. 13): (1) *efficiency*, related to the convective efficiency of the outer convective zone, and a function of T_{eff} and $\log g$; and (2) *energy*, the driving energy of a mode, and a function of the highest observed frequency amplitude and the associated frequency. Both observables are empirical and are constructed using only available measured variables. The impact and physical significance of the group separation in the $(\log(\text{efficiency}), \log(\text{energy}))$ -diagram needs to be investigated in more detail. The two new observables are a promising starting point for further investigations of the relation between δ Sct, γ Dor and hybrid stars.
- Our study indicates that $K_p = 14$ mag is a cut-off magnitude for detection of variations with amplitudes below 20 ppm in A-F type stars with *Kepler*.
- Sixteen percent of the sample stars show no clear variability within the expected range of frequencies for δ Sct and γ Dor stars. Faint and cool stars predominate this sample. Among the stars, we identified 75 candidate solar-like stars. No correlation between non-variability and the length of the available dataset or the available cadence mode is found. We find indications for the presence of constant stars inside the instability strips of A-F type pulsators.
- The remaining 21% of sample stars are identified as a Cepheid, B-type stars, red giant stars, stars that show stellar activity, or binaries. At least 12% of the sample are identified as a binary or multiple system, based on investigation of the *Kepler* light curve or on input from the literature. Many long-period binaries are expected to be among the remaining stars of the sample. 3.5% of the sample stars shows eclipses. Several of the EBs have variable components, including δ Sct, γ Dor, and hybrid stars.

Clearly, space missions are changing the landscape of γ Dor and δ Sct pulsators. We aimed at a global analysis of the sample stars. A careful seismic analysis of individual stars is needed to confirm their classification, clarify the observed variety in pulsational behaviour, fully characterize the properties of the δ Sct, γ Dor, and hybrid groups, understand their relationship, clarify the driving mechanism(s) for each group, and elaborate on the variables *energy* and *efficiency*. The observational results with *Kepler* presented here open up several new questions and theoretical challenges for the current models related to pulsational instability, thermodynamics, and stellar structure. We mention here some topics for further investigation.

To be able to place the stars confidently in the $(T_{\text{eff}}, \log g)$ -diagram, estimate the projected rotational velocity, and derive accurate abundances, at least one high-resolution spectrum is needed for each star. To this end, an observational campaign is ongoing (Uytterhoeven et al. 2010a,b). Most stars of the δ Sct, γ Dor, and hybrid stars in our sample with magnitude

$K_p \leq 10.5$ mag have recently been observed or are scheduled to be observed in the coming months. However, 70 % of the stars in Table 3 are fainter than magnitude $K_p = 10.5$ mag, for which it is time-consuming and less practical to observe them with the available 2-m class telescopes that are equipped with a high-resolution spectrograph.

Because the oscillation modes in A-F type stars do not produce evident frequency patterns in their mode spectra, as is the case for solar-like oscillators, the identification of pulsation modes benefits from high-resolution spectral or multi-colour time series. Here we encounter limitations owing to the relative faintness of the *Kepler* sample too. For instance, it is only feasible to efficiently spectroscopically monitor the few brightest ($K_p \leq 9$ mag) stars from the ground, while multi-colour photometry can go a few magnitudes fainter. Moreover, it will be impossible with the current instrumentation to detect the pulsation amplitudes of the order of a few μmag from the ground. Therefore, only for a limited selection of the stars in Table 3, i.e. bright stars exhibiting high-amplitude variations, will it be feasible to organize ground-based follow-up campaigns.

For all other stars, we will have to rely on extracting information on the pulsation modes directly from frequency patterns observed in the *Kepler* data. Quasi-periodic patterns have been observed before in δ Sct stars (Handler et al. 1997; García Hernández et al. 2009). But in fast rotating stars the rotation destroys regular frequency and period patterns of p- and g-modes, which complicates the mode identification (e.g. Lignières et al. 2006; Ballot et al. 2010). For slowly rotating g-mode pulsators ($V_{\text{rot}} < 70 \text{ km s}^{-1}$), a mode-identification technique has been developed that relies only on accurate values of at least three frequencies (Frequency Ratio Method, Moya et al. 2005; Suárez et al. 2005), which is ideal to apply to the information extracted from the *Kepler* white light, without colour or spectral information. Unfortunately, many of our stars are moderate-to-fast rotators (see Sect. 7.2). Hence, the mode identification will be very challenging and will require more investigation.

An individual analysis of the candidate hybrid stars is needed to confirm their hybrid status and to firmly characterize their pulsation properties. The current theoretical instability models for hybrid stars need to be revised to be able to accommodate all stars that have been proposed as hybrid candidates in this paper. This includes a revision of the mechanisms that allow driving of p- and g-modes in A-F type stars with a broad range of temperatures. Additional processes that can be investigated with possible effect on the driving are stochastic excitation (Houdek et al. 1999; Samadi et al. 2002), a convective driving mechanism similar to g-mode pulsations in white dwarfs (Goldreich & Wu 1999), a κ mechanism-related effect presented by Gautschy and Löffler (1996) and Löffler (2000), and radiative levitation (Turcotte et al. 2000). Asteroseismic diagnostics have been studied to find signatures of stochastic mechanisms at the origin of the instability of γ Dor oscillators (Pereira et al. 2007). In that work, this possibility was not discarded, but continuous and precise space data were not yet available. The *Kepler* time series of the sample of stars studied here will be an ideal new testbed for this method.

The long, continuous time series that *Kepler* will deliver during its lifetime will unveil a large number of amplitudes at μmag level. This precision will open up opportunities to search for signatures of granulation in the variable star light (Kallinger & Matthews 2010). Spectroscopically, convective signatures have been detected in the microturbulence and line broadening of A-F type stars cooler than $T_{\text{eff}} = 10,000 \text{ K}$ (Landstreet et al. 2009).

Also the theoretical instability strips of the γ Dor and δ Sct pulsators need revision. As shown in Fig. 1, stars exhibiting purely γ Dor or δ Sct pulsations seem to exist beyond the current blue and red edge of the respective instability strips. Moreover, it is worth investigating if the evolutionary phase of γ Dor stars can be derived from properties in their frequency spectra, as is recently suggested by Bouabid et al. (2011), based on a theoretical study of seismic properties of MS and pre-MS γ Dor pulsators.

Another open question is the existence of non-variable A-F type stars inside the instability strips. So far, it is suggested (Poretti et al. 2003; Breger 2004) that all seemingly constant stars in the instability strip are low-amplitude pulsators. In this study we find indications that non-variability exists within the instability strip, but a more in-depth investigation based on a more comprehensive sample of stars with precise values of T_{eff} and $\log g$ is needed to confirm this.

Furthermore, candidate γ Dor stars with only a few excited dominant modes deserve to be looked at in more detail. The relation between rotation and pulsations is not yet clear. Moreover, the differentiation between pulsations and rotational variability proves to be very difficult (Breger 2011; Monnier et al. 2010). In the pilot study by Balona et al. (2011d) it was suggested that pulsation and rotation periods might be very closely related. It needs to be investigated to which extent the rotation influences the excitation of the observed modes. To help this investigation, $v \sin i$ values are needed.

Constraints on important physical parameters that are crucial for seismic modelling, such as stellar radius and mass, can be derived directly for pulsators in binary systems (e.g. Tango et al. 2006; Desmet et al. 2010). Our sample consists of several binaries and eclipsing systems with (a) pulsating component(s) (see Table 4). Hence, these targets in particular are very promising for dedicated ground-based follow-up observations, and a seismic analysis. Moreover, it will be interesting to investigate the effect of tidal interactions on pulsation frequencies (e.g. Uytterhoeven et al. 2004; Derekas et al. 2011).

Four of the EBs with a candidate γ Dor, δ Sct, or hybrid component in our sample are known as chemically peculiar stars (see Table 1). Three candidate hybrid stars (out of 61 stars with known spectral type), four candidate δ Sct stars (out of 67 stars), and one candidate γ Dor star (out of 25 stars) are also Ap or Am stars. So far, we detected both p- and g-mode pulsators among the chemically peculiar stars. Balona et al. (2011c) stated that the instability strip of pulsating Am type stars and δ Sct stars do not differ much. With the current small number statistics, it is not clear whether Ap/Am stars are indeed rare among γ Dor stars (Handler & Shobbrook 2002). One of the open questions is if chemical peculiarity is related to hybridity. The first discovered hybrid HD 8801 (Henry & Fekel 2005) intriguingly turned out to be an Am star. In a recent abundance study by Hareter et al. (2011) one of the two studied hybrid stars is also confirmed as being a chemically peculiar star. Together with the results of this study, this brings the total of known chemically peculiar hybrid stars to five. There is currently no evidence for a direct link between chemical peculiarity and hybrid behaviour, but a careful abundance analysis of a representative sample of hybrid stars is needed to confirm this.

Many more (candidate) δ Sct, γ Dor, and hybrid stars are expected to be among the stars observed by *Kepler*. Debosscher et al. (2011) reported the discovery of many additional δ Sct and γ Dor candidates in the public *Kepler* Q1 data. Also, a considerable fraction of the host stars of the recently published 1235 *Kepler* planet candidates (Borucki et al. 2011) turn out to be A-F type stars. Hence, we have promising prospects in studying

and understanding the A-F type star variable behaviour in detail through a much larger and more complete sample of A-F stars in the *Kepler* field when longer timestrings of *Kepler* data will become publicly available. *Kepler* is definitely opening the window towards the accurate characterization of pulsating A-F stars.

Acknowledgements. We are grateful to Joanna Molenda-Żakowicz, James Nemeč and the anonymous referee for their suggestions and comments to improve this paper. Funding for the *Kepler* mission is provided by NASA's Science Mission Directorate. We thank the entire *Kepler* team for the development and operations of this outstanding mission. KU acknowledges financial support by the Deutsche Forschungsgemeinschaft (DFG) in the framework of project UY 52/1-1, and by the Spanish National Plan of R&D for 2010, project AYA2010-17803. AM acknowledges the funding of AstroMadrid (CAM.S2009/ESP-1496). EN and AP acknowledge the financial support of the NN 203 405139 and NN 203 302635 grant, respectively, from the MNiSW. The work by GH and VA was supported by the Austrian Fonds zur Förderung der wissenschaftlichen Forschung under grant P20526-N16. LFM acknowledge financial support from the UNAM under grant PAPIIT IN114309. RSz and LLK have been supported by the 'Lendület' program of the Hungarian Academy of Sciences and the Hungarian OTKA grants K83790 and MB08C 81013. RSz was supported by the János Bolyai Research Scholarship of the Hungarian Academy of Sciences. SH acknowledges financial support from the Netherlands Organisation for Scientific Research (NWO). This research has been funded by the Spanish grants ESP2007-65475-C02-02, AYA 2010-21161-C02-02 and CSD2006-00070. The research leading to these results has received funding from the European Community's Seventh Framework Programme (FP7/2007-2013) under grant agreement no. 269194. This research has made use of the SIMBAD database, operated at CDS, Strasbourg, France, and is partly based on observations obtained at the Observatorio Astronómico Nacional-San Pedro Mártir (OAN-SPM), Baja California, Mexico, at the Observatoire de Haute Provence, France, and at the Thüringer Landessternwarte Tautenburg, Germany. We acknowledge with thanks the variable star observations from the AAVSO International Database contributed by observers worldwide and used in this research.

References

- Abt, H.A. 1984, *ApJ*, 285, 247
 Abt, H.A. 2004, *ApJS*, 155, 175
 Abt, H.A., & Cardona, O. 1984, *ApJ*, 285, 190
 Aerts, C. 2001, *ApJ*, 553, 814
 Aerts, C., Eyer, L., & Kestens, E. 1998, *A&A*, 337, 790
 Allende Prieto, C., & Lambert, D. L. 1999, *A&A*, 352, 555
 Antoci, V., Handler, G., Campante, T.L., et al., 2011, *Nature*, accepted
 Baglin, A., Auvergne, M., Barge, P., et al. 2006, in *The CoRoT Mission, Pre-Launch Status, Stellar Seismology and Planet Finding*, eds. M. Fridlund, A. Baglin, J. Lochard, & L. Conroy, (ESA SP-1306, ESA Publications Division, Noordwijk, Netherlands), 33
 Ballot, J., Lignières, F., Reese, D.R., & Rieutord, M. 2010, *A&A*, 518, A30
 Balona, L.A., Krisciunas, K., & Cousins, A.W.J. 1994, *MNRAS*, 270, 905
 Balona, L.A., Cunha, M.S., Kurtz, D.W., et al. 2011a, *MNRAS*, 410, 517
 Balona, L.A., Pigulski, A., De Cat, P., et al. 2011b, *MNRAS*, 413, 2403
 Balona, L.A., Ripepi, V., Catanzaro, G., et al. 2011c, *MNRAS*, 414, 792
 Balona, L.A., Guzik, J., & Uytterhoeven, K., et al. 2011d, *MNRAS*, in press
 Benkő, J.M., Kolenberg, K., Szabó, R., et al. 2010, *MNRAS*, 409, 1585
 Bidelman, W.P., Ratcliff, S.J., & Svolopoulos, S. 1988, *PASP*, 100, 828
 Böhm-Vitense, E. 1958, *Zeitschrift für Astrophysik*, 46, 108
 Borucki, W.J., Koch, D.G., Brown, T. M., et al. 2010, *Science*, 327, 977
 Borucki, W.J., Koch, D.G., Basri, G., et al. 2011, *ApJ*, 728, 117
 Bouabid, M.-P., Montalbán, J., Miglio, A., et al. 2009, in *AIP Conf. Proc. 1170, Stellar Pulsation: Challenges for Theory and Observation*, eds. J. A. Guzik, P. A. Bradley (Melville, NY: AIP), 477
 Bouabid, M.-P., Montalbán, J., Miglio, A., et al. 2011, *A&A*, in press (arXiv:1103.4389)
 Breger, M., Handler, G., Garrido, R., et al. 1997, *A&A*, 324, 566
 Breger, M. 2000, in *Delta Scuti and Related Stars*, eds. M. Breger & M. H. Montgomery, ASP Conf. Ser., 210, 3
 Breger, M. 2011, *Carnegie Observatories Astrophysics Series*, 5, in press (arXiv:1104.4392)
 Breger, M. 2004, in *The A-Star Puzzle*, eds. J. Zverko, J. Žižnovský, S.J. Adelman, & W.W. Weiss, *Proceedings IAU Symposium*, 224, (Cambridge University Press), 335
 Breger, M., Lenz, P., Antoci, V., et al. 2005, *A&A*, 435, 955
 Breger, M., Balona, L., Lenz, P., et al. 2011, *MNRAS*, 414, 1721

- Brown, T.M., Latham, D.W., Everett, M.E., & Esquerdo, G.A. 2011, *AJ*, in press (arXiv:1102.0342)
- Bruntt, H., De Cat, P., & Aerts, C. 2008, *A&A*, 478, 487
- Cannon, A.J. 1925, *Ann. Astron. Obs. Harvard Coll.*, 100, 17
- Carrier, F., North, P., Udry, S., & Babel, J. 2002, *A&A*, 394, 151
- Catanzaro, G., Frasca, A., Molenda-Žakowicz, J., & Marilli, E. 2010, *A&A*, 517, A3
- Catanzaro, G., Ripepi, V., Bernabei, S. et al. 2011, *MNRAS*, 411, 1167
- Chapellier, E., Rodríguez, E., Auvergne, M., et al. 2011, *A&A*, 525, A23
- Cox, J. P., & Giuli, R. T. 1968, *Principles of stellar structure*, New York, Gordon and Breach
- Cuypers, J., Aerts, C., De Cat, P., et al. 2009, *A&A*, 499, 967
- Debosscher, J., Sarro, L.M., López, M., et al. 2009, *A&A*, 506, 519
- Debosscher, J., Blomme, J., Aerts, C., & De Ridder, J. 2011, *A&A*, A89
- Derekas, A., Kiss, L.L., Borkovits, T., et al. 2011, *Science*, 332, 216
- De Cat, P., Eyer, L., Cuypers, J., et al. 2006, *A&A*, 449, 281
- Desmet, M., Frémat, Y., Baudin, F., et al. 2010, *MNRAS*, 401, 418
- Dupret, M.-A., Grigahcène, A., Garrido, R., Gabriel, M., & Scuflaire, R. 2004, *A&A*, 414, L17
- Dupret, M.-A., Grigahcène, A., Garrido, R., Gabriel, M., & Scuflaire, R. 2005, *A&A*, 435, 927
- Eyer, L., & Aerts, C. 2000, *A&A*, 361, 201
- Floquet, M. 1970, *A&AS*, 1, 1
- Floquet, M. 1975, *A&AS*, 21, 25
- García, R.A., Hekker, S., Stello, D., et al. 2011, *MNRAS*, 414, 6
- García Hernández, A., Moya, A., Michel, E., et al. 2009, *A&A*, 506, 79
- Gautschi, A., & Löffler, W. 1996, *DSSN*, 10, 13
- Gilliland, R.L., Brown, T.M., Christensen-Dalsgaard, J., et al. 2010a, *PASP*, 122, 131
- Gilliland, R.L., Jenkins, J.M., Borucki, W.J., et al. 2010b, *ApJ*, 713, 160
- Glebocki, R. & Stawikowski, A. 2000, *AcA*, 50, 509
- Goldreich, P., & Wu, Y. 1999, *ApJ*, 511, 904
- Grenier, S., Baylac, M.-O., Rolland, et al. 1999, *A&AS*, 137, 451
- Grigahcène, A., Dupret, M.-A., Gabriel, M., Garrido, R., & Scuflaire, R. 2005, *A&A*, 434, 1055
- Grigahcène, A., Antoci, V., Balona, L., et al. 2010, *ApJ*, 713, L192
- Gray, R.O., & Kaye, A.B. 1999, *AJ*, 118, 2993
- Guetter, H.H. 1968, *PASP*, 80, 197
- Guinan, E.F., Bochanski, J.J., Depasquale, J.M., Ribas, I., & McCook, G.P. 2001, *IAU Inform. Bull. Var. Stars*, 5062, 1
- Guzik, J. A., Kaye, A. B., Bradley, P. A., Cox, A. N., Neuforge, C. 2000, *AJ*, 542, 57
- Handler, G. 1999, *MNRAS*, 309, L19
- Handler, G. 2009a, *AIPC*, 1170, 403
- Handler, G. 2009b, *MNRAS*, 398, 1339
- Handler, G. Pikall, H., O'Donoghue, D. et al. 1997, *MNRAS*, 286, 303
- Handler, G., & Shobbrook, R.R. 2002, *MNRAS*, 333, 251
- Hareter, M., Reegen, P., Miglio, A., et al. 2010, *AN*, P49 (arXiv:1007.3176)
- Hareter, M., Fossati, L., Weiss, W., et al. 2011, *ApJ*, submitted
- Hartman, J.D., Bakos, G., Stanek, K.Z., & Noyes, R.W. 2004, *AJ*, 128, 1761
- Hauck B. & Mermilliod M. 1998, *A&AS*, 129, 431
- Henry, G.W., Fekel, F.C., Kaye, A.B., & Kaul, A. 2001, *AJ*, 122, 3383
- Henry, G.W., & Fekel, F.C. 2005, *AJ*, 129, 2026
- Henry, G.W., Fekel, F.C., & Henry, S.M. 2005, *AJ*, 129, 2815
- Henry, G.W., Fekel, F.C., & Henry, S.M. 2011, *AJ*, in press (arXiv:1105.4161)
- Hill, P.W., & Lynas-Gray, A.E. 1977, *MNRAS*, 180, 691
- Hill, S.J. & Schilt, J. 1952, *Contributions from the Rutherford Observatory of Columbia University New York*, 32, 1
- Hoffleit, D. 1951, *Harvard College Observatory Bulletin*, 920, 32
- Horn, M., & Vollandt, R. 1995, in "Multiple Tests und Auswahlverfahren", Gustav Fischer Verlag Stuttgart
- Houdek, G., Balmforth, N.J., Christensen-Dalsgaard, J., & Gough, D.O. 1999, *A&A*, 351, 582
- Jenkins, J.M., Caldwell, D.A., Chandrasekaran H., et al. 2010a, *ApJ*, 713, L120
- Jenkins, J.M., Caldwell, D.A., Chandrasekaran, H., et al. 2010b, *ApJ*, 713, L87
- Kallinger, T., & Matthews, J.M. 2010, *ApJ*, 711, L35
- Kaye, A.B., Handler, G., Krisciunas, K., Poretti, E., & Zerbi, F.M. 1999a, *PASP*, 111, 840
- Kaye, A.B., Henry, G.W., Fekel, F.C., & Hall, D.S. 1999b, *MNRAS*, 308, 1081
- Keiner, J., Kunis, S., and Potts, D. 2009, in *Using NFFT 3 - a software library for various nonequispaced fast Fourier transforms ACM Trans. Math. Software*, 36, 4
- Kharchenko, N.V., & Roeser, S. 2009, *VizieR On-line Data Catalog: I/280B*
- King, H., Matthews, J.M., Rowe, J.F., et al. 2006, *CoAst*, 148, 28
- Koch, D.J., Borucki, W.J., Basri, G., et al. 2010, *ApJ*, 713, L79
- Kolenberg, K., Szabó, R., Kurtz, D. et al. 2010, *ApJ*, 713, L198
- Kurucz, R.L. 1993, *Kurucz CD-ROM 13. (Smithsonian Astrophysical Observatory, Cambridge, USA)*
- Lafrasse, S., Mella, G., Bonneau, D., et al. 2010, in *Optical and Infrared Interferometry II*, Eds. W.C. Danchi, F. Delplancke, & J.K. Rajagopal, *Proceedings of the SPIE*, 7734, 140
- Lampens, P., & Boffin, H.M.J. 2000, in *Delta Scuti and Related Stars*, eds. M. Breger & M. H. Montgomery, *ASP Conf. Ser.*, 210, 309
- Landstreet, J.D., Kupka, F., Ford, H.A., et al. 2009, *A&A*, 503, 973
- Latham, D.W., Brown, T.M., Monet, D.G., et al. 2005, *BAAS*, 37, 1340
- Lehmann, H., Tkachenko, A., Semaan, T, et al. 2011, *A&A*, 526, A124
- Lenz, P., & Breger, M. 2005, *CoAst*, 146, 53
- Lignières, F., Rieutord, M., & Reese, D. 2006, *A&A*, 455, 607
- Lindoff, U. 1972, *A&A*, 16, 315
- Löffler, W. 2000, in *The Impact of Large-Scale Surveys on Pulsating Star Research*, eds L. Szabados & D. Kurtz, *ASP Conf. Ser.*, 203, 447
- Macrae, D.A. 1952, *ApJ*, 116, 592
- Magalashvili, N.L., & Kumishvili, J.I. 1976, *IAU Inform. Bull. Var. Stars*, 1167, 1
- Malkov, O.Y., Oblak, E., Snegireva, E.A., & Torra, J. 2006, *A&A*, 446, 785
- Martín, S., Bossi, M., & Zerbi, F.M. 2003, *A&A*, 401, 1077
- Masana, E., Jordi, C., & Ribas, I. 2006, *A&A*, 450, 735
- Mason, B.D., Wycoff, G.L., Hartkopf, W.I., Douglass, G.G., & Worley, C.E. 2001, *AJ*, 122, 3466
- Mathias, P., Le Contel, J.-M., Chapellier, E., et al. 2004, *A&A*, 417, 189
- Molenda-Zakowicz J., Frasca A., Latham D. W., 2008, *AcA*, 58, 419
- Molenda-Žakowicz, J., Latham, D. W., Catanzaro, G., Frasca, A., & Quinn, S. N. 2011, *MNRAS*, 412, 1210
- Monnier, J.D., Townsend, R.H.D., Che, X., et al. 2010, *ApJ*, 725, 1192
- Moon, T.T. 1985, *Comm. from the Univ. of London Obs.*, 78
- Moore, J.H. & Paddock, G.F. 1950, *ApJ*, 112, 48
- Moya, A., Suárez, J.C., Amado, P.J., et al. 2005, *A&A*, 432, 289
- Moya, A., & Rodríguez-López, C. 2010, *ApJ*, 710, L7
- Niemczura, E., Morel, T., & Aerts, C. 2009, *A&A*, 506, 213
- Nordström, B., Mayor, M., Andersen, J., et al. 2004, *A&A*, 418, 989
- Otero S. 2007, *Open European Journal on Variable stars*, 72, 10
- Østensen, R.H., Silvotti, R., Charpinet, S., et al. 2010, *MNRAS*, 409, 1470
- Pereira, T. M. D., Suárez, J.C., Lopes, I., et al. 2007, *A&A*, 464, 659
- Perryman, M.A.C., Lindgren, L., Kovalevsky, J., et al. 1997, *A&A*, 323, L49
- Pigulski, A., Pojmański, G., Pilecki, B., & Szczygieł, D.M. 2009, *AcA*, 59, 33
- Poretti, E., Koen, C., Martinez, et al. 1997, *MNRAS*, 292, 621
- Poretti, E., Garido, R., Amado, P.J., et al. 2003, *A&A*, 406, 203
- Poretti, E., Michel, E., Garrido, R., et al. 2009, *A&A*, 506, 85
- Press, W.H., Teukolsky, S.A., Vetterling, W.T., & Flannery, B.P. 1992, *Numerical Recipes, 2nd Edition*, Cambridge University Press, New York, New York
- Prša, A., Batalha, N.M., Slawson, R.W., et al. 2011, *AJ*, 141, 83
- Reegen, P. 2007, *A&A*, 467, 1353
- Reegen, P. 2011, *CoAst*, in press (arXiv:1006.5081)
- Rodríguez, E., & Breger, M. 2001, *A&A*, 366, 178
- Rodríguez, E., López-González, M.J., & López de Coca, P. 2000, *A&AS*, 144, 469
- Rowe, J.F., Matthews, J. M., Cameron, C., et al. 2006, *CoAst*, 148, 34
- Samadi, R., Goupil, M.-J., & Houdek, G. 2002, *A&A*, 395, 563
- Sato, K. & Kuji, S. 1990, *A&AS*, 85, 1069
- Scargle, J. D. 1982, *ApJ*, 263, 835
- Scuflaire, R., Théado, S., Montalbán, J., et al. 2008, *A&AS*, 316, 83
- Shulyak, D., Tsymbal, V., Ryabchikova, et al. 2004, *A&A*, 428, 993
- Skiff, B.A. 2007, *VizieR On-line Data Catalog*, 1, 2023
- Slawson, R.W., Prša, A., Welsh, W.F., et al. 2011, *AJ*, in press (arXiv:1103.1659)
- Smalley, B. & Kupka, F. 1997, *A&A*, 328, 349
- Soubiran, C., Le Campion, J.-F., Cayrel de Strobel, G., & Caillo, A. 2010, *A&A*, 515, 111
- Stephenson, C.B. 1986, *ApJ*, 301, 927
- Strömgren, B. 1966, *ARA&A*, 4, 433
- Suárez, J.C., Moya, A., Martín-Ruiz, S., et al. 2005, *A&A*, 443, 271
- Szabó, R., Szabados, L., Ngeow, C.-C., et al. 2011, *MNRAS*, 413, 2709
- Tango, W.J., Davis, J., Ireland, M., et al. 2006, *MNRAS*, 370, 884
- Trampedach, R., & Stein, R. F. 2011, *ApJ*, 731, A78
- Tsymbal, V. 1996, *ASPC* 108, 198
- Turcotte, S., Richer, J., Michaud, G., & Christensen-Dalsgaard, J. 2000, *A&A*, 360, 603
- Unno, W., Osaki, Y., Ando, H., Saio, H., & Shibahashi, H. 1989, *Nonradial oscillations of stars*, Tokyo: University of Tokyo Press
- Uytterhoeven, K., Telting, J.H., Aerts, C., & Willems, B. 2004, *A&A*, 427, 593
- Uytterhoeven, K., Mathias, P., Poretti, E., et al. 2008, *A&A*, 489, 2213
- Uytterhoeven, K., Szabo, R., Southworth, J., et al. 2010a, *AN*, 331, P30 (arXiv:1003.6089)
- Uytterhoeven, K., Briquet, M., Bruntt, H., et al. 2010b, *AN*, 331, 993
- Vysotsky, A.N. 1958, *Publications of the Leander Mc Cormick Observatory of the University of Virginia, Charlottesville*, 13, V
- Walker, G., Matthews, J., Kuschnig, R., et al. 2003, *PASP*, 115, 1023

- Watson, C.L. 2006, SASS, 25, 47 (AAVSO International Variable Star Index VSX, Watson+, 2006-2010)
- Worley, C.E., & Douglass, G.G. 1997, A&AS, 125, 523
- Wright, C.O., Egan, M.P., Kraemer, K.E., & Price, S.D. 2003, AJ, 125, 359
- Zechmeister, M., & Kürster, M. 2009, A&A, 496, 577
- Zerbi, F.M., Rodríguez, E., Garrido, R., et al. 1997, MNRAS, 292, 43
- Zerbi, F.M., Rodríguez, E., Garrido, R., et al. 1999, MNRAS, 303, 275
- 38205 La Laguna, Tenerife, Spain
e-mail: katrien@iac.es
- ⁴ Laboratorio de Astrofísica Estelar y Exoplanetas, LAEX-CAB (INTA-CSIC), PO BOX 78, 28691 Villanueva de la Cañada, Madrid, Spain
- ⁵ Centro de Astrofísica, Faculdade de Ciências, Universidade do Porto, Rua das Estrelas, 4150-762 Porto, Portugal
- ⁶ Los Alamos National Laboratory, XTD-2, Los Alamos, NM 87545-2345, USA
- ⁷ Instituto de Astrofísica de Andalucía (CSIC), Apartado 3004, 18080 Granada, Spain
- ⁸ LESIA, Observatoire de Paris, CNRS, UPMC, Université Paris-Diderot, 92195 Meudon, France
- ⁹ Valentian International University, Prolongación C/ José Pradas Gallen, s/n 12006 Castellón de la Plana - Spain
- ¹⁰ Astrophysics Group, Keele University, Staffordshire, ST5 5BG, United Kingdom
- ¹¹ Institut für Astronomie, Türkenschanzstraße 17, 1180 Wien, Austria
- ¹² Nicolaus Copernicus Astronomical Center, Bartycka 18, 00-716 Warsaw, Poland
- ¹³ South African Astronomical Observatory, P.O. Box 9, Observatory 7935, South Africa
- ¹⁴ Instytut Astronomiczny, Uniwersytet Wrocławski, Kopernika 11, 51-622 Wrocław, Poland
- ¹⁵ Observatorio Astronómico Nacional, Instituto de Astronomía, INAM, Ensenada B.C., Apdo. Postal 877, México
- ¹⁶ CISAS, Padova University, Via Venezia 15, 35131 Padova, Italy
- ¹⁷ INAF - Astronomical Observatory of Padova, Vicolo Osservatorio 5, 35122 Padova, Italy
- ¹⁸ UMR 6525 H. Fizeau, UNS, CNRS, OCA, Campus Valrose, 06108 Nice Cedex 2, France
- ¹⁹ Instituut voor Sterrenkunde, K.U.Leuven, Celestijnenlaan 200D, 3001 Leuven, Belgium
- ²⁰ Konkoly Observatory of the Hungarian Academy of Sciences, 1525 Budapest PO Box 67, Hungary
- ²¹ INAF - Osservatorio Astronomico di Capodimonte, Via Moiariello 16, 80131 Napoli, Italy
- ²² Lab. d'Astrophysique de Toulouse-Tarbes, Université de Toulouse, CNRS, 57 avenue d'Azereix, 65000 Tarbes, France
- ²³ Thüringer Landessternwarte Tautenburg, 07778 Tautenburg, Germany
- ²⁴ Department of Astronomy, New Mexico State University, Las Cruces, NM 88001, USA
- ²⁵ Astronomical Institute 'Anton Pannekoek', University of Amsterdam, Science Park 904, 1098 XH Amsterdam, The Netherlands
- ²⁶ University of Birmingham, School of Physics and Astronomy, Edgbaston, Birmingham B15 2TT, UK
- ²⁷ Department of Astronomy and Physics, Saint Marys University, Halifax, NS B3H 3C3, Canada
- ²⁸ Observatoire de Genève, Université de Genève, 51 ch. des Maillettes, 1290 Sauverny, Switzerland
- ²⁹ Los Alamos National Laboratory, XCP-6, MS T-087, Los Alamos, NM 87545-2345, USA
- ³⁰ Jeremiah Horrocks Institute of Astrophysics, University of Central Lancashire, Preston PR1 2HE, UK
- ³¹ Royal Observatory of Belgium, Ringlaan 3, 1180 Brussel, Belgium
- ³² Department of Physics and Astronomy, University of Aarhus, bygn. 1520, Ny Munkegade, 8000 Aarhus C., Denmark
- ³³ Department of Astronomy, University of Texas, Austin, TX 78712, USA
- ³⁴ Sydney Institute for Astronomy, School of Physics, A28, The University of Sydney, NSW, 2006, Australia
- ³⁵ Bay Area Environmental Research Inst./NASA Ames Research Center, Moffett Field, CA 94035, USA
- ³⁶ SETI Institute/NASA Ames Research Center, Moffett Field, CA 94035, USA
-
- ¹ Laboratoire AIM, CEA/DSM-CNRS-Université Paris Diderot; CEA, IRFU, SAp, Centre de Saclay, 91191, Gif-sur-Yvette, France
- ² Kiepenheuer-Institut für Sonnenphysik, Schöneckstraße 6, 79104 Freiburg im Breisgau, Germany
- ³ Instituto de Astrofísica de Canarias, 38200 La Laguna, Tenerife, Spain; Departamento de Astrofísica, Universidad de La Laguna,

Table 1. Database of 750 *Kepler* A-F type stars

KIC ID	RA (J2000)	DEC (J2000)	Kp	Spectral Type	Name	Variable	N Datapoints	ΔT (d)	δT (d)	Quarters LC	Quarters SC
01162150	19 24 53.76	+36 53 13.6	11.2	binary	44 232	321.5	248.4	Q0-Q1	Q4.3
01294756	19 25 41.35	+36 58 16.6	9.1	A2 ³⁵	BD+36 3554	binary	15 856	44.4	1.2	Q1	Q0
01432149	19 25 29.23	+37 05 57.0	11.2	...	TYC2666-352-1	binary ¹	41 318	79.6	4.5	Q0-Q1	Q2.1
01571152	19 23 40.56	+37 09 54.8	9.3	F0 ³⁵	BD+36 3535	binary	43 057	79.6	5.1	Q0-Q1	Q2.1
01571717	19 24 10.54	+37 06 34.5	11.2	...	TYC 2666-579-1	...	44 418	321.5	248.3	Q0-Q1	Q4.3
01573064	19 25 24.07	+37 06 21.2	12.8	460	9.5	0.0	Q0	...
01718594	19 23 19.37	+37 16 21.3	10.4	...	TYC 2666-751-1	...	40 062	137.7	66.5	Q0-Q1	Q2.3
01995489	19 04 33.82	+37 29 48.7	12.2	461	9.5	0.0	Q0-Q1	...
02020966	19 31 26.64	+37 27 26.9	12.1	457	9.5	0.0	Q0-Q1	...
02162283	19 27 34.03	+37 33 24.6	9.6	F2 ³⁵	BD+37 3464	binary ³⁸	43 716	79.6	4.5	Q0-Q1	Q2.1
02163434	19 28 33.84	+37 34 46.3	13.4	461	9.5	0.0	Q0	...
02166218	19 30 57.05	+37 30 35.8	9.5	F0 ³⁵	BD+37 3490	...	39 459	137.7	66.5	Q0-Q1	Q2.3
02168333	19 32 44.59	+37 35 36.2	10.1	...	TYC 3135-203-1	...	15 857	44.4	1.2	Q1	Q0
02300165	19 23 16.78	+37 39 59.5	11.1	...	TYC3134-1646-1	...	49 244	44.2	1.2	Q0	Q1
02303365	19 26 08.76	+37 41 00.0	11.1	...	TYC 3134-205-1	...	43 946	79.6	4.5	Q0-Q1	Q2.1
02306469	19 28 52.06	+37 36 41.4	12.6	462	9.5	0.0	Q0	...
02306716	19 29 03.79	+37 41 19.2	12.0	461	9.5	0.0	Q0	...
02310479	19 32 24.58	+37 40 21.6	10.8	460	9.5	0.0	Q0	...
02311130	19 33 00.07	+37 39 41.6	11.9	461	9.5	0.0	Q0	...
02423932	19 05 59.69	+37 46 42.6	13.0	462	9.5	0.0	Q0-Q1	...
02439660	19 22 17.76	+37 43 23.2	11.6	40 046	228.8	158.5	Q0-Q1	Q3.3
02443055	19 25 31.08	+37 46 05.9	13.4	462	9.5	0.0	Q0	...
02444598	19 26 53.83	+37 44 14.9	12.3	2 070	44.2	1.6	Q0-Q1	...
02556297	19 05 53.09	+37 50 27.9	12.5	460	9.5	0.0	Q0	...
02556387	19 06 01.30	+37 53 10.6	11.1	2 086	44.2	1.2	Q0-Q1	...
02557115	19 06 59.52	+37 49 16.3	12.6	binary ³⁸	460	9.5	0.0	Q0	...
02557430	19 07 22.87	+37 48 57.2	11.5	binary ³⁶	38 573	79.6	4.5	Q0-Q1	Q2.1
02558273	19 08 24.84	+37 53 38.9	11.3	38 464	292.5	219.4	Q0-Q1	Q4.2
02568519	19 20 03.94	+37 52 27.4	11.3	...	BD+37 3418a	...	59 804	321.4	4.9	Q0-Q4	Q4.1
02569639	19 20 46.80	+37 50 13.8	10.6	...	CI*NGC 6791 SBG 5986	NGC 6791	39 847	228.8	158.6	Q0-Q1	Q3.3
02571868	19 22 17.62	+37 53 08.4	8.7	A0 ³⁵	HD 182271	...	40 134	228.8	158.5	Q0-Q1	Q3.3
02572386	19 22 45.89	+37 53 02.9	13.3	2 073	44.2	1.2	Q0-Q1	...
02575161	19 25 17.66	+37 49 25.2	10.9	F0 ³⁵	BD+37 3452	binary	1 999	44.2	2.7	Q0-Q1	...
02578251	19 27 51.65	+37 49 54.1	11.7	2 021	44.2	2.3	Q0-Q1	...
02583658	19 32 34.58	+37 51 32.0	12.6	463	9.5	0.0	Q0	...
02584202	19 33 03.19	+37 48 57.9	11.8	2 065	44.2	1.2	Q0-Q1	...
02584908	19 33 41.47	+37 50 41.7	10.8	binary ³⁸	38 098	292.5	219.3	Q0-Q1	Q4.2
02694337	19 05 08.62	+37 54 34.8	10.4	...	TYC 3120-1608-1	...	40 233	137.7	66.4	Q0-Q1	Q2.3
02707479	19 20 33.10	+37 59 54.0	11.2	...	TYC 3134-833-1	...	43 921	79.6	4.5	Q0-Q1	Q2.1
02718596	19 30 35.78	+37 55 51.5	13.4	464	9.5	0.0	Q0	...
02720582	19 32 21.19	+37 59 09.0	11.4	44 183	321.5	248.4	Q0-Q1	Q4.3
02834796	19 06 47.62	+38 04 32.4	12.5	461	9.5	0.0	Q0	...
02835795	19 08 06.53	+38 00 26.4	12.6	2 070	44.2	1.4	Q0-Q1	...
02853280	19 26 27.98	+38 02 05.2	11.0	...	TYC 3134-92-1	...	44 400	321.5	248.3	Q0-Q1	Q4.3
02855687	19 28 31.20	+38 01 40.7	10.3	...	TYC 3134-10-1	...	462	9.5	0.0	Q0	...
02860123	19 32 16.42	+38 03 36.6	13.7	463	9.5	0.0	Q0	...
02969151	19 02 17.76	+38 11 27.8	11.9	460	9.5	0.0	Q0	...
02970244	19 03 42.34	+38 08 14.2	12.5	463	9.5	0.0	Q0	...

Table 1. continued.

KIC ID	RA (J2000)	Dec (J2000)	Kp	Spectral Type	Name	Variable	N Datapoints	ΔT (d)	δT (d)	Quarters LC	Quarters SC
02972401	19 06 35.86	+38 08 59.3	13.5	460	9.5	0.0	Q0	...
02975832	19 11 01.99	+38 08 56.6	12.6	2 090	44.2	1.2	Q0-Q1	...
02987660	19 23 57.46	+38 06 51.7	8.0	F2 ¹⁶ ,A3 ³⁵	HD 182634	δ Sct ²	45 196	169.8	95.2	Q0-Q1	Q3.1
02989746	19 25 49.34	+38 09 13.6	13.2	2 078	44.2	1.2	Q0-Q1	...
02995525	19 30 50.23	+38 11 41.6	13.2	464	9.5	0.0	Q0	...
02997802	19 32 48.14	+38 08 35.9	13.2	2 062	44.2	1.2	Q0-Q1	...
03097912	19 03 36.72	+38 12 08.2	9.4	A5 ³⁵	BD+37 3324	binary	45 378	109.5	35.3	Q0-Q1	Q2.2
03111451	19 20 37.54	+38 15 08.2	13.5	463	9.5	0.0	Q0	...
03119604	19 28 30.50	+38 16 09.4	10.7	...	TYC 3134-70-1	...	47 547	262.8	187.3	Q0-Q1	Q4.1
03119825	19 28 42.19	+38 16 47.1	11.0	2 090	44.2	1.2	Q0-Q1	...
03215800	19 01 03.65	+38 18 24.3	13.2	2 070	44.2	1.6	Q0-Q1	...
03217554	19 03 51.02	+38 21 28.8	9.6	A5 ³⁵	BD+38 3415	binary ^o	40 426	137.7	66.3	Q0-Q1	Q2.3
03218637	19 05 31.68	+38 20 07.4	10.6	...	TYC 3120-564-1	...	40 072	228.8	158.5	Q0-Q1	Q3.3
03219256	19 06 27.53	+38 21 13.9	8.3	A3 ³⁵	HD 178306	...	58 430	321.4	32.9	Q0-Q4	Q3.2
03220783	19 08 43.49	+38 19 32.8	13.6	460	9.5	0.0	Q0	...
03222364	19 10 59.54	+38 21 19.9	11.1	...	TYC 3121-1831-1	...	2 063	44.2	1.2	Q0-Q1	...
03230227	19 20 27.02	+38 23 59.5	9.0	A5 ³⁵	HD 181850	binary ³⁸	48 466	44.2	1.2	Q0	Q1
03231406	19 21 43.73	+38 18 53.3	10.5	...	TYC 3134-1188-1	...	45 158	169.8	95.2	Q0-Q1	Q3.1
03240556	19 31 15.98	+38 18 46.4	10.3	...	TYC 3135-607-1	...	45 394	109.5	35.3	Q0-Q1	Q2.2
03245420	19 35 58.61	+38 18 21.2	10.6	...	TYC 3135-396-1	...	40 135	228.8	158.5	Q0-Q1	Q3.3
03248627	19 38 54.29	+38 21 04.1	12.3	463	9.5	0.0	Q0	...
03327681	19 08 12.48	+38 29 02.3	11.3	...	TYC 3120-1051-1	binary [*]	44 399	321.5	248.3	Q0-Q1	Q4.3
03331147	19 13 07.75	+38 27 34.3	10.1	...	TYC 3121-1178-1	...	15 791	44.4	1.2	Q1	Q0
03337002	19 20 04.25	+38 24 41.0	10.8	...	TYC 3134-2162-1	binary	38 681	292.5	219.3	Q0-Q1	Q4.2
03347643	19 31 16.22	+38 24 02.9	8.0	A2 ³⁵	HD 184105	...	45 121	109.0	35.4	Q0-Q1	Q2.2
03348390	19 32 00.62	+38 24 18.0	11.4	...	TYC 3135-135-1	pulsating ³	40 286	137.7	66.3	Q0-Q1	Q2.3
03354022	19 37 33.10	+38 27 51.8	12.1	461	9.5	0.0	Q0	...
03355066	19 38 29.66	+38 25 24.9	13.6	464	9.5	0.0	Q0	...
03424493	19 00 37.54	+38 30 20.2	9.6	A5 ³⁵	BD+38 3391	...	40 427	137.7	66.3	Q0-Q1	Q2.3
03425802	19 02 50.26	+38 34 04.0	11.2	...	TYC 3120-1011-1	...	43 321	79.6	4.5	Q0-Q1	Q2.1
03427144	19 04 53.21	+38 35 24.4	13.4	460	9.5	0.0	Q0	...
03427365	19 05 12.86	+38 32 46.6	13.6	462	9.5	0.0	Q0	...
03429637	19 08 38.04	+38 30 31.8	7.7	kF2hA9mF3 ¹⁸	HD 178875	binary, Am star	14 006	310.5	4.5	Q1-Q4	...
03437940	19 19 22.01	+38 31 49.4	8.5	F0 ³⁵	HD 181569	...	58 013	321.4	32.9	Q0-Q4	Q3.2
03440495	19 22 12.36	+38 30 32.6	10.5	...	TYC 3134-632-1	...	45 140	169.8	95.2	Q0-Q1	Q3.1
03449373	19 31 35.98	+38 30 34.6	12.7	2 062	44.2	1.2	Q0-Q1	...
03449625	19 31 49.30	+38 34 50.6	13.4	2 034	44.2	1.9	Q0-Q1	...
03453494	19 35 31.73	+38 34 54.4	9.6	A5 ³⁵	BD+38 3666	...	40 408	137.7	66.3	Q0-Q1	Q2.3
03457434	19 39 18.86	+38 32 18.4	12.4	462	9.5	0.0	Q0	...
03458097	19 39 53.33	+38 33 25.9	11.7	2 086	44.2	1.2	Q0-Q1	...
03458318	19 40 03.91	+38 35 51.6	12.8	2 090	44.2	1.2	Q0-Q1	...
03525951	19 00 34.73	+38 40 26.4	12.9	462	9.5	0.0	Q0	...
03528578	19 04 56.78	+38 38 56.5	13.5	461	9.5	0.0	Q0	...
03539153	19 19 32.71	+38 39 04.9	11.4	...	TYC 3121-379-1	...	39 889	137.7	66.3	Q0-Q1	Q2.3
03546061	19 27 13.94	+38 38 19.2	10.9	462	9.5	0.0	Q0	...
03558145	19 39 13.06	+38 38 05.1	11.3	...	TYC 3135-189-1	...	43 958	310.5	248.3	Q1	Q4.3
03629080	19 04 07.22	+38 42 20.2	13.5	459	9.5	0.0	Q0	...
03633693	19 11 21.65	+38 43 48.4	12.6	463	9.5	0.0	Q0	...

Table 1. continued.

KIC ID	RA (J2000)	Dec (J2000)	Kp	Spectral Type	Name	Variable	N Datapoints	ΔT (d)	δT (d)	Quarters LC	Quarters SC
03634384	19 12 20.28	+38 43 34.1	11.2	43 854	79.6	4.5	Q0-Q1	Q2.1
03643717	19 23 43.75	+38 47 30.2	12.9	463	9.5	0.0	Q0	...
03644116	19 24 10.73	+38 43 01.1	10.9	...	TYC 3134-1328-1	...	38 681	292.5	219.3	Q0-Q1	Q4.2
03655513	19 35 53.30	+38 47 03.7	10.5	...	TYC 3135-142-1	...	2 090	44.2	1.2	Q0-Q1	...
03655608	19 35 59.16	+38 44 45.3	11.4	43 807	321.5	248.3	Q0-Q1	Q4.3
03663141	19 42 39.17	+38 43 05.7	13.2	binary*	2 067	44.2	1.6	Q0-Q1	...
03733735	19 09 01.92	+38 53 59.6	8.4	F5 ³⁵	HD 178971	...	57 376	321.4	35.3	Q0-Q4	Q2.2
03758717	19 37 42.14	+38 51 20.4	11.8	...	TYC 3135-360-1	...	2 061	44.2	1.6	Q0-Q1	...
03759814	19 38 46.25	+38 51 32.5	10.7	G0 ³⁵	TYC 3135-77-1	...	45 382	109.5	35.3	Q0-Q1	Q2.2
03760002	19 38 58.01	+38 52 43.6	10.6	...	TYC 3135-708-1	...	46 068	200.7	126.4	Q0-Q1	Q3.2
03760826	19 39 48.22	+38 53 47.9	8.8	A1V ¹⁷	HD 185894	...	464	9.5	0.0	Q0	...
03761641	19 40 30.24	+38 51 59.9	11.0	A0 ¹⁸	HD 225341	...	15 851	44.4	1.2	Q1	Q0
03836911	19 08 30.05	+38 54 42.7	12.5	2 089	44.2	1.2	Q0-Q1	...
03850810	19 26 24.72	+38 58 32.7	10.0	...	TYC 3134-3-1	...	15 860	44.4	1.2	Q1	Q0
03851151	19 26 47.54	+38 56 16.7	9.8	A2 ³⁵	BD+38 3594	...	15 771	44.4	1.4	Q1	Q0
03868032	19 43 07.58	+38 56 49.9	10.4	A0 ¹⁸	HD 225504	...	44 909	169.8	95.3	Q0-Q1	Q3.1
03941283	19 09 43.68	+39 02 45.6	10.3	...	TYC 3120-867-1	...	45 449	109.5	35.3	Q0-Q1	Q2.2
03942911	19 12 16.27	+39 04 16.9	10.8	...	TYC 3121-719-1	...	38 658	292.5	219.3	Q0-Q1	Q4.2
03966357	19 38 24.10	+39 04 58.9	11.2	45 196	109.5	35.3	Q0-Q1	Q2.2
03970729	19 42 18.60	+39 00 46.8	11.5	...	TYC 3136-1008-1	...	45 175	169.8	95.2	Q0-Q1	Q3.1
04035667	18 58 29.57	+39 10 56.7	10.0	...	TYC 3119-347-1	...	15 842	44.4	1.2	Q1	Q0
04044353	19 11 00.82	+39 10 15.3	9.8	A2 ³⁵	BD+38 3465	...	15 856	44.4	1.2	Q1	Q0
04048488	19 16 32.78	+39 10 30.1	11.6	A5 ³⁵	...	binary	39 583	126.8	66.5	Q1	Q2.3
04048494	19 16 33.07	+39 10 28.7	9.5	A5 ³⁵	BD+38 3512	binary	45 465	109.5	35.3	Q0-Q1	Q2.2
04069477	19 38 38.52	+39 08 25.2	11.2	...	TYC 3135-485-1	...	44 118	321.5	248.3	Q0-Q1	Q4.3
04075519	19 43 50.02	+39 08 48.5	12.5	F0 ¹⁸	HD 225644	...	2 070	44.2	1.6	Q0-Q1	...
04077032	19 45 03.17	+39 11 26.0	9.7	F0 ³⁵	43 905	79.6	4.5	Q0-Q1	Q2.1
04144300	19 11 26.11	+39 12 18.0	12.3	2 075	44.2	1.2	Q0-Q1	...
04150611	19 18 58.20	+39 16 01.4	7.9	A5V ¹⁷ ,A2 ³⁵	HD 181469	binary ³⁸	43 160	109.4	35.3	Q0-Q1	Q2.2
04160876	19 29 29.16	+39 13 17.6	10.2	...	TYC 3134-81-1	...	45 235	109.5	35.4	Q0-Q1	Q2.2
04164363	19 32 50.54	+39 14 26.5	11.4	40 285	137.7	66.3	Q0-Q1	Q2.3
04168574	19 36 41.02	+39 15 17.9	10.3	...	TYC 3135-437-1	...	40 321	137.7	66.3	Q0-Q1	Q2.3
04170631	19 38 33.07	+39 14 18.7	10.8	...	TYC 3135-641-1	...	38 628	292.5	219.3	Q0-Q1	Q4.2
04180199	19 46 02.35	+39 12 19.7	10.1	A7 ¹⁸	HD 225718	...	15 829	44.4	1.2	Q1	Q0
04252757	19 15 35.28	+39 20 07.2	10.9	...	TYC 3121-1037-1	...	38 629	292.5	219.3	Q0-Q1	Q4.2
04269337	19 33 12.96	+39 22 23.8	10.9	A8II ³⁵	...	binary	39 692	126.8	66.3	Q1	Q2.3
04281581	19 43 57.00	+39 20 47.4	9.4	A2 ¹⁸	HD 225569	...	45 460	109.5	35.3	Q0-Q1	Q2.2
04383117	19 43 34.10	+39 24 24.0	11.0	A3 ¹⁸	HD 225535	...	49 453	44.2	1.2	Q0	Q1
04476836	19 39 31.42	+39 34 57.8	11.5	45 434	109.5	35.3	Q0-Q1	Q2.2
04480321	19 42 38.38	+39 33 40.4	10.3	A3 ¹⁸	HD 225479	...	45 390	109.5	35.3	Q0-Q1	Q2.2
04488840	19 49 27.58	+39 32 15.3	11.4	...	TYC 3140-568-1	...	40 338	137.7	66.3	Q0-Q1	Q2.3
04550962	19 14 05.11	+39 36 56.9	10.5	...	TYC 3125-3570-1	...	40 112	228.8	158.5	Q0-Q1	Q3.3
04556345	19 20 28.85	+39 36 36.4	10.8	...	TYC 3138-1615-1	...	47 527	262.8	187.3	Q0-Q1	Q4.1
04570326	19 36 09.02	+39 37 43.0	9.8	...	BD+39 3858	variable ^{4,38}	14 474	321.5	4.5	Q0-Q4	...
04588487	19 51 21.82	+39 41 37.5	10.9	A0 ¹⁸	HD 226196	...	43 254	310.5	248.4	Q1	Q4.3
04647763	19 18 41.14	+39 42 26.7	10.8	...	TYC 3125-307-1	...	45 196	109.5	35.4	Q0-Q1	Q2.2
04649476	19 20 35.90	+39 47 01.5	9.4	A2 ³⁵	BD+39 3732	...	45 459	109.5	35.3	Q0-Q1	Q2.2

Table 1. continued.

KIC ID	RA (J2000)	Dec (J2000)	Kp	Spectral Type	Name	Variable	N Datapoints	ΔT (d)	δT (d)	Quarters LC	Quarters SC
04671225	19 43 40.08	+39 45 33.1	10.0	A7 ¹⁸	HD 225544	...	54 194	137.9	66.3	Q1	Q0,Q2.3
04677684	19 48 44.71	+39 47 32.5	10.2	A0 ¹⁸	HD 225950	...	40 407	137.7	66.3	Q0-Q1	Q2.3
04758316	19 39 41.69	+39 48 04.6	11.1	...	TYC 3139-1185-1	...	47 354	262.8	187.3	Q0-Q1	Q4.1
04768677	19 48 23.95	+39 52 58.0	11.2	A ¹⁸	HD 225906	...	40 676	79.6	5.1	Q0-Q1	Q2.1
04840675	19 32 57.94	+39 58 45.3	9.6	...	TYC 3139-1403-1	...	40 137	228.8	158.5	Q0-Q1	Q3.3
04850899	19 43 04.49	+39 59 49.6	7.0	F0IV ¹⁹ ,A5 ³⁵	HD 186505	...	451	9.5	0.0	Q0	...
04856630	19 47 46.58	+39 58 56.3	11.4	40 317	137.7	66.3	Q0-Q1	Q2.3
04857678	19 48 44.06	+39 54 60.0	7.0	F0 ³⁵	HD 187523	...	14 420	321.5	4.7	Q0-Q4	...
04863077	19 53 13.85	+39 56 48.3	11.1	A0 ¹⁸	HD 226381	...	49 510	44.2	1.2	Q0	Q1
04909697	19 08 48.00	+40 04 06.0	10.7	...	TYC 3124-2306-1	binary	47 579	262.8	187.3	Q0-Q1	Q4.1
04919818	19 22 10.66	+40 03 17.1	10.7	...	TYC 3138-36-1	...	47 370	262.8	187.3	Q0-Q1	Q4.1
04920125	19 22 35.04	+40 03 47.2	11.1	F0 ³⁵	BD+39 3745	...	49 479	44.2	1.2	Q0	Q1
04936524	19 40 48.31	+40 02 28.9	13.1	49 504	44.2	1.2	Q0	Q1
04937257	19 41 27.31	+40 04 54.8	13.5	10 188	228.7	4.9	Q0-Q3	...
04989900	18 55 25.66	+40 10 37.7	6.9	A2 ³⁵	HD 175841	...	37 933	25.9	0.0	...	Q3.3
05024150	19 41 06.58	+40 10 19.6	13.2	48 935	33.4	0.0	...	Q1
05024454	19 41 17.02	+40 10 34.8	13.7	...	NGC 6819 609	NGC 6819	48 970	33.4	0.0	...	Q1
05024455	19 41 17.02	+40 06 04.0	14.8	...	NGC 6819 960	NGC 6819	48 955	33.4	0.0	...	Q1
05024456	19 41 17.04	+40 10 51.9	11.1	...	NGC 6819 550	NGC 6819	13 835	309.7	4.9	Q1-Q4	...
05024750	19 41 26.59	+40 11 41.8	11.2	...	NGC 6819 975	NGC 6819	10 327	228.7	4.5	Q0-Q3	...
05038228	19 52 43.85	+40 10 56.0	11.4	44 407	321.5	248.3	Q0-Q1	Q4.3
05080290	18 59 19.10	+40 12 54.8	9.5	F8 ³⁵	BD+40 3547	...	41 935	79.6	5.0	Q0-Q1	Q2.1
05088308	19 13 27.19	+40 14 32.1	8.7	F5 ³⁵	HD 180099	binary ³⁸	40 304	137.7	66.3	Q0-Q1	Q2.3
05105754	19 34 31.15	+40 17 36.6	11.4	...	TYC 3139-2577-1	...	40 240	137.7	66.3	Q0-Q1	Q2.3
05112786	19 41 23.69	+40 12 35.5	11.5	...	NGC 6819 972	NGC 6819	14 461	321.5	4.5	Q0-Q4	...
05112932	19 41 28.99	+40 13 15.5	13.2	...	NGC 6819 995	NGC 6819	48 925	33.4	0.0	...	Q1
05113797	19 42 12.62	+40 17 46.0	9.1	A3 ¹⁸	HD 225447	...	43 613	79.6	4.5	Q0-Q1	Q2.1
05164767	18 53 54.19	+40 19 25.6	7.8	F2IV ²⁰	HD 175537	...	14 422	321.5	4.6	Q0-Q4	...
05180796	19 19 49.58	+40 19 18.7	10.2	...	TYC 3125-269-1	...	44 855	109.5	35.4	Q0-Q1	Q2.2
05197256	19 38 33.82	+40 19 25.7	11.0	...	TYC 3139-1882-1	binary	44 430	321.5	248.3	Q0-Q1	Q4.3
05199464	19 40 45.48	+40 22 03.1	14.8	48 927	33.4	0.0	...	Q1
05200084	19 41 20.66	+40 23 31.7	9.2	A0 ³⁹	HD 225410	binary*	41 302	79.6	5.1	Q0-Q1	Q2.1
05201088	19 42 12.05	+40 18 02.8	13.6	A3 ³⁵	48 950	33.4	0.0	...	Q1
05209712	19 49 21.98	+40 21 13.2	11.3	A2 ³⁹	HD 226009	...	45 346	109.5	35.3	Q0-Q1	Q2.2
05217733	19 55 44.76	+40 23 30.3	7.4	B1V ²² ,B2II ²¹	HD 188891	binary	42 261	28.9	0.0	...	Q4.3
05219533	19 57 09.91	+40 22 50.5	9.2	A2 ³⁹ ,kA2hA8mA8 ²³	HD 226766	binary	49 385	44.2	1.2	Q0	Q1
05272673	19 24 19.87	+40 24 27.6	10.4	...	TYC 3138-994-1	...	45 175	169.8	95.2	Q0-Q1	Q3.1
05294571	19 47 12.53	+40 28 02.4	10.5	F2 ³⁹	HD 225808	...	47 206	262.8	187.3	Q0-Q1	Q4.1
05296877	19 49 04.75	+40 24 36.6	12.3	...	HAT 199-27597	variable ^{5,38}	28 722	321.9	75.3	Q0-Q4	Q0
05356349	19 19 36.10	+40 35 07.3	8.1	A0 ³⁵	HD 181680	binary	45 292	189.7	126.4	Q1	Q3.2
05371747	19 37 43.49	+40 35 38.4	10.5	F ³⁵	BD+40 3811	...	45 893	200.7	126.4	Q0-Q1	Q3.2
05391416	19 55 14.78	+40 33 12.8	10.2	A7 ³⁹	HD 226570	...	45 456	109.5	35.3	Q0-Q1	Q2.2
05428254	18 56 52.80	+40 37 47.4	10.5	...	TYC 3123-1722-1	...	46 080	200.7	126.4	Q0-Q1	Q3.2
05436432	19 11 27.91	+40 41 26.6	9.0	A2 ³⁵	HD 179618	...	49 499	44.2	1.2	Q0	Q1
05437206	19 12 43.56	+40 37 57.1	8.4	A2 ³⁵	HD 179936	...	46 078	200.7	126.4	Q0-Q1	Q3.2
05446068	19 24 18.10	+40 38 58.8	9.7	...	BD+40 3704	binary	43 937	79.6	4.5	Q0-Q1	Q2.1
05473171	19 52 17.88	+40 41 10.1	9.0	A2 ³⁹	HD 226284	...	15 859	44.4	1.2	Q1	Q0

Table 1. continued.

KIC ID	RA (J2000)	Dec (J2000)	Kp	Spectral Type	Name	Variable	N Datapoints	ΔT (d)	δT (d)	Quarters LC	Quarters SC
05474427	19 53 21.14	+40 39 12.9	11.4	...	TYC 3141-2904-1	...	44 428	321.5	248.3	Q0-Q1	Q4.3
05476495	19 54 53.11	+40 36 55.2	10.2	A3 ³⁹	HD 226528	...	42 944	79.6	4.6	Q0-Q1	Q2.1
05476864	19 55 09.22	+40 39 20.7	11.5	41 682	68.6	5.1	Q1	Q2.1
05513861	18 57 24.53	+40 42 53.0	11.6	...	TYC 3123-2012-1	binary ³⁸	45 178	109.5	113.0	Q0-Q1	Q2.2
05603049	19 03 43.90	+40 48 17.2	11.2	...	TYC 3124-1423-1	...	44 428	321.5	248.3	Q0-Q1	Q4.3
05630362	19 39 19.25	+40 53 58.9	10.5	...	TYC 3139-1246-1	...	40 134	228.8	158.5	Q0-Q1	Q3.3
05632093	19 41 04.78	+40 53 17.4	10.9	A ³⁹	HD 225391	...	15 846	44.4	1.2	Q1	Q0
05641711	19 49 38.38	+40 53 49.8	10.4	F0 ³⁹	HD 226029	...	40 404	137.7	66.3	Q0-Q1	Q2.3
05709664	19 32 25.58	+40 54 03.0	11.3	...	TYC 3139-826-1	...	45 456	109.5	35.3	Q0-Q1	Q2.2
05722346	19 45 32.76	+40 56 41.9	11.2	...	TYC 3140-925-1	...	47 575	262.8	187.3	Q0-Q1	Q4.1
05724048	19 47 00.46	+40 56 10.0	11.4	44 067	321.5	248.4	Q0-Q1	Q4.3
05724440	19 47 19.78	+40 59 39.6	7.9	A5 ³⁵	HD 187234	...	57 568	321.5	4.5	Q0-Q4	Q3.1
05724810	19 47 39.24	+40 54 41.5	10.9	A7 ³⁹	HD 225842	binary*	15 856	44.4	1.2	Q1	Q0
05768203	18 51 36.46	+41 05 27.7	10.8	...	TYC 3123-19-1	...	45 448	109.5	35.3	Q0-Q1	Q2.2
05772411	18 59 59.59	+41 00 54.3	10.6	binary	37 713	292.5	219.9	Q0-Q1	Q4.2
05774557	19 04 01.78	+41 01 49.6	11.0	...	TYC 3124-2058-1	...	44 425	321.5	248.3	Q0-Q1	Q4.3
05785707	19 20 31.70	+41 04 48.4	9.0	A2 ³⁵	HD 181902	...	43 397	79.6	4.5	Q0-Q1	Q2.1
05810113	19 47 39.34	+41 01 32.5	11.6	binary ³⁸	45 383	109.5	35.3	Q0-Q1	Q2.2
05857714	18 58 46.37	+41 09 56.0	11.2	...	TYC 3123-742-1	...	38 656	292.5	219.3	Q0-Q1	Q4.2
05880360	19 32 23.26	+41 08 09.2	8.8	A0 ³⁵	HD 184380	...	49 507	44.2	1.2	Q0	Q1
05940273	18 55 48.17	+41 15 40.5	10.5	F0 ³⁵	BD+41 3185	...	40 102	228.8	158.5	Q0-Q1	Q3.3
05954264	19 19 27.19	+41 13 25.6	8.2	F0 ³⁵	HD 181654	...	57 187	321.5	35.3	Q0-Q4	Q2.2
05965837	19 34 06.50	+41 15 03.3	9.2	F2 ³⁵	BD+40 3786	variable ⁶	24 079	228.5	4.5	Q0-Q3	Q0
05980337	19 48 24.29	+41 16 51.3	10.1	F0 ³⁹	HD 225912	binary	43 796	79.0	5.0	Q0-Q1	Q2.1
05988140	19 55 10.03	+41 17 10.1	8.9	F0 ³⁷	HD 188774	...	10 332	321.5	93.4	Q0-Q4	...
06032730	19 14 22.30	+41 18 26.4	8.7	A2 ³⁷	HD 180349	...	46 077	200.7	126.4	Q0-Q1	Q3.2
06067817	19 53 54.89	+41 23 33.4	10.2	A3 ³⁹	HD 226443	...	43 924	79.6	4.5	Q0-Q1	Q2.1
06123324	19 27 01.51	+41 29 09.1	8.7	F0 ³⁵	HD 183281	binary	40 431	137.7	66.3	Q0-Q1	Q2.3
06141372	19 46 37.94	+41 28 33.6	11.1	...	HAT 199-04866	variable	44 408	321.5	248.3	Q0-Q1	Q4.3
06142919	19 47 55.85	+41 26 58.9	10.6	...	TYC 3144-608-1	binary*	40 021	228.8	158.5	Q0-Q1	Q3.3
06187665	19 01 38.06	+41 30 26.9	11.5	...	TYC 3128-1790-1	...	45 465	109.5	35.3	Q0-Q1	Q2.2
06199731	19 20 31.94	+41 35 19.5	10.9	...	TYC 3142-175-1	...	15 820	44.4	1.2	Q1	Q0
06268890	19 02 28.39	+41 36 11.4	11.2	...	TYC 3128-2125-1	...	45 464	109.5	35.3	Q0-Q1	Q2.2
06279848	19 20 19.44	+41 39 39.9	8.9	F0 ³⁵	HD 181877	...	2 087	44.2	1.2	Q0-Q1	...
06289468	19 33 00.60	+41 39 13.4	9.4	A2 ³⁵	BD+41 3389	...	45 438	109.5	35.3	Q0-Q1	Q2.2
06301745	19 45 51.36	+41 37 54.0	10.9	...	TYC 3144-787-1	...	45 248	109.5	35.4	Q0-Q1	Q2.2
06381306	19 46 36.34	+41 44 16.9	8.7	A0 ³⁵	HD 187141	...	39 980	228.8	158.5	Q0-Q1	Q3.3
06432054	19 12 09.53	+41 50 15.3	8.2	F0 ³⁵	HD 179837	...	46 058	200.7	126.4	Q0-Q1	Q3.2
06440930	19 24 33.79	+41 53 24.0	10.6	...	TYC 3142-1367-1	...	45 857	200.7	126.4	Q0-Q1	Q3.2
06443122	19 27 36.34	+41 49 39.9	11.2	...	TYC 3142-1661-1	...	45 463	109.5	35.3	Q0-Q1	Q2.2
06446951	19 32 35.93	+41 53 32.3	11.3	...	TYC 3143-1362-1	...	44 431	321.5	248.3	Q0-Q1	Q4.3
06448112	19 34 02.57	+41 53 03.1	10.0	A2 ³⁵	BD+41 3395	...	15 813	44.4	1.2	Q1	Q0
06462033	19 48 33.72	+41 49 49.3	10.7	...	TYC 3144-646-1	...	40 066	228.8	158.5	Q0-Q1	Q3.3
06500578	18 53 24.94	+41 59 16.9	10.8	...	TYC 3127-1666-1	...	38 671	292.5	219.3	Q0-Q1	Q4.2
06509175	19 09 08.64	+41 56 59.8	10.0	A2 ³⁵	BD+41 3248	...	15 859	44.4	1.2	Q1	Q0
06519869	19 24 03.26	+41 56 54.4	10.5	...	TYC 3142-733-1	...	44 879	169.8	95.2	Q0-Q1	Q3.1
06586052	18 58 02.14	+42 01 05.7	11.3	45 465	109.5	35.3	Q0-Q1	Q2.2

Table 1. continued.

KIC ID	RA (J2000)	Dec (J2000)	Kp	Spectral Type	Name	Variable	N Datapoints	ΔT (d)	δT (d)	Quarters LC	Quarters SC
06587551	19 00 54.70	+42 02 23.9	9.8	A0 ³⁵	BD+41 3207	...	15 844	44.4	1.2	Q1	Q0
06590403	19 05 53.35	+42 02 14.5	10.6	...	TYC 3128-2036-1	...	40 133	228.8	158.5	Q0-Q1	Q3.3
06606229	19 27 25.34	+42 00 31.0	11.1	...	TYC 3142-717-1	...	47 569	262.7	187.3	Q0-Q1	Q4.1
06614168	19 36 27.50	+42 04 26.8	11.4	40 405	137.7	66.3	Q0-Q1	Q2.3
06629106	19 50 38.40	+42 01 23.2	10.1	F0 ³⁹	HD 226135	...	15 861	44.4	1.2	Q1	Q0
06668729	18 53 50.62	+42 10 15.8	8.6	A2 ³⁵	HD 175536	...	46 078	200.7	126.4	Q0-Q1	Q3.2
06670742	18 57 19.82	+42 07 37.5	9.3	A5 ³⁵	BD+41 3195	...	43 924	79.6	4.5	Q0-Q1	Q2.1
06678614	19 10 46.30	+42 06 40.7	10.8	...	TYC 3129-800-1	...	37 918	292.5	219.4	Q0-Q1	Q4.2
06694649	19 31 01.20	+42 10 11.2	10.4	binary	45 188	169.8	95.2	Q0-Q1	Q3.1
06756386	18 55 54.24	+42 12 37.9	8.7	A2 ³⁵	HD 175939	...	15 860	44.4	1.2	Q1	Q0
06756481	18 56 01.87	+42 13 34.7	9.3	F0 ³⁵	BD+42 3197	...	43 844	79.6	4.5	Q0-Q1	Q2.1
06761539	19 05 03.58	+42 13 18.7	10.3	...	TYC 3128-1341-1	...	45 451	109.5	35.3	Q0-Q1	Q2.2
06776331	19 25 59.47	+42 16 45.3	10.9	...	TYC 3142-511-1	...	44 411	321.5	248.3	Q0-Q1	Q4.3
06790335	19 41 30.74	+42 12 11.1	10.5	...	TYC 3144-1756-1	...	46 068	200.7	126.4	Q0-Q1	Q3.2
06804821	19 54 04.99	+42 17 29.9	10.6	A ³⁵	HD 226454	variable ⁷	40 121	228.8	158.5	Q0-Q1	Q3.3
06865077	19 29 39.38	+42 23 25.4	9.8	...	TYC 3142-1206-1	...	15 858	44.4	1.2	Q1	Q0
06922690	18 46 11.06	+42 24 02.5	10.4	...	TYC 3126-780-1	...	45 167	169.8	95.2	Q0-Q1	Q3.1
06923424	18 47 49.73	+42 26 27.6	11.3	...	TYC 3126-1059-1	...	44 223	321.5	248.4	Q0-Q1	Q4.3
06937758	19 13 01.18	+42 29 58.4	9.8	A2 ³⁵	BD+42 3278	...	15 860	44.4	1.2	Q1	Q0
06939291	19 15 18.79	+42 26 19.2	10.1	...	TYC 3129-2577-1	...	42 750	79.6	4.5	Q0-Q1	Q2.1
06947064	19 25 17.66	+42 25 13.3	11.3	...	TYC 3142-1168-1	...	45 456	109.5	35.3	Q0-Q1	Q2.2
06951642	19 31 05.93	+42 29 53.2	9.7	A5 ³⁵	BD+42 3370	...	15 807	44.4	1.2	Q1	Q0
06965789	19 45 41.30	+42 29 34.4	10.1	A5 ³⁵	BD+42 3446	binary	43 926	79.6	4.5	Q0-Q1	Q2.1
07007103	18 43 57.19	+42 31 05.7	11.2	...	TYC 3126-2522-1	...	38 311	292.5	219.3	Q0-Q1	Q4.2
07106205	19 11 57.48	+42 40 22.6	11.4	...	TYC 3129-879-1	binary*	43 945	79.6	4.5	Q0-Q1	Q2.1
07106648	19 12 39.79	+42 38 40.5	10.5	...	TYC 3129-2589-1	...	44 969	169.8	95.3	Q0-Q1	Q3.1
07109598	19 16 56.81	+42 38 11.7	10.6	...	TYC 3129-2517-1	...	46 064	200.7	126.4	Q0-Q1	Q3.2
07119530	19 29 19.03	+42 38 29.1	8.5	A3 ³⁵	HD 183787	...	14 473	321.5	4.5	Q0-Q4	...
07122746	19 33 10.10	+42 38 26.9	10.9	...	TYC 3143-1631-1	...	15 833	44.4	1.2	Q1	Q0
07204237	19 32 01.34	+42 42 21.5	10.8	...	TYC 3143-261-1	...	47 584	262.8	187.3	Q0-Q1	Q4.1
07211759	19 40 30.77	+42 47 02.9	11.0	...	TYC 3144-1426-1	...	49 467	44.2	1.2	Q0	Q1
07212040	19 40 49.03	+42 47 05.6	10.9	...	TYC 3144-2042-1	...	38 635	292.5	219.3	Q0-Q1	Q4.2
07215607	19 44 11.64	+42 45 09.5	10.5	...	TYC 3144-1656-1	...	47 487	262.8	187.3	Q0-Q1	Q4.1
07217483	19 45 57.86	+42 45 23.1	10.6	...	TYC 3144-856-1	...	49 511	44.2	1.2	Q0	Q1
07220356	19 48 28.15	+42 44 36.9	11.5	44 194	321.5	248.4	Q0-Q1	Q4.3
07265427	19 03 27.89	+42 49 54.6	11.5	40 413	137.7	66.3	Q0-Q1	Q2.3
07287118	19 33 31.34	+42 50 11.3	10.7	...	TYC 3143-1359-1	...	47 575	262.8	187.3	Q0-Q1	Q4.1
07300387	19 47 19.51	+42 52 02.0	10.5	...	TYC 3144-1600-1	...	46 064	200.7	126.4	Q0-Q1	Q3.2
07304385	19 50 51.55	+42 48 06.0	10.0	...	TYC 3145-901-1	...	10 289	228.7	4.5	Q0-Q3	...
07338125	18 48 49.75	+42 55 05.4	11.1	...	TYC 3126-3094-1	...	48 494	44.2	1.8	Q0	Q1
07350486	19 10 48.22	+42 54 38.6	11.3	45 279	109.5	35.3	Q0-Q1	Q2.2
07352425	19 13 48.70	+42 57 28.8	10.6	...	TYC 3129-1319-1	...	38 650	292.5	219.3	Q0-Q1	Q4.2
07352776	19 14 23.02	+42 55 27.7	11.1	...	TYC 3129-2485-1	...	49 484	44.2	1.2	Q0	Q1
07385478	19 50 57.86	+42 59 45.9	11.5	...	TYC 3145-171-1	binary ³⁸	42 442	109.5	35.3	Q0-Q1	Q2.2
07436266	19 16 34.20	+43 01 26.7	11.4	40 402	137.7	66.3	Q0-Q1	Q2.3
07450284	19 33 37.68	+43 05 49.2	10.4	A5 ³⁵	BD+42 3380	...	45 192	169.8	95.2	Q0-Q1	Q3.1
07502559	18 48 17.69	+43 07 06.6	11.3	...	TYC 3126-2023-1	...	44 216	321.5	248.3	Q0-Q1	Q4.3
07533694	19 34 12.91	+43 07 03.5	10.4	...	TYC 3143-1179-1	...	40 429	137.7	66.3	Q0-Q1	Q2.3

Table 1. continued.

KIC ID	RA (J2000)	Dec (J2000)	Kp	Spectral Type	Name	Variable	N Datapoints	ΔT (d)	δT (d)	Quarters LC	Quarters SC
07548061	19 48 15.46	+43 07 36.8	8.8	G2 ²⁴ ,G2Ib ⁴¹	V1154 Cyg	Cepheid ⁸	63 501	321.5	319.7	Q0-Q4	Q1
07548479	19 48 36.50	+43 06 32.0	8.4	A3 ³⁵	HD 187547	...	46077	200.7	126.4	Q0-Q1	Q3.2
07553237	19 52 43.10	+43 06 00.1	11.3	44 428	321.5	248.3	Q0-Q1	Q4.3
07583939	18 47 32.06	+43 17 04.7	9.7	A0 ³⁵	BD+43 3078	...	40 086	228.8	158.5	Q0-Q1	Q3.3
07596250	19 11 03.60	+43 13 07.8	11.3	44 419	321.5	248.3	Q0-Q1	Q4.3
07662076	18 50 56.93	+43 18 13.6	10.0	F0 ³⁵	BD+43 3097	...	15 812	44.4	1.2	Q1	Q0
07668791	19 05 23.64	+43 20 05.6	9.3	A2 ³⁵	HD 178120	...	43 532	79.6	4.5	Q0-Q1	Q2.1
07669848	19 07 19.99	+43 18 55.2	7.4	F2III ²⁰	HD 178615	...	10 175	228.7	4.7	Q0-Q3	...
07694191	19 42 09.29	+43 23 37.4	10.8	...	TYC 3148-1126-1	...	38 456	292.5	219.4	Q0-Q1	Q4.2
07697795	19 46 20.83	+43 22 36.0	11.0	...	TYC 3148-1808-1	...	49 510	44.2	1.2	Q0	Q1
07699056	19 47 39.43	+43 20 19.4	10.5	...	TYC 3148-431-1	...	40 113	228.8	158.5	Q0-Q1	Q3.3
07702705	19 50 55.42	+43 19 03.0	11.4	40 368	137.7	66.3	Q0-Q1	Q2.3
07732458	18 49 27.38	+43 28 12.1	10.8	...	TYC 3130-150-1	...	38 452	292.5	219.4	Q0-Q1	Q4.2
07742739	19 11 16.92	+43 24 24.8	11.3	...	TYC 3133-2367-1	...	44 582	109.5	35.3	Q0-Q1	Q2.2
07748238	19 20 38.21	+43 29 03.7	9.5	A5 ³⁵	HD 181985	...	40 114	137.7	66.5	Q0-Q1	Q2.3
07756853	19 32 39.12	+43 26 11.2	9.0	A0 ³⁵	HD 184449	...	49 461	44.2	1.2	Q0	Q1
07767565	19 45 39.00	+43 29 43.0	9.3	A5 ³⁵	HD 186995	binary	2 069	44.2	1.2	Q0-Q1	...
07770282	19 48 33.12	+43 27 04.2	9.7	F0 ³⁵	BD+43 3370	...	15 796	44.4	1.2	Q1	Q0
07771991	19 50 06.55	+43 29 05.9	11.1	...	TYC 3149-1784-1	...	49 327	44.2	1.2	Q0	Q1
07773133	19 51 13.75	+43 27 43.0	10.9	...	TYC 3149-1852-1	...	46 078	200.7	126.4	Q0-Q1	Q3.2
07777435	19 55 24.38	+43 29 47.9	10.7	47 583	262.8	187.3	Q0-Q1	Q4.1
07798339	18 41 34.99	+43 32 58.9	7.9	F0 ³⁵	HD 173109	...	57 256	321.5	35.3	Q0-Q4	Q2.2
07827131	19 33 47.14	+43 31 02.2	8.0	A2 ³⁵	HD 184695	variable ⁹	43 088	30.3	0.7	...	Q3.1
07831302	19 39 00.86	+43 35 03.4	11.3	...	TYC 3147-982-1	...	44 562	98.6	35.3	Q1	Q2.2
07834612	19 43 04.87	+43 35 32.8	10.3	...	TYC 3148-2091-1	...	40 432	137.7	66.3	Q0-Q1	Q2.3
07842286	19 51 14.45	+43 30 41.8	9.9	A2 ³⁵	BD+43 3384	...	15 840	44.4	1.2	Q1	Q0
07842621	19 51 35.69	+43 31 10.1	11.1	...	TYC 3149-1211-1	...	43 215	79.6	4.9	Q0-Q1	Q2.1
07848288	19 56 52.27	+43 30 14.8	10.8	...	TYC 3149-2143-1	binary*	38 034	281.5	219.3	Q1	Q4.2
07890526	19 26 27.53	+43 40 53.8	11.3	...	TYC 3146-1192-1	...	45 435	109.5	35.3	Q0-Q1	Q2.2
07900367	19 39 44.95	+43 41 45.3	11.3	...	TYC 3147-12-1	...	38 681	292.5	219.3	Q0-Q1	Q4.2
07908633	19 49 06.89	+43 41 22.8	11.2	...	TYC 3148-660-1	...	45 163	109.5	35.4	Q0-Q1	Q2.2
07959867	19 26 58.34	+43 44 40.1	9.8	A2 ³⁵	BD+43 3245	...	15 836	44.4	1.2	Q1	Q0
07977996	19 49 50.50	+43 46 28.6	11.5	...	TYC 3148-597-1	...	46 074	200.7	126.4	Q0-Q1	Q3.2
07985370	19 56 59.74	+43 45 08.3	9.8	G5 ³⁵	HD 189210	...	55 936	321.5	4.5	Q0-Q4	Q2.1
08029546	19 28 22.46	+43 52 16.0	11.0	...	TYC 3146-1256-1	...	49 145	44.2	1.2	Q0	Q1
08043961	19 46 55.49	+43 50 27.8	10.7	...	TYC 3148-1402-1	...	45 467	109.5	112.9	Q0-Q1	Q2.2
08054146	19 56 53.35	+43 49 27.0	11.3	39 284	137.7	66.5	Q0-Q1	Q2.3
08103917	19 36 07.25	+43 55 08.0	11.5	45 192	169.8	95.2	Q0-Q1	Q3.1
08104589	19 37 00.82	+43 55 56.5	11.5	44 217	321.5	248.3	Q0-Q1	Q4.3
08123127	19 57 04.13	+43 55 31.7	11.0	...	TYC 3149-534-1	...	86 902	321.5	248.3	Q0-Q1	Q4.3
08143903	18 46 15.74	+44 00 13.4	13.8	13 373	310.5	6.0	Q1-Q4	...
08144674	18 48 20.42	+44 00 12.4	11.6	...	TYC 3130-1700-1	...	39 858	228.8	158.6	Q0-Q1	Q3.3
08145477	18 50 15.98	+44 03 16.7	14.8	14 007	310.5	325.1	Q1-Q4	...
08149341	18 58 28.85	+44 02 41.5	10.9	...	TYC 3131-1906-1	...	46 057	200.7	126.4	Q0-Q1	Q3.2
08159135	19 17 59.83	+44 01 12.6	13.8	12 238	310.5	7.3	Q1-Q4	...
08197761	20 04 09.31	+44 04 16.0	10.7	F2 ³⁵	BD+43 3473s	NGC 6866 ¹⁰	49 023	44.2	1.2	Q0	Q1
08197788	20 04 11.18	+44 05 33.3	13.0	45 246	109.5	35.3	Q0-Q1	Q2.2
08211500	18 46 12.19	+44 08 08.3	8.1	A5 ³⁵	HD 173978	binary	56 868	310.5	4.9	Q1-Q4	Q3.1

Table 1. continued.

KIC ID	RA (J2000)	Dec (J2000)	Kp	Spectral Type	Name	Variable	N Datapoints	ΔT (d)	δT (d)	Quarters LC	Quarters SC
08218419	19 00 34.61	+44 08 29.0	11.9	14 436	321.5	4.5	Q0-Q4	...
08222685	19 10 07.49	+44 08 18.5	8.9	F0V ²⁵ ,F2 ³⁵	HD 179336	...	2 080	44.2	1.2	Q0-Q1	...
08223568	19 11 56.54	+44 08 49.9	11.5	F2 ²⁵	52 274	321.5	4.5	Q0-Q4	Q2.3
08223987	19 12 46.30	+44 06 18.9	14.2	5 678	310.5	187.5	Q1,Q4	...
08230025	19 22 29.45	+44 06 16.2	10.9	F0 ²⁵	TYC 3146-1037-1	...	15 850	44.4	1.2	Q1	Q0
08245366	19 43 33.91	+44 06 19.5	11.2	...	TYC 3148-1360-1	...	40 134	228.8	158.5	Q0-Q1	Q3.3
08248630	19 47 23.30	+44 07 59.0	11.2	...	TYC 3148-484-1	...	44 407	321.5	248.3	Q0-Q1	Q4.3
08264061	20 03 27.94	+44 09 19.2	13.5	NGC 6866	44 106	98.6	35.3	Q1	Q2.2
08264075	20 03 28.34	+44 07 55.2	13.7	NGC 6866	39 585	126.8	66.3	Q1	Q2.3
08264274	20 03 39.67	+44 09 23.3	13.8	NGC 6866	39 285	126.8	66.5	Q1	Q2.3
08264404	20 03 47.14	+44 09 25.7	12.2	NGC 6866	45 464	109.5	35.3	Q0-Q1	Q2.2
08264546	20 03 54.84	+44 09 50.3	13.4	...	NGC 6866 17	NGC 6866	49 495	44.2	1.2	Q0	Q1
08264583	20 03 57.36	+44 09 33.6	11.3	...	HIP 98797	NGC 6866	45 272	109.5	35.3	Q0-Q1	Q2.2
08264588	20 03 57.62	+44 08 37.5	10.7	NGC 6866	49 512	44.2	1.2	Q0	Q1
08264617	20 03 59.35	+44 10 25.8	13.9	NGC 6866	44 828	98.1	35.3	Q1	Q2.2
08264674	20 04 02.86	+44 11 55.4	11.2	42 120	79.6	5.1	Q0-Q1	Q2.1
08264698	20 04 03.96	+44 10 20.5	12.4	44 937	98.6	35.3	Q1	Q2.2
08283796	18 58 53.09	+44 16 40.3	14.5	13 965	310.5	69.8	Q1-Q4	...
08293302	19 18 03.67	+44 14 36.1	13.4	13 721	321.3	6.9	Q0-Q4	...
08323104	19 55 37.82	+44 14 32.9	9.7	kA2mF0 ²⁶	39 147	79.6	6.0	Q0-Q1	Q2.1
08330056	20 03 33.05	+44 12 06.5	13.8	39 755	126.8	66.3	Q1	Q2.3
08330092	20 03 34.92	+44 14 50.1	13.5	43 475	68.6	4.5	Q1	Q2.1
08330463	20 03 58.63	+44 14 09.7	14.9	37 687	281.5	219.3	Q1	Q4.2
08330778	20 04 16.18	+44 12 04.6	13.4	41 890	79.6	4.5	Q0-Q1	Q2.1
08352420	19 04 11.40	+44 21 44.7	12.6	40 433	137.7	66.3	Q0-Q1	Q2.3
08355130	19 10 01.61	+44 22 29.9	10.3	F0III ²⁵	BD+44 3072	binary	57 395	321.5	35.3	Q0-Q4	Q2.2
08355837	19 11 27.07	+44 22 46.7	13.3	13 332	310.5	6.2	Q1-Q4	...
08397426	20 05 34.30	+44 20 09.8	11.1	49 505	44.2	1.2	Q0	Q1
08415752	19 00 00.02	+44 27 48.5	10.7	...	TYC 3132-1272-1	...	46 040	200.7	126.4	Q0-Q1	Q3.2
08429756	19 25 43.13	+44 26 26.3	10.5	...	TYC 3146-1441-1	...	46 052	200.7	126.4	Q0-Q1	Q3.2
08446738	19 48 49.37	+44 24 12.6	11.1	...	TYC 3148-665-1	...	49 502	44.2	1.2	Q0	Q1
08454553	19 56 37.15	+44 25 54.7	11.5	...	TYC 3149-213-1	...	40 298	137.7	66.3	Q0-Q1	Q2.3
08459354	20 01 37.63	+44 24 51.1	11.1	...	TYC 3162-1077-1	...	43 947	79.6	4.5	Q0-Q1	Q2.1
08460025	20 02 22.08	+44 29 31.3	13.7	43 968	98.6	35.9	Q1	Q2.2
08460993	20 03 41.30	+44 24 54.1	11.2	38 282	292.5	219.3	Q0-Q1	Q4.2
08479107	18 56 30.14	+44 33 02.1	14.9	13 570	310.5	324.9	Q1-Q4	...
08482540	19 04 31.01	+44 35 20.1	14.1	13 467	310.5	5.4	Q1-Q4	...
08488065	19 16 14.83	+44 33 57.3	14.2	13 161	310.5	5.9	Q1-Q4	...
08489712	19 18 59.50	+44 33 43.7	8.6	A2 ²⁵	HD 181598	...	46 063	200.7	126.4	Q0-Q1	Q3.2
08499639	19 34 14.23	+44 30 13.4	10.5	...	TYC 3147-849-1	...	47 548	262.7	187.3	Q0-Q1	Q4.1
08507325	19 44 27.10	+44 33 21.1	10.5	...	TYC 3148-1229-1	...	46 058	200.7	126.4	Q0-Q1	Q3.2
08516008	19 53 42.72	+44 35 42.6	10.6	A ³⁵	...	binary*	47 109	251.8	187.3	Q1	Q4.1
08516686	19 54 22.56	+44 34 20.0	10.9	...	TYC 3149-863-1	...	38 572	292.5	219.3	Q0-Q1	Q4.2
08525286	20 03 36.36	+44 35 50.4	13.4	41 777	68.6	5.1	Q1	Q2.1
08545456	19 00 22.73	+44 39 58.5	11.7	15 859	44.4	1.2	Q1	Q0
08560996	19 28 46.42	+44 40 08.5	10.6	...	TYC 3146-802-1	...	40 130	228.8	158.5	Q0-Q1	Q3.3
08565229	19 35 28.32	+44 40 09.6	11.1	...	TYC 3147-509-1	...	49 509	44.2	1.2	Q0	Q1
08579615	19 52 44.14	+44 36 58.0	11.2	...	TYC 3149-571-1	...	44 402	321.5	248.3	Q0-Q1	Q4.3

Table 1. continued.

KIC ID	RA (J2000)	Dec (J2000)	Kp	Spectral Type	Name	Variable	N Datapoints	ΔT (d)	δT (d)	Quarters LC	Quarters SC
08583770	19 56 58.51	+44 40 59.2	10.1	B9III ³⁵	HD 189177	binary	55 306	321.5	4.5	Q0-Q4	Q2.1
08590553	20 04 13.46	+44 40 18.9	11.2	44 398	321.5	248.3	Q0-Q1	Q4.3
08608260	18 56 07.42	+44 47 24.9	10.9	...	TYC 3131-1633-1	...	38 676	292.5	219.3	Q0-Q1	Q4.2
08623953	19 25 59.76	+44 44 45.3	9.4	A5 ³⁵	BD+44 3134	...	45 466	109.5	35.3	Q0-Q1	Q2.2
08651452	19 59 54.19	+44 42 18.6	10.8	...	TYC 3149-307-1	...	45 275	109.5	35.3	Q0-Q1	Q2.2
08655712	20 04 50.98	+44 44 57.7	11.0	44 401	321.5	248.3	Q0-Q1	Q4.3
08695156	19 36 27.74	+44 50 14.8	10.9	...	TYC 3147-395-1	...	15 857	44.4	1.2	Q1	Q0
08703413	19 47 11.45	+44 50 53.6	8.7	kA2mF0 ²⁶	HD 187254	...	39 574	228.8	158.6	Q0-Q1	Q3.3
08714886	19 59 10.18	+44 51 44.9	10.9	F ³⁵	HD 189637	...	14 442	321.5	4.5	Q0-Q4	...
08717065	20 01 40.54	+44 52 47.4	10.9	...	TYC 3162-71-1	...	15 850	44.4	1.2	Q1	Q0
08738244	18 57 58.94	+44 59 17.2	8.2	A3V ²⁰	HD 176390	...	46 035	200.7	126.4	Q0-Q1	Q3.2
08742449	19 07 33.17	+44 57 56.3	14.0	13 862	310.5	4.5	Q1-Q4	...
08746834	19 16 37.06	+44 56 01.4	13.0	14 043	321.4	6.3	Q0-Q4	...
08747415	19 17 39.50	+44 58 05.0	11.8	14 093	321.4	5.9	Q0-Q4	...
08748251	19 19 07.73	+44 57 54.0	11.2	F0 ²⁵	95 046	262.7	187.3	Q0-Q1	Q4.1
08750029	19 21 54.91	+44 59 42.0	9.7	A5p ²⁵	BD+44 3113	...	15 834	44.4	1.2	Q1	Q0
08766619	19 46 09.19	+44 59 09.8	10.8	binary	44 792	98.6	35.3	Q1	Q2.2
08827821	19 40 41.38	+45 05 58.7	11.1	...	TYC 3556-3407-1	...	43 942	79.6	4.5	Q0-Q1	Q2.1
08838457	19 53 09.36	+45 05 53.6	11.2	...	TYC 3558-2497-1	...	77 120	292.5	219.3	Q0-Q1	Q4.2
08869302	18 58 45.58	+45 10 42.0	14.1	13 803	310.5	4.5	Q1-Q4	...
08869892	19 00 00.74	+45 08 03.5	12.6	40 429	137.7	66.3	Q0-Q1	Q2.3
08871304	19 02 56.93	+45 11 42.2	10.8	...	TYC 3541-1172-1	...	50 616	321.5	34.8	Q0-Q4	Q4.2
08881697	19 21 36.02	+45 07 06.9	10.6	A5 ²⁵	15 854	44.4	1.2	Q1	Q0
08915335	20 03 45.55	+45 10 02.9	9.6	A2 ³⁵	HD 190566	...	45 192	169.8	95.2	Q0-Q1	Q3.1
08933391	18 52 06.41	+45 13 39.4	8.9	F0 ³⁵	HD 175201	...	49 159	44.2	1.2	Q0	Q1
08940640	19 06 33.89	+45 14 24.9	12.8	A5 ²⁵	45 195	169.8	95.2	Q0-Q1	Q3.1
08972966	19 51 32.42	+45 15 51.8	11.5	45 194	169.8	95.2	Q0-Q1	Q3.1
08975515	19 53 45.58	+45 13 09.3	9.5	A2 ³⁵	HD 188538	...	40 206	137.7	66.5	Q0-Q1	Q2.3
09020157	19 24 43.66	+45 21 01.2	10.8	F2III ²⁵	BD+45 2892	...	45 344	109.1	35.3	Q0-Q1	Q2.2
09020199	19 24 48.48	+45 20 48.9	8.9	F2CrEu ²⁵ ,F0V ³⁷	HD 182895	Ap variable ¹¹	15 845	44.4	1.2	Q1	Q0
09052363	20 02 07.70	+45 22 07.6	10.7	A2 ³⁵	HD 190226	...	47 457	262.8	187.3	Q0-Q1	Q4.1
09072011	18 53 55.80	+45 28 35.9	10.7	...	TYC 3540-2380-1	...	45 179	169.8	95.2	Q0-Q1	Q3.1
09073007	18 56 09.07	+45 26 59.2	10.6	...	TYC 3540-2491-1	...	40 433	137.7	66.3	Q0-Q1	Q2.3
09073985	18 58 15.29	+45 29 45.6	13.4	14 112	321.5	5.7	Q0-Q4	...
09077192	19 05 34.85	+45 26 47.0	14.5	13 975	310.5	4.5	Q1-Q4	...
09108615	19 51 37.61	+45 27 04.4	11.4	...	TYC 3557-2024-1	...	42 088	79.6	4.5	Q0-Q1	Q2.1
09111056	19 54 07.15	+45 24 06.7	10.5	F0 ³⁵	BD+45 3006	...	38 573	292.5	219.3	Q0-Q1	Q4.2
09117875	20 01 46.73	+45 28 35.9	7.5	kA2mF2 ³⁷	15 828	44.4	1.2	Q1	Q0
09138872	18 55 47.57	+45 31 27.5	10.1	...	TYC 3540-1966-1	...	43 944	79.6	4.5	Q0-Q1	Q2.1
09143785	19 06 42.17	+45 33 12.6	12.1	A5 ²⁵	15 847	44.4	1.2	Q1	Q0
09147229	19 14 11.59	+45 34 59.1	10.7	F0V ²⁵	TYC 3542-1223-1	...	94 344	262.8	187.3	Q0-Q1	Q4.1
09156808	19 30 53.18	+45 33 12.7	11.3	...	TYC 3556-1431-1	binary*	45 464	109.5	35.3	Q0-Q1	Q2.2
09201644	18 52 58.58	+45 36 43.7	11.0	...	TYC 3540-3014-1	...	46 072	200.7	126.4	Q0-Q1	Q3.2
09204672	18 59 58.82	+45 40 35.7	9.8	G ³⁵	BD+45 2812	...	14 392	321.5	4.5	Q0-Q4	...
09204718	19 00 03.36	+45 36 27.5	8.8	kA3mF0 ³⁷	HD 176843	Am star	40 057	228.5	158.5	Q0-Q1	Q3.3
09210037	19 12 07.37	+45 38 11.9	13.5	40 134	228.8	158.5	Q0-Q1	Q3.3
09216367	19 24 20.86	+45 39 16.7	12.1	A2p: ²⁵	15 842	44.4	1.2	Q1	Q0

Table 1. continued.

KIC ID	RA (J2000)	Dec (J2000)	Kp	Spectral Type	Name	Variable	N Datapoints	ΔT (d)	δT (d)	Quarters LC	Quarters SC
09222942	19 34 45.65	+45 41 22.1	10.5	...	TYC 3556-929-1	...	45 039	169.8	95.2	Q0-Q1	Q3.1
09229318	19 43 51.82	+45 41 09.0	9.6	F0 ³⁵	BD+45 2962	...	40 433	137.7	66.3	Q0-Q1	Q2.3
09246481	20 03 33.70	+45 37 13.7	9.0	A0 ³⁵	HD 190548	...	15 840	44.4	1.2	Q1	Q0
09264399	18 53 05.98	+45 44 20.3	14.3	13 393	310.3	7.6	Q1-Q4	...
09264462	18 53 13.32	+45 45 08.3	13.0	13 992	320.9	5.0	Q0-Q4	...
09267042	18 58 52.06	+45 44 58.2	13.4	40 132	228.8	158.5	Q0-Q1	Q3.3
09268087	19 01 09.07	+45 47 36.5	12.1	28 654	322.0	4.6	Q0-Q4	Q0
09272082	19 10 33.79	+45 45 04.0	9.0	A7 ²⁷	HD 179458	...	44 436	109.5	35.4	Q0-Q1	Q2.2
09274000	19 14 57.79	+45 42 32.2	14.2	13 243	310.5	7.0	Q1-Q4	...
09291618	19 43 36.74	+45 43 57.1	9.7	A5 ³⁵	BD+45 2961	...	40 135	228.8	158.5	Q0-Q1	Q3.3
09306095	20 00 41.90	+45 47 59.3	12.4	45 467	109.5	35.3	Q0-Q1	Q2.2
09324334	18 49 26.86	+45 53 38.4	13.7	47 113	251.8	187.3	Q1	Q4.1
09327993	18 57 59.76	+45 53 29.7	9.8	K0 ³⁵	BD+45 2805	...	14 398	321.5	4.6	Q0-Q4	...
09336219	19 16 36.91	+45 52 16.5	13.3	13 911	320.7	5.7	Q0-Q4	...
09351622	19 41 26.86	+45 53 53.1	9.1	F0 ³⁵	BD+45 2955	...	43 586	79.6	4.5	Q0-Q1	Q2.1
09353572	19 43 58.61	+45 53 54.7	10.6	...	TYC 3557-1126-1	...	40 133	228.8	158.5	Q0-Q1	Q3.3
09368220	20 01 18.62	+45 52 05.7	11.3	38 680	292.5	219.3	Q0-Q1	Q4.2
09386259	18 49 12.55	+45 54 26.8	13.3	...	J18491255+4554268	...	13 252	320.4	7.7	Q0-Q4	...
09391395	19 01 29.78	+45 55 14.4	11.4	...	TYC 3541-2014-1	...	40 405	137.7	66.3	Q0-Q1	Q2.3
09395246	19 10 06.41	+45 58 27.0	11.8	F2 ²⁵	15 859	44.4	1.2	Q1	Q0
09408694	19 34 45.60	+45 54 16.3	11.5	15 860	44.4	47.9	Q1	Q0
09413057	19 41 19.15	+45 57 45.8	9.6	A2 ³⁵	BD+45 2954	...	40 419	137.7	66.3	Q0-Q1	Q2.3
09450940	18 58 53.42	+46 00 17.7	12.7	45 194	169.8	95.2	Q0-Q1	Q3.1
09451598	19 00 28.58	+46 03 02.2	13.6	39 664	217.8	158.5	Q1	Q3.3
09453075	19 03 44.09	+46 03 46.0	12.4	43 912	79.6	4.5	Q0-Q1	Q2.1
09458750	19 16 37.49	+46 02 11.4	13.8	13 429	310.5	6.5	Q1-Q4	...
09473000	19 39 48.67	+46 01 38.5	10.1	...	TYC 3556-3291-1	...	15 859	44.4	1.2	Q1	Q0
09489590	19 59 40.42	+46 01 56.3	10.9	...	TYC 3558-16-1	...	38 682	292.5	219.3	Q0-Q1	Q4.2
09490042	20 00 11.69	+46 05 43.3	10.5	...	TYC 3558-1852-1	...	44 756	169.8	95.2	Q0-Q1	Q3.1
09490067	20 00 12.86	+46 03 33.0	10.6	...	TYC 3558-1208-1	...	77 094	292.5	219.3	Q0-Q1	Q4.2
09509296	18 50 55.32	+46 06 48.5	9.9	...	TYC 3540-1568-1	...	15 841	44.4	1.2	Q1	Q0
09514879	19 03 49.58	+46 06 58.1	10.7	...	TYC 3541-30-1	...	63 454	321.5	4.9	Q0-Q4	Q1
09520434	19 16 48.22	+46 09 49.7	14.5	13 290	310.5	6.0	Q1-Q4	...
09520864	19 17 41.62	+46 10 17.4	11.1	14 428	321.5	4.5	Q0-Q4	...
09532644	19 37 26.47	+46 10 07.4	12.7	49 449	44.2	1.2	Q0	Q1
09533449	19 38 37.37	+46 11 16.9	11.3	...	TYC 3556-3494-1	...	45 449	109.5	35.3	Q0-Q1	Q2.2
09533489	19 38 41.71	+46 07 21.6	13.0	48 961	33.4	0.0	...	Q1
09550886	20 00 06.74	+46 07 30.5	11.0	...	TYC 3558-1238-1	...	44 429	321.5	248.3	Q0-Q1	Q4.3
09551281	20 00 33.60	+46 11 55.4	10.4	A3 ³⁵	HD 189916	...	45 192	169.8	95.2	Q0-Q1	Q3.1
09580794	19 14 08.02	+46 16 00.1	11.3	F0V ²⁵	15 859	44.4	1.2	Q1	Q0
09582720	19 18 17.18	+46 12 46.6	12.7	binary*	14 440	321.5	4.6	Q0-Q4	...
09593997	19 36 47.76	+46 17 34.0	12.6	38 532	292.5	219.3	Q0-Q1	Q4.2
09594100	19 36 55.99	+46 15 18.5	13.0	49 454	44.2	1.2	Q0	Q1
09604762	19 50 59.64	+46 16 03.3	10.6	A5 ³⁵	TYC 3557-1418-1	...	39 877	228.8	158.6	Q0-Q1	Q3.3
09630640	18 46 31.25	+46 19 16.1	13.7	13 939	310.5	4.5	Q1-Q4	...
09632537	18 52 00.24	+46 21 51.6	12.0	15 861	44.4	1.2	Q1	Q0
09640204	19 10 14.09	+46 20 42.6	11.5	F5 ²⁵	63 481	321.5	4.5	Q0-Q4	Q1
09642894	19 16 18.07	+46 21 16.1	11.1	F0 ²⁵	TYC 3542-1780-1	...	46 081	200.7	126.4	Q0-Q1	Q3.2

Table 1. continued.

KIC ID	RA (J2000)	Dec (J2000)	Kp	Spectral Type	Name	Variable	N Datapoints	ΔT (d)	δT (d)	Quarters LC	Quarters SC
09643982	19 18 38.69	+46 21 27.9	12.9	13 969	320.7	6.5	Q0-Q4	...
09650390	19 29 17.81	+46 21 26.1	9.4	A0 ³⁵	HD 183829	...	45 231	109.5	35.3	Q0-Q1	Q2.2
09651065	19 30 25.63	+46 22 52.2	11.1	...	TYC 3556-768-1	...	49510	44.2	1.2	Q0	Q1
09654789	19 36 28.80	+46 18 39.2	13.3	40 227	137.7	66.3	Q0-Q1	Q2.3
09655055	19 36 51.91	+46 23 20.4	11.4	A4 ²⁸	NGC 6811 26	NGC 6811	40 429	137.7	66.3	Q0-Q1	Q2.3
09655114	19 36 58.18	+46 20 22.6	12.1	A4 ²⁸	NGC 6811 18	NGC 6811	52 782	321.5	4.5	Q0-Q4	Q2.3
09655151	19 37 01.18	+46 22 59.4	13.2	...	NGC 6811 16	NGC 6811	48 853	33.4	0.0	...	Q1
09655177	19 37 03.24	+46 19 25.7	10.9	A4 ²⁸	NGC 6811 70	NGC 6811	43 883	79.6	4.5	Q0-Q1	Q2.1
09655393	19 37 21.38	+46 19 53.3	12.6	47 574	262.8	187.3	Q0-Q1	Q4.1
09655422	19 37 24.10	+46 23 52.1	11.5	...	NGC 6811 39	NGC 6811	45 605	189.7	126.4	Q1	Q3.2
09655433	19 37 24.86	+46 18 39.0	11.9	B7 ²⁸	NGC 6811 114	NGC 6811, binary*	12 994	310.5	6.8	Q1-Q4	...
09655438	19 37 25.22	+46 19 35.7	12.3	47 505	262.8	187.3	Q0-Q1	Q4.1
09655487	19 37 29.21	+46 22 39.1	13.1	48 956	33.4	0.0	...	Q1
09655501	19 37 31.22	+46 21 31.9	12.4	A5 ²⁸	NGC 6811 49	NGC 6811	47 543	262.8	187.3	Q0-Q1	Q4.1
09655514	19 37 32.11	+46 19 15.0	11.5	A4 ²⁸	NGC 6811 113	NGC 6811, binary	63 523	321.5	4.5	Q0-Q4	Q1
09655800	19 37 53.16	+46 18 28.8	12.7	77 242	292.5	219.3	Q0-Q1	Q4.2
09656348	19 38 45.29	+46 18 23.6	10.3	...	TYC 3556-3198-1	...	49 500	44.2	1.2	Q0	Q1
09664869	19 50 12.10	+46 18 52.3	11.2	...	TYC 3557-368-1	...	49 510	44.2	1.2	Q0	Q1
09673293	20 00 11.23	+46 19 17.0	10.6	A0 ³⁵	HD 189861	...	39 895	228.8	158.6	Q0-Q1	Q3.3
09693282	18 51 14.90	+46 26 56.1	10.4	...	TYC 3540-1359-1	...	45 385	109.5	35.3	Q0-Q1	Q2.2
09696853	18 59 33.43	+46 24 11.3	11.3	...	TYC 3541-967-1	...	41 869	79.6	5.1	Q0-Q1	Q2.1
09699950	19 06 55.32	+46 25 08.0	13.4	40 133	228.8	158.5	Q0-Q1	Q3.3
09700145	19 07 23.57	+46 28 21.7	12.7	40 426	137.7	66.3	Q0-Q1	Q2.3
09700322	19 07 50.71	+46 29 11.9	12.7	...	ASAS J190751+4629.2	...	45 194	169.8	95.2	Q0-Q1	Q3.1
09700679	19 08 42.53	+46 24 14.8	9.9	G2III ²⁵	BD+46 2633	...	40 416	137.7	66.3	Q0-Q1	Q2.3
09703601	19 15 25.03	+46 28 10.6	14.3	13 495	310.5	5.7	Q1-Q4	...
09716107	19 36 56.76	+46 26 58.0	13.1	48 446	33.4	0.1	...	Q1
09716350	19 37 17.98	+46 27 45.3	12.5	binary*	49 401	44.2	1.2	Q0	Q1
09716947	19 38 11.95	+46 28 02.5	12.9	49 302	44.2	1.2	Q0	Q1
09760531	19 06 59.78	+46 32 20.4	9.5	F0 ³⁵	BD+46 2621	...	43 946	79.6	4.5	Q0-Q1	Q2.1
09762713	19 12 12.26	+46 30 50.3	11.1	F0 ²⁵	40 134	228.8	158.5	Q0-Q1	Q3.3
09764712	19 16 49.58	+46 32 01.7	13.9	13 158	310.5	6.3	Q1-Q4	...
09764965	19 17 24.91	+46 35 35.2	8.9	A5mp ²⁵	HD 181206	Ap or Am star	49 507	44.2	1.2	Q0	Q1
09773512	19 32 21.77	+46 35 29.8	10.0	A2 ³⁵	BD+46 2714	...	15 860	44.4	1.2	Q1	Q0
09775385	19 35 24.70	+46 35 26.9	11.1	...	TYC 3556-1982-1	...	43 914	79.6	4.5	Q0-Q1	Q2.1
09775454	19 35 32.02	+46 35 22.3	8.2	FIIV ²⁹	HD 185115	hybrid ¹⁵	10 327	228.7	4.5	Q0-Q3	...
09776474	19 37 00.19	+46 31 14.2	13.0	63 426	321.5	4.5	Q0-Q4	Q1
09777532	19 38 31.06	+46 31 34.1	10.9	...	TYC 3556-3228-1	...	57 342	321.5	4.5	Q0-Q4	Q3.1
09790479	19 55 05.57	+46 35 05.1	9.9	A2 ³⁵	HD 188833	...	15 822	44.4	1.2	Q1	Q0
09812351	18 46 10.32	+46 37 51.0	7.9	A0 ³⁵	HD 174019	...	45 192	169.8	95.2	Q0-Q1	Q3.1
09813078	18 48 21.55	+46 41 43.7	11.9	15 859	44.4	1.2	Q1	Q0
09818269	19 00 40.73	+46 39 58.7	11.4	15 851	44.4	1.2	Q1	Q0
09836020	19 35 43.10	+46 40 03.0	12.8	14 463	321.5	4.5	Q0-Q4	...
09845907	19 49 30.46	+46 40 01.7	11.6	15 860	44.4	1.2	Q1	Q0
09851142	19 55 12.05	+46 39 55.9	7.6	kA5hA7mF3 ²⁰ , A7pCrEu ⁴⁰	V2094 Cyg	Am star, or α^2 CVn ¹²	47 787	310.5	4.5	Q1-Q4	Q2.3
09874181	18 51 26.57	+46 46 48.0	10.8	38 670	292.5	219.3	Q0-Q1	Q4.2

Table 1. continued.

KIC ID	RA (J2000)	Dec (J2000)	Kp	Spectral Type	Name	Variable	N Datapoints	ΔT (d)	δT (d)	Quarters LC	Quarters SC
09881909	19 10 03.58	+46 42 16.1	11.4	F2 ²⁵	43 845	79.6	4.5	Q0-Q1	Q2.1
09885882	19 18 45.05	+46 44 27.8	14.1	13 809	310.5	5.0	Q1-Q4	...
09909300	19 53 27.17	+46 45 39.5	11.5	88 778	321.5	248.3	Q0-Q1	Q4.3
09913481	19 58 20.76	+46 45 55.9	10.9	...	TYC 3558-637-1	...	13 759	44.1	4.6	Q1	Q0
09944208	19 13 58.44	+46 50 00.2	14.2	13 980	310.5	4.5	Q1-Q4	...
09944730	19 15 11.54	+46 48 52.2	14.1	13 980	310.5	4.6	Q1-Q4	...
09970568	19 55 01.15	+46 52 29.2	9.6	A2 ³⁵	HD 188832	...	40 424	137.7	66.3	Q0-Q1	Q2.3
09991621	18 44 43.25	+46 55 47.6	13.9	13 276	310.5	6.1	Q1-Q4	...
09991766	18 45 08.02	+46 58 02.0	14.2	13 495	310.5	5.7	Q1-Q4	...
09994789	18 52 50.45	+46 59 48.0	13.8	13 322	310.5	6.4	Q1-Q4	...
09995464	18 54 26.02	+46 59 11.5	13.2	14 360	321.5	4.9	Q0-Q4	...
10000056	19 05 07.51	+46 59 01.5	14.2	36 583	28.9	3.9	...	Q4.2
10002897	19 11 41.71	+46 55 12.7	12.2	15 853	44.4	1.2	Q1	Q0
10004510	19 14 55.08	+46 55 02.6	14.2	13 941	310.5	4.5	Q1-Q4	...
10006158	19 18 07.39	+46 57 26.2	9.7	K0 ³⁵	BD+46 2665	...	14 431	321.5	4.5	Q0-Q4	...
10014548	19 32 14.23	+46 54 20.9	10.7	...	TYC 3560-2590-1	...	47 550	262.8	187.3	Q0-Q1	Q4.1
10030943	19 54 12.43	+46 56 12.6	11.3	...	TYC 3562-2361-1	...	38 677	292.5	219.3	Q0-Q1	Q4.2
10035772	20 00 05.26	+46 54 22.8	11.1	...	TYC 3562-32-1	...	43 903	79.6	4.5	Q0-Q1	Q2.1
10056217	18 50 47.52	+47 00 23.3	12.9	13 699	320.6	6.8	Q0-Q4	...
10056297	18 51 00.24	+47 00 11.3	13.4	40 137	228.8	158.5	Q0-Q1	Q3.3
10057129	18 52 50.38	+47 00 27.8	13.9	13 930	310.5	4.9	Q1-Q4	...
10062593	19 04 12.91	+47 03 05.0	13.3	14 399	321.5	4.6	Q0-Q4	...
10064111	19 07 24.91	+47 05 13.2	10.3	A5 ³⁵	BD+46 2624	binary	44 462	109.5	35.9	Q0-Q1	Q2.2
10065244	19 09 47.30	+47 04 34.5	12.3	43 945	79.6	4.5	Q0-Q1	Q2.1
10068892	19 17 00.31	+47 05 38.4	11.4	14 433	321.5	4.6	Q0-Q4	...
10069934	19 18 56.14	+47 05 14.4	11.3	...	TYC 3547-470-1	...	88 326	321.5	248.3	Q0-Q1	Q4.3
10073601	19 24 48.70	+47 02 41.1	11.5	...	TYC 3547-20-1	...	433 213	321.6	4.5	...	Q0-Q4.3
10090345	19 49 00.12	+47 05 05.2	11.3	...	TYC 3561-258-1	...	45 170	109.5	35.4	Q0-Q1	Q2.2
10096499	19 55 54.07	+47 05 24.2	6.9	A3V ³⁰	HD 189013	...	37 977	25.9	0.0	...	Q3.3
10119517	18 45 55.46	+47 07 21.6	9.9	...	TYC 3544-1245-1	...	52 795	321.5	4.5	Q0-Q4	Q2.3
10130777	19 10 00.34	+47 11 12.1	12.6	40 348	137.7	66.3	Q0-Q1	Q2.3
10134600	19 17 02.93	+47 08 52.0	13.6	14 282	321.3	4.9	Q0-Q4	...
10134800	19 17 24.60	+47 08 32.4	11.8	15 858	44.4	1.2	Q1	Q0
10140513	19 26 25.46	+47 06 05.4	11.0	435 810	321.6	4.5	...	Q0-Q4.3
10140665	19 26 38.47	+47 06 08.0	12.1	432 553	321.6	4.5	...	Q0-Q4.3
10164569	19 57 20.35	+47 09 58.8	11.4	...	TYC 3562-1846-1	...	39 573	137.7	66.5	Q0-Q1	Q2.3
10206340	19 24 58.82	+47 14 57.3	11.2	B1	V850 Cyg	binary ¹³	403 034	321.6	324.3	...	Q0-Q4.3
10208303	19 28 12.58	+47 14 04.0	11.9	432 367	321.6	4.5	...	Q0-Q4.3
10208345	19 28 17.04	+47 17 14.6	11.6	46 069	200.7	126.4	Q0-Q1	Q3.2
10213987	19 37 05.16	+47 17 19.5	11.4	...	TYC 3560-2645-1	binary*	39 155	126.8	66.7	Q1	Q2.3
10253943	18 47 24.48	+47 18 05.7	10.2	...	TYC 3544-2546-1	...	43 944	79.6	4.5	Q0-Q1	Q2.1
10254547	18 48 46.27	+47 22 26.3	13.9	13 393	310.5	5.6	Q1-Q4	...
10264728	19 10 59.66	+47 20 21.6	9.9	A2 ³⁵	BD+47 2769	...	15 840	44.4	1.2	Q1	Q0
10266959	19 15 19.42	+47 22 59.2	15.0	13 598	310.5	5.6	Q1-Q4	...
10273246	19 26 05.76	+47 21 30.1	10.9	432 872	321.6	4.5	...	Q0-Q4.3
10273384	19 26 19.54	+47 23 36.7	11.5	436 154	321.6	4.5	...	Q0-Q4.3
10273960	19 27 17.42	+47 18 39.2	11.7	431 979	321.6	4.5	...	Q0-Q4.3
10274244	19 27 44.74	+47 18 34.9	11.5	373 959	321.6	35.3	...	Q0-Q4.3

Table 1. continued.

KIC ID	RA (J2000)	Dec (J2000)	Kp	Spectral Type	Name	Variable	N Datapoints	ΔT (d)	δT (d)	Quarters LC	Quarters SC
10281360	19 38 39.22	+47 23 24.5	11.1	...	TYC 3560-1923-1	...	43 712	30.0	0.0	Q1	Q3.2
10289211	19 48 58.75	+47 23 25.7	10.2	A2 ³⁵	BD+47 2927	...	45 449	109.5	35.3	Q0-Q1	Q2.2
10338279	19 25 28.94	+47 26 07.8	12.0	436 158	321.6	4.5	...	Q0-Q4.3
10339342	19 27 05.35	+47 24 08.2	12.0	432 133	321.6	4.5	...	Q0-Q4.3
10340511	19 28 56.16	+47 24 44.0	11.6	431 104	321.6	4.5	...	Q0-Q4.3
10341072	19 29 46.20	+47 24 09.4	9.0	F8 ³⁵	HD 183954	...	147 978	109.7	4.5	...	Q0-Q2.2
10355055	19 49 16.61	+47 24 27.3	9.3	A2 ³⁵	HD 187709	...	45 466	109.5	35.3	Q0-Q1	Q2.2
10361229	19 56 08.93	+47 28 30.5	10.9	...	TYC 3562-1455-1	...	40 046	137.7	66.3	Q0-Q1	Q2.3
10383933	18 44 15.65	+47 34 09.2	13.3	13 729	320.9	5.8	Q0-Q4	...
10385459	18 48 19.39	+47 32 07.6	10.5	...	TYC 3544-2086-1	...	10 335	228.7	4.5	Q0-Q4	Q4.1
10389037	18 56 44.62	+47 32 01.8	10.4	K ³⁵	BD+47 2721	...	14 423	321.5	4.6	Q0-Q4	...
10394332	19 08 02.76	+47 33 08.8	13.3	14 457	321.5	4.5	Q0-Q4	...
10448764	18 44 12.41	+47 40 31.0	10.8	45 194	169.8	95.2	Q0-Q1	Q3.1
10450550	18 48 44.04	+47 36 50.9	13.2	13 719	321.2	4.6	Q0-Q4	...
10450675	18 49 01.15	+47 36 27.9	12.8	13 804	321.4	6.2	Q0-Q4	...
10451090	18 49 55.92	+47 38 14.4	9.2	A2 ³⁵	HD 174789	...	43 946	79.6	4.5	Q0-Q1	Q2.1
10451250	18 50 15.94	+47 38 22.5	14.1	13 274	310.5	5.7	Q1-Q4	...
10453475	18 55 16.63	+47 37 33.0	14.2	13 907	310.1	4.5	Q1-Q4	...
10467969	19 23 32.47	+47 40 28.6	12.0	431 107	321.6	4.5	...	Q0-Q4.3
10471914	19 30 03.02	+47 36 18.6	10.7	...	TYC 3560-2319-1	...	47 572	262.8	187.3	Q0-Q1	Q4.1
10484808	19 48 04.58	+47 40 45.0	10.6	...	TYC 3561-1801-1	...	40 134	228.8	158.5	Q0-Q1	Q3.3
10526137	19 11 42.82	+47 45 27.1	10.2	M7 ³¹	TYC 3546-1494-1	...	13 014	320.5	8.2	Q0-Q4	...
10526615	19 12 39.94	+47 47 43.4	14.4	13 450	310.4	6.0	Q1-Q4	...
10533506	19 24 50.42	+47 43 47.5	11.5	433 130	321.6	4.5	...	Q0-Q4.3
10533616	19 25 00.91	+47 47 49.8	9.6	A5 ³⁵	BD+47 2828	...	40 147	137.7	66.5	Q0-Q1	Q2.3
10534629	19 26 43.27	+47 46 08.7	11.3	431 681	321.6	4.5	...	Q0-Q4.3
10536147	19 29 11.93	+47 44 43.0	11.6	449 999	321.9	4.5	Q0-Q4	Q0-Q4.3
10537907	19 32 08.18	+47 42 28.8	9.9	F0 ³⁵	BD+47 2856	...	15 860	44.4	1.2	Q1	Q0
10549292	19 48 10.56	+47 45 33.3	11.0	44 427	321.5	248.3	Q0-Q1	Q4.3
10549371	19 48 16.15	+47 42 28.8	9.5	A5 ³⁵	BD+47 2922	...	43 939	79.6	4.5	Q0-Q1	Q2.1
10586837	19 03 02.38	+47 48 48.9	12.4	45 316	109.5	35.3	Q0-Q1	Q2.2
10590857	19 11 38.54	+47 53 45.3	10.0	F0 ³⁵	BD+47 2773	...	15 851	44.4	1.2	Q1	Q0
10604429	19 34 36.46	+47 50 14.0	9.9	F0 ³⁵	BD+47 2868	binary*	52 538	137.9	101.1	...	Q0-Q2.3
10615125	19 48 58.92	+47 51 56.6	10.3	40 385	137.7	66.3	Q0-Q1	Q2.3
10647493	18 51 45.14	+47 57 29.4	11.7	15 860	44.4	1.2	Q1	Q0
10647611	18 52 04.49	+47 59 54.2	12.0	15 851	44.4	1.2	Q1	Q0
10647860	18 52 37.75	+47 55 26.2	13.3	13 667	321.0	7.4	Q0-Q4	...
10648728	18 54 35.76	+47 56 52.3	11.4	44 102	321.5	248.4	Q0-Q1	Q4.3
10652134	19 02 08.28	+47 55 45.2	11.9	11 249	252.5	4.5	Q0-Q4	...
10658302	19 15 07.68	+47 54 19.0	13.1	43 591	79.6	4.5	Q0-Q1	Q2.1
10658802	19 16 03.00	+47 57 27.0	11.9	15 854	44.4	1.2	Q1	Q0
10663892	19 24 45.10	+47 58 53.9	11.8	430 810	321.6	4.5	...	Q0-Q4.3
10664703	19 26 02.47	+47 58 53.9	10.9	...	TYC 3547-1575-1	...	44 427	321.5	248.3	Q0-Q1	Q4.3
10664975	19 26 28.49	+47 58 11.7	7.6	A2 ³⁵	HD 183280	...	38 016	25.9	0.0	...	Q3.3
10675762	19 43 05.02	+47 57 32.6	10.9	...	TYC 3561-371-1	...	15 842	44.4	1.2	Q1	Q0
10684587	19 53 36.67	+47 59 53.1	11.0	...	TYC 3562-461-1	...	44 430	321.5	248.3	Q0-Q1	Q4.3
10684673	19 53 42.41	+47 58 27.2	11.1	...	TYC 3562-805-1	...	49 511	44.2	1.2	Q0	Q1
10685653	19 54 50.30	+47 55 43.1	11.1	...	TYC 3562-301-1	...	49 465	44.2	1.2	Q0	Q1

Table 1. continued.

KIC ID	RA (J2000)	Dec (J2000)	Kp	Spectral Type	Name	Variable	N Datapoints	ΔT (d)	δT (d)	Quarters LC	Quarters SC
10686752	19 56 03.43	+47 58 55.8	11.3	...	TYC 3562-707-1	...	45 455	109.5	35.3	Q0-Q1	Q2.2
10709716	18 45 29.64	+48 05 33.0	13.9	13 501	310.5	6.1	Q1-Q4	...
10713398	18 53 42.43	+48 02 25.8	11.2	...	TYC 3544-1186-1	...	15 860	44.4	1.2	Q1	Q0
10717871	19 03 14.88	+48 02 56.6	10.5	...	TYC 3545-2523-1	...	40 421	137.7	66.3	Q0-Q1	Q2.3
10723718	19 15 05.93	+48 00 40.9	14.2	13 650	310.5	5.9	Q1-Q4	...
10730618	19 26 30.48	+48 05 34.8	10.5	...	TYC 3547-1205-1	...	411 665	321.6	7.3	...	Q0-Q4.3
10775968	18 45 15.58	+48 06 56.6	10.6	...	TYC 3544-733-1	...	39 910	228.8	158.6	Q0-Q1	Q3.3
10777541	18 48 50.14	+48 06 45.9	14.1	12 652	310.5	7.3	Q1-Q4	...
10777903	18 49 40.42	+48 07 13.9	10.2	...	BD+47 2705	...	43 945	79.6	4.5	Q0-Q1	Q2.1
10778640	18 51 17.76	+48 06 19.5	13.8	13 190	310.5	7.4	Q1-Q4	...
10783150	19 01 20.76	+48 08 30.9	13.1	11 299	252.5	4.5	Q0-Q4	...
10788451	19 12 37.80	+48 08 15.5	11.1	...	TYC 3546-1364-1	...	40 136	228.8	158.5	Q0-Q1	Q3.3
10797526	19 27 49.37	+48 10 36.3	8.3	B5 ³²	HD 183558	...	147 727	109.7	4.5	...	Q0-Q2.2
10797849	19 28 20.69	+48 10 57.2	10.8	...	TYC 3547-1020-1	binary	435 432	321.6	5.1	...	Q0-Q4.3
10813970	19 50 47.21	+48 10 17.3	11.3	...	TYC 3561-1538-1	...	40 408	137.7	66.3	Q0-Q1	Q2.3
10815466	19 52 28.63	+48 10 28.0	11.2	...	TYC 3561-434-1	binary*	43 946	79.6	4.5	Q0-Q1	Q2.1
10853783	19 13 30.60	+48 12 21.2	11.0	...	TYC 3546-374-1	...	44 428	321.5	248.3	Q0-Q1	Q4.3
10861649	19 27 58.37	+48 17 37.9	12.1	431 057	321.6	4.5	...	Q0-Q4.3
10902738	18 45 46.99	+48 23 01.6	12.5	9 706	217.8	5.4	Q1-Q3	...
10920182	19 27 36.17	+48 19 09.9	11.8	430 256	321.6	4.5	...	Q0-Q4.3
10920273	19 27 45.77	+48 19 45.4	11.9	430 371	321.6	4.5	...	Q0-Q4.3
10920447	19 28 04.97	+48 18 27.6	11.2	...	TYC 3547-1099-1	...	44 429	321.5	248.3	Q0-Q1	Q4.3
10971674	19 19 09.79	+48 26 53.3	13.8	12 734	310.5	5.7	Q1-Q4	...
10975247	19 26 34.37	+48 29 14.9	11.1	48 556	44.2	1.3	Q0	Q1
10977859	19 31 37.99	+48 26 33.1	8.8	A2 ³⁵	HD 184333	...	49 510	44.2	1.2	Q0	Q1
10988009	19 48 08.23	+48 27 37.8	10.2	...	TYC 3561-622-1	...	43 947	79.6	4.5	Q0-Q1	Q2.1
11013201	18 48 00.07	+48 32 32.0	9.3	A2 ³⁵	BD+48 2768	...	43 656	79.6	4.5	Q0-Q1	Q2.1
11017401	18 59 53.81	+48 33 17.0	14.6	10 873	241.5	150.6	Q1-Q4	...
11020521	19 07 39.65	+48 34 19.4	11.4	338 509	252.7	5.1	...	Q0-Q4.1
11021188	19 09 15.58	+48 33 38.9	11.3	342 509	252.7	4.5	...	Q0-Q4.1
11027270	19 22 35.14	+48 35 49.5	11.3	...	TYC 3547-1058-1	...	88 810	321.5	248.3	Q0-Q1	Q4.3
11067972	18 48 26.30	+48 36 16.9	14.3	12 550	310.5	7.2	Q1-Q4	...
11069435	18 52 28.25	+48 40 08.7	14.5	13 300	310.5	5.9	Q1-Q4	...
11082830	19 24 46.87	+48 38 19.8	10.9	...	TYC 3547-759-1	binary	38 597	292.5	219.3	Q0-Q1	Q4.2
11090405	19 39 12.38	+48 36 24.2	9.6	A5 ³⁵	BD+48 2925	...	40 423	137.7	66.3	Q0-Q1	Q2.3
11122763	18 52 27.24	+48 47 55.6	13.9	13 297	310.5	5.8	Q1-Q4	...
11125764	19 01 09.67	+48 42 57.5	11.1	...	TYC 3545-69-1	...	49 041	33.4	0.0	...	Q1
11127190	19 04 37.85	+48 46 32.4	11.4	15 856	44.4	1.2	Q1	Q0
11128041	19 06 59.26	+48 43 27.7	10.8	339 574	252.7	4.6	...	Q0-Q4.1
11128126	19 07 12.19	+48 47 45.1	11.3	338 231	252.7	5.1	...	Q0-Q4.1
11129289	19 10 15.19	+48 44 32.1	11.7	336 245	252.7	5.1	...	Q0-Q4.1
11180361	19 04 04.61	+48 52 00.3	7.7	A2/3V ²⁰	HD 177876	...	39 548	217.8	158.5	Q1	Q3.3
11182716	19 10 24.26	+48 50 41.5	12.0	337 715	252.7	5.1	...	Q0-Q4.1
11183399	19 12 06.29	+48 52 21.4	12.8	11 324	252.5	4.6	Q0-Q4	...
11183539	19 12 25.80	+48 50 21.2	10.8	...	TYC 3550-456-1	...	45 180	169.8	95.2	Q0-Q1	Q3.1
11193046	19 32 45.31	+48 52 07.6	9.6	A2 ³⁵	BD+48 2912	...	40 255	137.7	66.3	Q0-Q1	Q2.3
11197934	19 41 29.06	+48 48 22.0	11.0	...	TYC 3565-514-1	...	44 324	321.5	248.3	Q0-Q1	Q4.3
11199412	19 43 51.58	+48 48 07.5	10.9	...	TYC 3565-674-1	...	58 160	321.6	248.3	Q1	Q0-Q4.3

Table 1. continued.

KIC ID	RA (J2000)	Dec (J2000)	Kp	Spectral Type	Name	Variable	N Datapoints	ΔT (d)	δT (d)	Quarters LC	Quarters SC
11230518	18 55 50.50	+48 55 32.1	13.6	10 454	241.5	5.7	Q1-Q4	...
11232922	19 02 17.33	+48 54 33.0	14.1	10 290	241.5	6.2	Q1-Q4	...
11233189	19 02 52.42	+48 56 31.6	13.5	10 545	251.5	5.6	Q0-Q4	...
11234888	19 07 00.22	+48 56 07.0	11.9	337 220	252.7	5.1	...	Q0-Q4.1
11235721	19 09 10.61	+48 55 39.1	11.9	338 373	252.7	5.1	...	Q0-Q4.1
11236253	19 10 39.34	+48 56 39.3	12.0	328 959	252.7	5.1	...	Q0-Q4.1
11240653	19 19 53.18	+48 54 03.6	10.6	...	TYC 3551-523-1	...	77 272	292.5	219.3	Q0-Q1	Q4.2
11253226	19 43 39.62	+48 55 44.2	8.4	F5 ³⁵	HD 186700	...	56 546	321.5	35.3	Q0-Q4	Q2.2
11285767	19 01 12.19	+49 02 05.6	10.3	F2 ³⁵	BD+48 2815	...	45 466	109.5	35.3	Q0-Q1	Q2.2
11288686	19 08 39.31	+49 03 12.5	11.8	...	TYC 3550-892-1	...	15 861	44.4	1.2	Q1	Q0
11290197	19 12 40.70	+49 02 36.3	11.4	...	TYC 3550-42-1	...	337 111	252.7	5.1	...	Q0-Q4.1
11309335	19 48 47.21	+49 05 50.0	10.5	...	TYC 3565-1318-1	...	45 182	169.8	95.2	Q0-Q1	Q3.1
11340063	19 04 11.66	+49 10 52.6	14.4	10 617	241.5	4.9	Q1-Q4	...
11340713	19 05 42.79	+49 08 47.4	13.0	46 076	200.7	126.4	Q0-Q1	Q3.2
11342032	19 09 19.63	+49 11 48.3	12.8	11 332	252.5	4.5	Q0-Q4	...
11393580	19 06 05.35	+49 17 49.7	11.5	340 340	252.7	4.5	...	Q0-Q4.1
11394216	19 07 48.43	+49 14 02.1	12.0	338 263	252.7	5.1	...	Q0-Q4.1
11395018	19 09 55.49	+49 15 04.5	10.8	...	TYC 3550-300-1	...	335 442	252.7	5.1	...	Q0-Q4.1
11395028	19 09 57.86	+49 16 44.4	11.7	336 659	252.7	4.5	...	Q0-Q4.1
11395392	19 10 54.34	+49 17 04.6	12.6	45 461	109.5	35.3	Q0-Q1	Q2.2
11402951	19 27 32.81	+49 15 23.5	8.1	kF3hA9mF5 ¹⁴	HD 183489	Am star ¹⁴	28 721	322.0	4.5	Q0-Q4	Q0
11445774	19 05 21.00	+49 18 01.6	11.9	341 474	252.7	5.1	...	Q0-Q4.1
11445913	19 05 40.63	+49 18 20.8	8.5	kA7hA9mF5 ¹⁴	HD 178327	Am, hybrid ^{14,15}	24 170	228.5	4.5	Q0-Q3	Q0
11446143	19 06 19.22	+49 20 52.2	11.8	334 372	252.7	5.1	...	Q0-Q4.1
11446181	19 06 24.36	+49 22 19.3	11.9	338 310	252.7	4.8	...	Q0-Q4.1
11447883	19 11 04.92	+49 19 22.3	9.8	F0 ³⁵	BD+49 2951	...	351 517	253.0	4.5	Q0-Q4	Q0-Q4.1
11447953	19 11 13.92	+49 22 41.1	11.3	342 439	252.7	4.5	...	Q0-Q4.1
11448266	19 12 02.93	+49 18 46.2	11.5	339 553	252.7	4.5	...	Q0-Q4.1
11449931	19 15 46.08	+49 19 42.5	12.1	12 780	320.0	7.8	Q0-Q4	...
11454008	19 24 45.94	+49 23 03.2	11.1	...	TYC 3551-2195-1	...	94 458	262.8	187.5	Q0-Q1	Q4.1
11494765	18 57 57.77	+49 24 56.4	11.1	...	TYC 3549-1627-1	...	49 461	44.2	1.2	Q0	Q1
11497012	19 03 53.04	+49 25 39.1	9.7	F0 ³⁵	BD+49 2927	...	49 507	44.2	1.2	Q0	Q1
11498538	19 07 46.85	+49 29 07.3	7.3	F5 ³⁵	HD 178874	...	104 958	79.7	4.5	...	Q0-Q2.1
11499354	19 09 50.93	+49 25 10.5	12.0	298 877	252.7	30.9	...	Q0-Q4.1
11499453	19 10 05.35	+49 25 47.5	10.7	...	TYC 3550-1330-1	...	342 562	252.7	4.5	...	Q0-Q4.1
11502075	19 16 07.75	+49 28 46.6	14.2	13 788	309.6	4.6	Q1-Q4	...
11508397	19 29 38.30	+49 29 48.4	10.7	38 643	292.5	219.3	Q0-Q1	Q4.2
11509728	19 32 21.24	+49 27 49.4	9.7	A2 ³²	BD+49 3039	...	15 835	44.4	1.6	Q1	Q0
11515690	19 42 55.30	+49 25 27.0	10.6	...	TYC 3565-580-1	...	38 114	292.5	219.4	Q0-Q1	Q4.2
11549609	19 04 23.64	+49 32 58.2	13.2	10 898	252.1	4.8	Q0-Q4	...
11551622	19 10 12.67	+49 33 08.0	13.9	10 369	241.5	5.7	Q1-Q4	...
11572666	19 51 22.80	+49 35 28.8	9.9	...	TYC 3565-1155-1	...	15 857	44.4	1.2	Q1	Q0
11602449	19 08 13.78	+49 39 07.6	9.9	...	TYC 3550-1718-1	...	15 855	44.4	1.2	Q1	Q0
11607193	19 19 29.78	+49 41 07.8	12.6	14 393	321.5	4.6	Q0-Q4	...
11612274	19 30 41.54	+49 39 10.7	10.6	...	TYC 3564-1819-1	...	40 115	228.8	158.5	Q0-Q1	Q3.3
11622328	19 47 56.14	+49 39 14.1	9.5	A2 ³³	BD+49 3109	...	2 089	44.2	1.2	Q0-Q1	...
11651083	19 01 15.65	+49 46 57.8	11.3	11 057	252.5	4.6	Q0-Q4	...
11651147	19 01 26.57	+49 45 14.1	13.8	10 423	241.3	5.5	Q1-Q4	...

Table 1. continued.

KIC ID	RA (J2000)	Dec (J2000)	Kp	Spectral Type	Name	Variable	N Datapoints	ΔT (d)	δT (d)	Quarters LC	Quarters SC
11653958	19 08 57.19	+49 44 22.2	11.9	335 138	252.7	4.5	...	Q0-Q4.1
11654210	19 09 41.76	+49 47 37.4	11.9	334 440	252.7	4.5	...	Q0-Q4.1
11657840	19 18 15.26	+49 45 33.7	15.0	13 043	310.5	6.1	Q1-Q4	...
11661993	19 27 55.78	+49 45 43.5	9.4	F2 ³³	BD+49 3018	...	45 466	109.5	35.3	Q0-Q1	Q2.2
11671429	19 45 48.82	+49 47 11.6	11.0	...	TYC 3565-1003-1	...	41 580	321.5	248.3	Q0-Q1	Q4.3
11700370	18 57 38.28	+49 51 03.6	10.6	...	TYC 3549-677-1	...	39 786	228.7	158.6	Q0-Q1	Q3.3
11700604	18 58 21.74	+49 53 55.7	11.1	...	TYC 3549-914-1	...	49 100	44.2	1.3	Q0	Q1
11706449	19 13 34.66	+49 51 01.2	11.0	14 384	321.5	4.9	Q0-Q4	...
11706564	19 13 51.17	+49 51 34.5	12.4	14 380	321.5	4.8	Q0-Q4	...
11707341	19 15 32.38	+49 51 13.6	13.8	13 915	310.5	4.8	Q1-Q4	...
11708170	19 17 18.50	+49 51 00.8	7.2	F2 ³⁵	HD 181252	...	57 638	321.5	35.3	Q0-Q4	Q2.2
11714150	19 30 25.78	+49 53 09.0	10.3	...	TYC 3564-231-1	...	39 814	137.7	66.4	Q0-Q1	Q2.3
11718839	19 39 17.64	+49 48 06.1	10.9	...	TYC 3564-891-1	...	44 372	321.5	248.3	Q0-Q1	Q4.3
11753169	19 03 04.37	+49 54 06.3	14.7	10 563	241.5	5.7	Q1-Q4	...
11754974	19 08 15.94	+49 57 15.4	12.7	45 195	169.8	156.1	Q0-Q1	Q3.1
11821140	19 41 26.98	+50 03 11.0	10.0	F0 ³³	BD+49 3081	...	15 800	44.4	1.2	Q1	Q0
11822666	19 43 57.53	+50 04 31.8	10.7	47 515	262.8	187.3	Q0-Q1	Q4.1
11824964	19 47 43.10	+50 05 14.2	10.6	...	TYC 3565-247-1	...	39 824	228.8	158.6	Q0-Q1	Q3.3
11874676	19 47 15.31	+50 11 20.1	10.1	A5 ³⁵	BD+49 3106	...	15 861	44.4	1.2	Q1	Q0
11874898	19 47 35.95	+50 06 09.4	11.0	...	TYC 3565-1373-1	...	15 858	44.4	1.2	Q1	Q0
11910256	19 17 46.56	+50 16 17.4	10.6	binary*	46 863	251.8	187.5	Q1	Q4.1
11910642	19 18 33.77	+50 17 00.6	10.2	...	TYC 3550-1782-1	...	45 401	109.5	35.3	Q0-Q1	Q2.2
11973705	19 46 42.58	+50 21 01.3	9.1	B9 ³⁴	HD 234999	...	28 668	322.0	4.6	Q0-Q4	Q0
12018834	19 38 48.29	+50 24 13.8	10.8	...	TYC 3564-274-1	...	95 146	262.8	187.3	Q0-Q1	Q4.1
12020590	19 42 20.35	+50 27 38.8	10.0	...	TYC 3565-859-1	...	15 830	44.4	1.4	Q1	Q0
12058428	19 18 05.66	+50 33 35.9	11.1	...	TYC 3550-895-1	...	49 055	44.2	1.2	Q0	Q1
12062443	19 27 48.05	+50 31 10.2	10.9	...	TYC 3551-450-1	...	15 826	44.4	1.6	Q1	Q0
12068180	19 39 22.42	+50 32 03.4	10.4	...	TYC 3564-1358-1	...	40 428	137.7	66.3	Q0-Q1	Q2.3
12102187	19 04 01.97	+50 37 26.3	11.1	...	TYC 3549-88-1	...	49 308	44.2	1.2	Q0	Q1
12117689	19 40 37.25	+50 38 31.5	10.8	...	TYC 3568-996-1	...	45 441	109.5	35.3	Q0-Q1	Q2.2
12122075	19 48 15.07	+50 39 11.8	10.7	...	TYC 3569-391-1	binary*	47 568	262.8	187.3	Q0-Q1	Q4.1
12216817	19 43 11.14	+50 53 45.6	10.7	...	TYC 3569-368-1	...	40 433	137.7	66.3	Q0-Q1	Q2.3
12217281	19 44 00.38	+50 53 13.2	9.9	F2 ³⁴	HD 234984	...	15 841	44.4	1.2	Q1	Q0
12353648	19 18 07.97	+51 10 47.5	9.6	A2 ³⁴	HD 234859	...	40 397	137.7	66.3	Q0-Q1	Q2.3
12647070	19 21 51.14	+51 42 20.1	10.7	...	TYC 3555-1407-1	...	47 581	262.8	187.3	Q0-Q1	Q4.1
12784394	19 19 51.41	+52 05 39.6	9.8	A5 ³⁴	HD 234869	...	15 729	44.4	1.6	Q1	Q0

Notes. ⁽¹⁾ P = 9.3562 d, eclipsing binary (Hartman et al. 2004) ⁽²⁾ P = 0.0665 d (Henry et al. 2001) ⁽³⁾ P = 4.0303 d, pulsating star (Hartman et al. 2004) ⁽⁴⁾ P = 0.5607 d (Hartman et al. 2004) ⁽⁵⁾ P = 0.1886 d (Hartman et al. 2004) ⁽⁶⁾ P = 0.2948 d (Hartman et al. 2004) ⁽⁷⁾ P = 35.9 d (Watson 2006) ⁽⁸⁾ P = 4.924 d (Pigulski et al. 2009) ⁽⁹⁾ P = 2.18 d (Magalashvili & Kumishvili 1976) ⁽¹⁰⁾ P = 0.066677 d (Watson 2006) ⁽¹¹⁾ P = 0.38414 d (Watson 2006) ⁽¹²⁾ P = 8.4803 d (Otero 2007); 8.480322 d (Carrier et al. 2002) ⁽¹³⁾ P = 4.56427 d, eclipsing binary (Malkov et al. 2006) ⁽¹⁴⁾ Abt (1984) ⁽¹⁵⁾ Grigahcène et al. (2010) ⁽¹⁶⁾ Henry et al. (2001) ⁽¹⁷⁾ Sato & Kuji (1990) ⁽¹⁸⁾ Cannon (1925) ⁽¹⁹⁾ Abt (2004) ⁽²⁰⁾ Grenier et al. (1999) ⁽²¹⁾ Hill & Lynas-Gray (1977) ⁽²²⁾ Guetter (1968) ⁽²³⁾ Abt & Cardona (1984) ⁽²⁴⁾ Perryman et al. (1997) ⁽²⁵⁾ Macrae (1952) ⁽²⁶⁾ Floquet (1975) ⁽²⁷⁾ Floquet (1970) ⁽²⁸⁾ Lindoff (1972) ⁽²⁹⁾ Moore & Paddock (1950) ⁽³⁰⁾ Bidelman, Ratcliff & Svolopoulos (1988) ⁽³¹⁾ Stephenson (1986) ⁽³²⁾ Vyssotsky (1958) ⁽³³⁾ Hill & Schilt (1952) ⁽³⁴⁾ Cannon (1925) ⁽³⁵⁾ Kharchenko & Roeser (2009) ⁽³⁶⁾ Eclipsing binary (Prša et al. 2011) ⁽³⁷⁾ Balona et al. (2011c) ⁽³⁸⁾ Eclipsing binary (Slawson et al. 2011) ⁽³⁹⁾ Wright et al. (2003) ⁽⁴⁰⁾ Hoffleit (1951) ⁽⁴¹⁾ Molenda-Żakowicz et al. (2008)

★: binarity is suspected by inspection of Digitized Sky Survey and 2MASS images; °: spectroscopic binary

Table 2. Effective temperature (in K), $\log g$ (in dex), and $v \sin i$ values (in km s^{-1}) for the 750 sample stars

KIC ID	T_{eff} (K)		$\log g$ (dex)				$v \sin i$ (km s^{-1})				
	KIC ^a	Literature	Literature	Literature	Adopted*	KIC ^a	Literature	Literature	Adopted*	Spectra	Spectra
01162150	6870	6870 ± 290^a	3.47	3.5 ± 0.3^a
01294756	8410	8410 ± 290^a	3.92	3.9 ± 0.3^a
01432149	7270	7270 ± 290^a	3.99	4.0 ± 0.3^a
01571152°	7050	6500±130 ^b	7000± 75 ^g	...	7000 ± 75^g	3.16	4.49±0.21 ^b	4.15±0.26 ^g	4.2 ± 0.26^g	91±13 ^g	...
01571717	8110	8110 ± 290^a	3.98	4.0 ± 0.3^a
01573064	4639	4639 ± 290^a	2.54	2.5 ± 0.3^a
01718594	7500	7500 ± 290^a	3.95	4.0 ± 0.3^a
01995489	...	6410±120 ^b	6410 ± 120^b	...	4.43±0.21 ^b	...	4.43 ± 0.21^b
02020966	...	6560±130 ^b	6560 ± 130^b	...	3.50±0.23 ^b	...	3.50 ± 0.23^b
02162283	6680	6680 ± 290^a	4.07	4.1 ± 0.3^a
02163434	4590	4590 ± 290^a	2.67	2.7 ± 0.3^a
02166218	7150	7070± 80 ^g	7070 ± 80^g	3.35	3.84±0.21 ^b	2.69±0.19 ^g	2.69 ± 0.19^g	100± 3 ^g	...
02168333	8140	8140 ± 290^a	3.83	3.8 ± 0.3^a
02300165	7140	7140 ± 290^a	3.58	3.6 ± 0.3^a
02303365	7280	7280 ± 290^a	3.65	3.7 ± 0.3^a
02306469	4600	4600 ± 290^a	2.42	2.4 ± 0.3^a
02306716	4670	4670 ± 290^a	2.32	2.3 ± 0.3^a
02310479	4440	4440 ± 290^a	2.02	2.0 ± 0.3^a
02311130	4640	4640 ± 290^a	2.31	2.3 ± 0.3^a
02423932
02439660	7990	7990 ± 290^a	3.95	4.0 ± 0.3^a
02443055	4590	4590 ± 290^a	2.52	2.5 ± 0.3^a
02444598
02556297	4590	4590 ± 290^a	2.48	2.5 ± 0.3^a
02556387
02557115	4340	4340 ± 290^a	2.22	2.2 ± 0.3^a
02557430	6250	6250 ± 290^a	4.10	4.1 ± 0.3^a
02558273	6440	6440 ± 290^a	4.19	4.2 ± 0.3^a
02568519	6170	6170 ± 290^a	4.46	4.5 ± 0.3^a
02569639	8020	8020 ± 290^a	4.12	4.1 ± 0.3^a
02571868	7930	7930 ± 290^a	3.56	3.6 ± 0.3^a
02572386
02575161	...	6940±150 ^b	6940 ± 150^b	...	4.00±0.21 ^b	...	4.00 ± 0.21^b
02578251	...	6610±130 ^b	6610 ± 130^b	...	4.23±0.21 ^b	...	4.23 ± 0.21^b
02583658	4620	4620 ± 290^a	2.44	2.4 ± 0.3^a
02584202
02584908	8180	8180 ± 290^a	3.70	3.7 ± 0.3^a
02694337	7290	7290 ± 290^a	3.99	4.0 ± 0.3^a
02707479	7280	7280 ± 290^a	4.10	4.1 ± 0.3^a
02718596	4850	4850 ± 290^a	2.63	2.6 ± 0.3^a
02720582	7060	7060 ± 290^a	4.17	4.2 ± 0.3^a
02834796	4570	4570 ± 290^a	2.34	2.3 ± 0.3^a
02835795	...	6690±130 ^b	6690 ± 130^b	...	3.74±0.22 ^b	...	3.74 ± 0.22^b

Table 2. continued.

KIC ID			T_{eff} (K)			$\log g$ (dex)				$v \sin i$ (km s ⁻¹)	
	KIC ^a	Literature	Literature	Literature	Adopted*	KIC ^a	Literature	Literature	Adopted*	Spectra	Spectra
02853280	7320	7320 ± 290^a	3.59	3.6 ± 0.3^a
02855687	4770	4770 ± 290^a	2.52	2.5 ± 0.3^a
02860123	4620	4620 ± 290^a	2.53	2.5 ± 0.3^a
02969151	4700	4700 ± 290^a	2.37	2.4 ± 0.3^a
02970244	4720	4720 ± 290^a	2.24	2.2 ± 0.3^a
02972401	4660	4660 ± 290^a	2.59	2.6 ± 0.3^a
02975832
02987660	7310	7310 ± 290^a	3.59	3.6 ± 0.3^a
02989746
02995525	4850	4850 ± 290^a	2.64	2.6 ± 0.3^a
02997802
03097912	7880	7880 ± 290^a	3.56	3.6 ± 0.3^a
03111451
03119604	8210	8210 ± 290^a	4.04	4.0 ± 0.3^a
03119825
03215800
03217554 ^o	7800	7830±120 ^g	7830 ± 120^g	3.50	3.69±0.09 ^g	...	3.69 ± 0.09^g	228±18 ^g	...
03218637	7190	7190 ± 290^a	3.89	3.9 ± 0.3^a
03219256	7290	7500±150 ⁱ	7500 ± 150ⁱ	3.56	3.6± 0.1 ⁱ	...	3.6 ± 0.1ⁱ	90± 5 ⁱ	...
03220783	4590	4590 ± 290^a	2.58	2.6 ± 0.3^a
03222364	...	6750±130 ^b	6750 ± 130^b	...	3.82±0.21 ^b	...	3.82 ± 0.21^b
03230227	7970	7970 ± 290^a	3.89	3.9 ± 0.3^a
03231406	7800	7800 ± 290^a	3.76	3.8 ± 0.3^a
03240556	8420	8420 ± 290^a	3.85	3.9 ± 0.3^a
03245420	7870	7870 ± 290^a	3.66	3.7 ± 0.3^a
03248627	4660	4660 ± 290^a	2.32	2.3 ± 0.3^a
03327681	6500	6500 ± 290^a	3.68	3.7 ± 0.3^a
03331147	7020	7020 ± 290^a	3.55	3.6 ± 0.3^a
03337002	7200	7200 ± 290^a	3.60	3.6 ± 0.3^a
03347643	6780	6780 ± 290^a	4.07	4.1 ± 0.3^a
03348390	7140	6850±150 ^b	6850 ± 150^b	4.02	4.10±0.21 ^b	...	4.10 ± 0.21^b
03354022	4810	4810 ± 290^a	2.26	2.3 ± 0.3^a
03355066	4900	4900 ± 290^a	2.74	2.7 ± 0.3^a
03424493	7230	7230 ± 290^a	3.44	3.4 ± 0.3^a
03425802	8050	8050 ± 290^a	4.06	4.1 ± 0.3^a
03427144	4790	4790 ± 290^a	2.55	2.5 ± 0.3^a
03427365	4900	4900 ± 290^a	2.48	2.5 ± 0.3^a
03429637	6960	7200±150 ⁱ	7200 ± 150ⁱ	3.42	4.0± 0.1 ⁱ	...	4.0 ± 0.1ⁱ	50± 5 ⁱ	...
03437940	7430	7342±162 ^e	7700±120 ⁱ	...	7700 ± 120ⁱ	3.86	3.3 ± 0.2 ^e	4.1± 0.2 ⁱ	4.1 ± 0.2ⁱ	120± 5 ⁱ	...
03440495	7410	7410 ± 290^a	3.93	3.9 ± 0.3^a
03449373
03449625
03453494	7810	7750± 70 ^g	7750 ± 70^g	3.84	3.6 ± 0.3 ^g	...	3.6 ± 0.3^g	210±15 ^g	...

Table 2. continued.

KIC ID			T_{eff} (K)			$\log g$ (dex)				$v \sin i$ (km s ⁻¹)	
	KIC ^a	Literature	Literature	Literature	Adopted*	KIC ^a	Literature	Literature	Adopted*	Spectra	Spectra
03457434	4570	4570 ± 290^a	2.39	2.4 ± 0.3^a
03458097
03458318
03525951	4570	4570 ± 290^a	2.47	2.5 ± 0.3^a
03528578	5020	5020 ± 290^a	2.78	2.8 ± 0.3^a
03539153	7310	6790±140 ^b	6790 ± 140^b	3.81	3.73±0.21 ^b	...	3.73 ± 0.21^b
03546061	4770	4770 ± 290^a	2.34	2.3 ± 0.3^a
03558145	7340	7340 ± 290^a	4.11	4.1 ± 0.3^a
03629080	4830	4830 ± 290^a	2.74	2.7 ± 0.3^a
03633693	4530	4530 ± 290^a	2.38	2.4 ± 0.3^a
03634384	7480	7480 ± 290^a	3.86	3.9 ± 0.3^a
03643717	4410	4410 ± 290^a	2.02	2.0 ± 0.3^a
03644116	7500	7500 ± 290^a	4.11	4.1 ± 0.3^a
03655513
03655608	6600	6600 ± 290^a	4.33	4.3 ± 0.3^a
03663141
03733735	6440	6671±76 ^c	6760±0 ^d	6546±0 ^o	6671 ± 76^c	4.03	4.31±0.10 ^d	...	4.3 ± 0.1^d
03758717
03759814	4890	4890 ± 290^a	3.51	3.5 ± 0.3^a
03760002	7030	7030 ± 290^a	4.04	4.0 ± 0.3^a
03760826	8640	8640 ± 290^a	3.42	3.4 ± 0.3^a
03761641	8150	8150 ± 290^a	4.10	4.1 ± 0.3^a
03836911
03850810	7300	7300 ± 290^a	3.56	3.6 ± 0.3^a
03851151	8190	8190 ± 290^a	4.10	4.1 ± 0.3^a
03868032	8340	8340 ± 290^a	4.04	4.0 ± 0.3^a
03941283	7800	7800 ± 290^a	3.87	3.9 ± 0.3^a
03942911	7310	7310 ± 290^a	3.99	4.0 ± 0.3^a
03966357	7460	7460 ± 290^a	3.59	3.6 ± 0.3^a
03970729	7160	7160 ± 290^a	4.14	4.1 ± 0.3^a
04035667	7960	7960 ± 290^a	3.87	3.9 ± 0.3^a
04044353	8300	8300 ± 290^a	3.56	3.6 ± 0.3^a
04048488	5900	5900 ± 290^a	4.21	4.2 ± 0.3^a
04048494	7620	7620 ± 290^a	3.95	4.0 ± 0.3^a
04069477	7190	7190 ± 290^a	3.80	3.8 ± 0.3^a
04075519
04077032	6790	6790 ± 290^a	4.05	4.1 ± 0.3^a
04144300
04150611	6620	6620 ± 290^a	4.05	4.1 ± 0.3^a
04160876	8290	8290 ± 290^a	3.65	3.7 ± 0.3^a
04164363	7480	6470±120 ^b	6470 ± 120^b	3.83	3.84±0.22 ^b	...	3.84 ± 0.22^b
04168574	7710	7710 ± 290^a	3.50	3.5 ± 0.3^a
04170631	7500	7500 ± 290^a	3.47	3.5 ± 0.3^a

Table 2. continued.

KIC ID	T_{eff} (K)					$\log g$ (dex)				$v \sin i$ (km s $^{-1}$)	
	KIC ^a	Literature	Literature	Literature	Adopted*	KIC ^a	Literature	Literature	Adopted*	Spectra	Spectra
04180199	7220	7220 ± 290^a	3.91	3.9 ± 0.3^a
04252757	7650	7650 ± 290^a	3.72	3.7 ± 0.3^a
04269337	8000	8000 ± 290^a	3.58	3.6 ± 0.3^a
04281581	8140	8140 ± 290^a	3.84	3.8 ± 0.3^a
04383117	8250	8250 ± 290^a	3.63	3.6 ± 0.3^a
04476836	6760	6760 ± 290^a	3.88	3.9 ± 0.3^a
04480321	7150	7150 ± 290^a	3.87	3.9 ± 0.3^a
04488840	7130	7130 ± 290^a	3.54	3.5 ± 0.3^a
04550962	7290	7290 ± 290^a	3.54	3.5 ± 0.3^a
04556345	7290	7290 ± 290^a	3.87	3.9 ± 0.3^a
04570326	...	7000 ± 150 ⁱ	7000 ± 150ⁱ	...	4.0 ± 0.3 ⁱ	...	4.0 ± 0.3ⁱ	80 ± 20 ⁱ	...
04588487	7860	7860 ± 290^a	3.98	4.0 ± 0.3^a
04647763	6890	6850 ± 140 ^b	6850 ± 140^b	4.05	3.56 ± 0.22 ^b	...	3.56 ± 0.22^b
04649476	8330	8330 ± 290^a	3.87	3.9 ± 0.3^a
04671225	8230	8230 ± 290^a	3.27	3.3 ± 0.3^a
04677684	7860	7860 ± 290^a	3.32	3.3 ± 0.3^a
04758316	6980	6980 ± 290^a	4.07	4.1 ± 0.3^a
04768677	8360	8360 ± 290^a	3.97	4.0 ± 0.3^a
04840675	7110	7110 ± 290^a	3.55	3.6 ± 0.3^a
04850899	...	7132 ± 163 ^e	7244 ± 0 ^d	...	7132 ± 163^e	...	4.2 ± 0.2 ^e	4.26 ± 0.05 ^d	4.26 ± 0.05^d
04856630	7350	7350 ± 290^a	3.89	3.9 ± 0.3^a
04857678	...	6668 ± 0 ^o	6680 ± 290^o
04863077	7520	7520 ± 290^a	3.90	3.9 ± 0.3^a
04909697	7820	7820 ± 290^a	3.92	3.9 ± 0.3^a
04919818	7320	7320 ± 290^a	3.97	4.0 ± 0.3^a
04920125	7630	7630 ± 290^a	3.62	3.6 ± 0.3^a
04936524	7470	7470 ± 290^a	3.79	3.8 ± 0.3^a
04937257
04989900	7900	7900 ± 290^a	3.51	3.5 ± 0.3^a
05024150	5250	5250 ± 290^a
05024454	6210	6210 ± 290^a	4.11	4.1 ± 0.3^a
05024455	6760	6760 ± 290^a	4.44	4.4 ± 0.3^a
05024456	4300	4300 ± 290^a
05024750
05038228	6740	6740 ± 290^a	4.13	4.1 ± 0.3^a
05080290	5140	5140 ± 290^a	3.58	3.6 ± 0.3^a
05088308	6570	6740 ± 50 ^g	6740 ± 50^g	4.04	2.70 ± 0.13 ^g	...	2.70 ± 0.13^g	41 ± 1 ^g	...
05105754	7090	7090 ± 290^a	4.13	4.1 ± 0.3^a
05112786
05112932
05113797	8140	8140 ± 290^a	3.83	3.8 ± 0.3^a
05164767	...	6576 ± 121 ^e	6960 ± 80 ^g	6982 ± 0 ^o	6960 ± 80^g	...	3.11 ± 0.19 ^e	4.01 ± 0.37 ^g	3.11 ± 0.19^e	162 ± 9 ^g	...
05180796	7450	7450 ± 290^a	3.89	3.9 ± 0.3^a

Table 2. continued.

KIC ID	T_{eff} (K)					$\log g$ (dex)				$v \sin i$ (km s $^{-1}$)	
	KIC ^a	Literature	Literature	Literature	Adopted*	KIC ^a	Literature	Literature	Adopted*	Spectra	Spectra
05197256	7610	7610 ± 290^a	3.88	3.9 ± 0.3^a
05199464	6080	6080 ± 290^a	4.53	4.5 ± 0.3^a
05200084	7470	7470 ± 290^a	3.84	3.8 ± 0.3^a
05201088	5450	5450 ± 290^a
05209712	8360	8360 ± 290^a	3.95	4.0 ± 0.3^a
05217733	9120	9120 ± 290^a	4.22	4.2 ± 0.3^a
05219533	7410	7410 ± 290^a	3.94	3.9 ± 0.3^a	115 ⁿ	...
05272673	7120	7120 ± 290^a	3.76	3.8 ± 0.3^a
05294571	6580	6580 ± 290^a	4.07	4.1 ± 0.3^a
05296877	6660	6500±200 ⁱ	6500 ± 200ⁱ	4.11	3.8± 0.3 ⁱ	...	3.8 ± 0.3ⁱ	200±20 ⁱ	...
05356349	8290	8290 ± 290^a	3.91	3.9 ± 0.3^a
05371747	7070	7070 ± 290^a	4.03	4.0 ± 0.3^a
05391416	8060	8060 ± 290^a	3.89	3.9 ± 0.3^a
05428254	7390	7390 ± 290^a	3.93	3.9 ± 0.3^a
05436432	8330	8330 ± 290^a	3.90	3.9 ± 0.3^a
05437206	7710	7710 ± 290^a	3.67	3.7 ± 0.3^a
05446068 ^o	5340	5980±120 ^g	5980 ± 120^g	4.48	3.58±0.28 ^g	...	3.58 ± 0.28^g	11± 1 ^g	...
05473171	7450	7450 ± 290^a	3.63	3.6 ± 0.3^a
05474427	6880	6880 ± 290^a	4.14	4.1 ± 0.3^a
05476495	7360	7360 ± 290^a	3.92	3.9 ± 0.3^a
05476864	6580	6550±120 ^b	6550 ± 120^b	4.11	3.72±0.22 ^b	...	3.72 ± 0.22^b
05513861	6170	6610±140 ^b	6610 ± 140^b	4.43	4.48±0.21 ^b	...	4.48 ± 0.21^b
05603049	8000	8000 ± 290^a	3.71	3.7 ± 0.3^a
05630362	7360	7360 ± 290^a	3.53	3.5 ± 0.3^a
05632093	8090	8090 ± 290^a	4.07	4.1 ± 0.3^a
05641711	7160	7160 ± 290^a	3.97	4.0 ± 0.3^a
05709664	7200	7200 ± 290^a	4.04	4.0 ± 0.3^a
05722346	6670	6670 ± 290^a	4.21	4.2 ± 0.3^a
05724048	6520	6520 ± 290^a	4.08	4.1 ± 0.3^a
05724440	7290	7699± 81 ^c	7537±186 ^e	7350±120 ⁱ	7350 ± 120ⁱ	3.57	3.98±0.21 ^e	3.6± 0.3 ⁱ	3.6 ± 0.3ⁱ	220± 5 ⁱ	...
05724810	7330	7330 ± 290^a	3.88	3.9 ± 0.3^a
05768203	6450	6450 ± 290^a	3.95	3.9 ± 0.3^a
05772411	6760	6760 ± 290^a	4.18	4.2 ± 0.3^a
05774557	7050	7050 ± 290^a	3.99	4.0 ± 0.3^a
05785707	8010	7940± 80 ^g	7940 ± 80^g	3.62	3.44±0.26 ^g	...	3.44 ± 0.26^g	170±11 ^g	...
05810113	6360	6480±120 ^b	6480 ± 120^b	4.22	3.60±0.23 ^b	...	3.60 ± 0.23^b
05857714	6710	6710 ± 290^a	3.80	3.8 ± 0.3^a
05880360	7690	7690 ± 290^a	3.64	3.6 ± 0.3^a
05940273	8010	8010 ± 290^a	3.59	3.6 ± 0.3^a
05954264	6720	6900±146 ^e	6900 ± 146^e	4.15	3.86±0.21 ^e	...	3.86 ± 0.21^e
05965837	6520	6975±200 ⁱ	6975 ± 200ⁱ	4.15	4.0± 0.4 ⁱ	...	4.0 ± 0.3ⁱ	20±10 ⁱ	...
05980337	7680	7680 ± 290^a	3.76	3.8 ± 0.3^a
05988140	7450	7267±163 ^e	7400±150 ⁱ	...	7400 ± 150ⁱ	3.54	3.32±0.23 ^e	3.7± 0.3 ⁱ	3.32 ± 0.23^e	70±20 ⁱ	...

Table 2. continued.

KIC ID	T_{eff} (K)					$\log g$ (dex)				$v \sin i$ (km s^{-1})	
	KIC ^a	Literature	Literature	Literature	Adopted*	KIC ^a	Literature	Literature	Adopted*	Spectra	Spectra
06032730	7110	7110 ± 290^a	3.79	3.8 ± 0.3^a
06067817	7840	7840 ± 290^a	3.86	3.9 ± 0.3^a
06123324	6670	6700±130 ^b	6641±123 ^e	...	6700 ± 130^b	3.40	3.09±0.23 ^b	3.06±0.21 ^e	3.1 ± 0.3^b
06141372	7080	7080 ± 290^a	4.21	4.2 ± 0.3^a
06142919	7000	7000 ± 290^a	4.02	4.0 ± 0.3^a
06187665	6880	6025± 60 ^c	6025± 0 ^d	...	6025 ± 60^c	4.01	4.27±0.11 ^d	...	4.27 ± 0.11^d
06199731	7850	7850 ± 290^a	3.55	3.6 ± 0.3^a
06268890	7280	7280 ± 290^a	3.49	3.5 ± 0.3^a
06279848	...	6826±140 ^e	6826 ± 140^e	...	3.8±0.2 ^e	...	3.8 ± 0.2^e
06289468	8270	8150±100 ^g	8150 ± 100^g	3.74	3.29±0.09 ^g	...	3.29 ± 0.09^g	148± 7 ^g	...
06301745	6790	6740±130 ^b	6740 ± 130^b	4.13	4.01±0.21 ^b	...	4.01 ± 0.21^b
06381306	8060	8060 ± 290^a	3.63	3.6 ± 0.3^a
06432054	7090	7287±167 ^e	7400±150 ^l	...	7400 ± 150^l	3.85	3.81±0.19 ^e	3.9±0.2 ^l	3.81 ± 0.19^e
06440930	8320	8320 ± 290^a	4.09	4.1 ± 0.3^a
06443122	7480	7480 ± 290^a	3.54	3.5 ± 0.3^a
06446951	7380	7380 ± 290^a	4.06	4.1 ± 0.3^a
06448112	8150	8150 ± 290^a	4.01	4.0 ± 0.3^a
06462033	8390	8390 ± 290^a	4.32	4.3 ± 0.3^a
06500578	7840	7840 ± 290^a	3.64	3.6 ± 0.3^a
06509175	7300	7520± 60 ^g	7520 ± 60^g	3.52	3.29±0.3 ^g	...	3.3 ± 0.3^g	132± 8 ^g	...
06519869	7150	7150 ± 290^a	3.80	3.8 ± 0.3^a
06586052	7520	7520 ± 290^a	4.05	4.1 ± 0.3^a
06587551	8380	8870±190 ^g	8870 ± 190^g	3.93	3.78±0.09 ^g	...	3.78 ± 0.09^g	138± 9 ^g	...
06590403	7030	7030 ± 290^a	3.93	3.9 ± 0.3^a
06606229	6750	6750 ± 290^a	4.09	4.1 ± 0.3^a
06614168	7270	7270 ± 290^a	4.14	4.1 ± 0.3^a
06629106	7070	7070 ± 290^a	3.95	4.0 ± 0.3^a
06668729	7770	7770 ± 290^a	3.48	3.5 ± 0.3^a
06670742	7450	6386± 62 ^c	6386 ± 62^c	3.61	3.6 ± 0.3^a
06678614	7410	7410 ± 290^a	3.85	3.9 ± 0.3^a
06694649	7750	7750 ± 290^a	3.66	3.7 ± 0.3^a
06756386	7990	7900± 70 ^g	7900 ± 70^g	3.51	3.17±0.10 ^g	...	3.2 ± 0.1^g	190±12 ^g	...
06756481	7310	7310 ± 290^a	3.52	3.5 ± 0.3^a
06761539	7240	7240 ± 290^a	4.04	4.0 ± 0.3^a
06776331	7650	7650 ± 290^a	3.72	3.7 ± 0.3^a
06790335	7690	7690 ± 290^a	3.52	3.5 ± 0.3^a
06804821	7480	7480 ± 290^a	3.65	3.7 ± 0.3^a
06865077	7770	7770 ± 290^a	3.62	3.6 ± 0.3^a
06922690	7320	7320 ± 290^a	3.61	3.6 ± 0.3^a
06923424	7060	7060 ± 290^a	4.16	4.2 ± 0.3^a
06937758	7840	7840 ± 290^a	3.47	3.5 ± 0.3^a
06939291	7140	7140 ± 290^a	3.52	3.5 ± 0.3^a
06947064	8170	8170 ± 290^a	3.91	3.9 ± 0.3^a

Table 2. continued.

KIC ID	T_{eff} (K)					$\log g$ (dex)				$v \sin i$ (km s $^{-1}$)	
	KIC ^a	Literature	Literature	Literature	Adopted*	KIC ^a	Literature	Literature	Adopted*	Spectra	Spectra
06951642	7180	7180 ± 290^a	3.37	3.4 ± 0.3^a
06965789	7650	7650 ± 290^a	3.39	3.4 ± 0.3^a
07007103	6910	6910 ± 290^a	4.06	4.1 ± 0.3^a
07106205	6970	6900±140 ^b	6900 ± 140^b	4.05	3.73±0.21 ^b	...	3.73 ± 0.21^b
07106648	7010	7010 ± 290^a	4.11	4.1 ± 0.3^a
07109598	7270	7270 ± 290^a	4.08	4.1 ± 0.3^a
07119530	7780	7608±190 ^e	7500±200 ⁱ	...	7500 ± 200ⁱ	3.49	3.26±0.21 ^e	3.6± 0.3 ⁱ	3.26 ± 0.21^e	200±20 ⁱ	...
07122746	8340	7740±200 ^b	7740 ± 200^b	3.84	4.00±0.18 ^b	...	4.00 ± 0.18^b
07204237	8070	8070 ± 290^a	4.05	4.1 ± 0.3^a
07211759	8220	8220 ± 290^a	3.77	3.8 ± 0.3^a
07212040	7500	7500 ± 290^a	3.97	4.0 ± 0.3^a
07215607	6530	6530 ± 290^a	4.06	4.1 ± 0.3^a
07217483	6940	6940 ± 290^a	3.89	3.9 ± 0.3^a
07220356	6340	6340 ± 290^a	4.26	4.3 ± 0.3^a
07265427	7560	7560 ± 290^a	4.13	4.1 ± 0.3^a
07287118	7850	7850 ± 290^a	3.76	3.8 ± 0.3^a
07300387	7000	7000 ± 290^a	3.60	3.6 ± 0.3^a
07304385	6890	6890 ± 290^a	3.60	3.6 ± 0.3^a
07338125	7860	7860 ± 290^a	3.96	4.0 ± 0.3^a
07350486	7290	7290 ± 290^a	3.65	3.7 ± 0.3^a
07352425	6890	6890 ± 290^a	4.07	4.1 ± 0.3^a
07352776	7460	7460 ± 290^a	3.99	4.0 ± 0.3^a
07385478	6480	6480 ± 290^a	3.87	3.9 ± 0.3^a
07436266	7020	7020 ± 290^a	4.05	4.1 ± 0.3^a
07450284	7930	7930 ± 290^a	3.74	3.7 ± 0.3^a
07502559	7470	7470 ± 290^a	3.89	3.9 ± 0.3^a
07533694	7860	7860 ± 290^a	3.80	3.8 ± 0.3^a
07548061	5000	5370 ± 120 ^q	5370 ± 120^q	2.42	1.50±0.35 ^q	...	2.4 ± 0.3^a	12± 2 ^q	...
07548479	7340	7500±250 ^r	7500 ± 250^l	3.84	3.90±0.25 ^l	...	3.90 ± 0.25^l	10± 2 ^l	...
07553237	6930	6930 ± 290^a	4.12	4.1 ± 0.3^a
07583939	8310	8310 ± 290^a	3.95	3.9 ± 0.3^a
07596250	6870	6870 ± 290^a	3.90	3.9 ± 0.3^a
07662076	7050	7050 ± 290^a	4.01	4.0 ± 0.3^a
07668791	8150	8150 ± 290^a	3.89	3.9 ± 0.3^a
07669848	19 ^o	19.4±2.0 ^o
07694191	7850	7850 ± 290^a	3.54	3.5 ± 0.3^a
07697795	7480	7480 ± 290^a	3.56	3.6 ± 0.3^a
07699056	7410	7410 ± 290^a	3.67	3.7 ± 0.3^a
07702705	7310	6710±130 ^b	6710 ± 130^b	4.00	2.88±0.23 ^b	...	2.88 ± 0.23^b
07732458	7550	7550 ± 290^a	3.64	3.6 ± 0.3^a
07742739	7170	7170 ± 290^a	3.89	3.9 ± 0.3^a
07748238	7230	7260± 64 ^s	7260 ± 64^s	3.47	4.06±0.28 ^s	...	4.06 ± 0.28^s	119± 6 ^s	...
07756853	8060	8060 ± 290^a	3.94	3.9 ± 0.3^a

Table 2. continued.

KIC ID	T_{eff} (K)					$\log g$ (dex)				$v \sin i$ (km s ⁻¹)	
	KIC ^a	Literature	Literature	Literature	Adopted*	KIC ^a	Literature	Literature	Adopted*	Spectra	Spectra
07767565
07770282	7450	7450 ± 290^a	3.50	3.5 ± 0.3^a
07771991	7300	7300 ± 290^a	3.53	3.5 ± 0.3^a
07773133	6640	6640 ± 290^a	3.52	3.5 ± 0.3^a
07777435	8120	8120 ± 290^a	3.75	3.8 ± 0.3^a
07798339	6680	6880±144 ^e	6700±200 ⁱ	6745± 0 ^o	6880 ± 144^e	3.40	3.90±0.21 ^e	3.7± 0.3 ⁱ	3.90 ± 0.21^e	15.4±2.0 ⁿ	15± 5 ^{g,i}
07827131	8290	8290 ± 290^a	3.49	3.5 ± 0.3^a
07831302	8160	8160 ± 290^a	3.86	3.9 ± 0.3^a
07834612	7450	7450 ± 290^a	3.67	3.7 ± 0.3^a
07842286	7660	7660 ± 290^a	3.77	3.8 ± 0.3^a
07842621	7620	7620 ± 290^a	3.54	3.5 ± 0.3^a
07848288	7380	7380 ± 290^a	3.52	3.5 ± 0.3^a
07890526	7080	7080 ± 290^a	4.07	4.1 ± 0.3^a
07900367	6970	6970 ± 290^a	4.14	4.1 ± 0.3^a
07908633	7840	7840 ± 290^a	3.73	3.7 ± 0.3^a
07959867	8480	8480 ± 290^a	3.90	3.9 ± 0.3^a
07977996	7120	7120 ± 290^a	3.77	3.8 ± 0.3^a
07985370	5610	5610 ± 290^a	4.60	4.6 ± 0.3^a
08029546	7120	7120 ± 290^a	3.89	3.9 ± 0.3^a
08043961	6350	6350 ± 290^a	3.62	3.6 ± 0.3^a
08054146	8150	6770± 150 ^b	6770 ± 150^b	3.67	3.08± 0.27 ^b	...	3.7 ± 0.3^a
08103917	7130	7130 ± 290^a	4.16	4.2 ± 0.3^a
08104589	6510	6510 ± 290^a	4.29	4.3 ± 0.3^a
08123127	7160	7160 ± 290^a	3.69	3.7 ± 0.3^a
08143903	3680	3680 ± 290^a	4.22	4.2 ± 0.3^a
08144674	7290	7290 ± 290^a	3.85	3.9 ± 0.3^a
08145477	6800	6800 ± 290^a	4.06	4.1 ± 0.3^a
08149341	7540	7540 ± 290^a	4.00	4.0 ± 0.3^a
08159135	5020	5020 ± 290^a	4.14	4.1 ± 0.3^a
08197761	7070	7070 ± 290^a	4.09	4.1 ± 0.3^a
08197788	8010	7500±150 ⁱ	7500 ± 150ⁱ	3.98	4.0± 0.3 ⁱ	...	4.0 ± 0.3ⁱ	230±20 ⁱ	...
08211500	7400	7400 ± 290^a	3.91	3.9 ± 0.3^a
08218419	4550	4550 ± 290^a	2.20	2.2 ± 0.3^a
08222685
08223568	6790	6740±140 ^b	6740 ± 140^b	3.88	4.38±0.21 ^b	...	4.38 ± 0.21^b
08223987	5550	5550 ± 290^a	4.45	4.5 ± 0.3^a
08230025	7280	7280 ± 290^a	3.48	3.5 ± 0.3^a
08245366
08248630	7310	7310 ± 290^a	3.74	3.7 ± 0.3^a
08264061	7230	7230 ± 290^a	4.10	4.1 ± 0.3^a
08264075	7650	7650 ± 290^a	4.06	4.1 ± 0.3^a
08264274	7640	7640 ± 290^a	3.74	3.7 ± 0.3^a
08264404	7890	7500±200 ⁱ	7500 ± 200ⁱ	3.73	3.7± 0.3 ⁱ	...	3.7 ± 0.3ⁱ	250±20 ⁱ	...

Table 2. continued.

KIC ID	KIC ^a	Literature	T_{eff} (K)			KIC ^a	log g (dex)			$v \sin i$ (km s ⁻¹)	
			Literature	Literature	Adopted*		Literature	Literature	Adopted*	Spectra	Spectra
08264546	7630	7630 ± 290^a	3.96	4.0 ± 0.3^a
08264583	8360	7240±160 ^b	7240 ± 160^b	3.64	2.97±0.22 ^b	...	3.97 ± 0.22^b
08264588
08264617	7310	7310 ± 290^a	4.12	4.1 ± 0.3^a
08264674	8030	8030 ± 290^a	3.69	3.7 ± 0.3^a
08264698	8010	7500±200 ⁱ	7500 ± 200ⁱ	3.79	3.9± 0.2 ⁱ	...	3.9 ± 0.2ⁱ	210±20 ⁱ	...
08283796	5500	5500 ± 290^a	4.05	4.1 ± 0.3^a
08293302	6450	6450 ± 290^a	4.22	4.2 ± 0.3^a
08323104	7590	7590 ± 290^a	3.92	3.9 ± 0.3^a
08330056	7240	7240 ± 290^a	4.10	4.1 ± 0.3^a
08330092	6900	6900 ± 290^a	4.12	4.1 ± 0.3^a
08330463	6020	6020 ± 290^a	4.86	4.9 ± 0.3^a
08330778	7620	7620 ± 290^a	4.03	4.0 ± 0.3^a
08352420	6560	6560 ± 290^a	4.30	4.3 ± 0.3^a
08355130	7040	7040 ± 290^a	4.11	4.1 ± 0.3^a
08355837	5860	5860 ± 290^a	4.30	4.3 ± 0.3^a
08397426	7030	7030 ± 290^a	3.55	3.6 ± 0.3^a
08415752	7780	7780 ± 290^a	4.00	4.0 ± 0.3^a
08429756	7360	7360 ± 290^a	3.67	3.7 ± 0.3^a
08446738	7150	7150 ± 290^a	3.93	3.9 ± 0.3^a
08454553	6670	6670 ± 290^a	3.58	3.6 ± 0.3^a
08459354	7430	7430 ± 290^a	3.62	3.6 ± 0.3^a
08460025
08460993	6710	6710 ± 290^a	3.98	4.0 ± 0.3^a
08479107	5050	5050 ± 290^a	4.52	4.5 ± 0.3^a
08482540	6360	6360 ± 290^a	4.33	4.3 ± 0.3^a
08488065	6190	6190 ± 290^a	4.20	4.2 ± 0.3^a
08489712	8350	8350 ± 290^a	3.52	3.5 ± 0.3^a
08499639	6580	6580 ± 290^a	4.12	4.1 ± 0.3^a
08507325	7140	7140 ± 290^a	3.43	3.4 ± 0.3^a
08516008	8320	8320 ± 290^a	3.60	3.6 ± 0.3^a
08516686	8240	8240 ± 290^a	4.02	4.0 ± 0.3^a
08525286	7350	7350 ± 290^a	4.19	4.2 ± 0.3^a
08545456	7860	7860 ± 290^a	3.87	3.9 ± 0.3^a
08560996	7870	7870 ± 290^a	3.61	3.6 ± 0.3^a
08565229	7740	7740 ± 290^a	3.88	3.9 ± 0.3^a
08579615	8260	8260 ± 290^a	3.98	4.0 ± 0.3^a
08583770	7660	9000±200 ⁱ	9000 ± 200ⁱ	3.47	3.0± 0.2 ⁱ	...	3.0 ± 0.2ⁱ	130±10 ⁱ	...
08590553	7300	7300 ± 290^a	3.98	4.0 ± 0.3^a
08608260	7890	7890 ± 290^a	3.91	3.9 ± 0.3^a
08623953	7730	7720± 50 ^g	7720 ± 50^g	3.74	3.47±0.08 ^g	...	3.47 ± 0.08^g	84± 4 ^g	...
08651452	6940	6940 ± 290^a	4.07	4.1 ± 0.3^a
08655712	7380	7380 ± 290^a	3.45	3.4 ± 0.3^a

Table 2. continued.

KIC ID	T_{eff} (K)		$\log g$ (dex)			$v \sin i$ (km s $^{-1}$)					
	KIC ^a	Literature	Literature	Literature	Adopted*	KIC ^a	Literature	Literature	Adopted*	Spectra	Spectra
08695156	7640	7640 ± 290^a	3.37	3.4 ± 0.3^a
08703413	7710	7710 ± 290^a	3.77	3.8 ± 0.3^a
08714886	9140	19 000±0 ^f	19 000±290^f	4.09	4.3 ^f	...	4.3 ± 0.3^f
08717065	7440	7440 ± 290^a	3.76	3.8 ± 0.3^a
08738244	8170	8260±160 ^g	8260 ± 160^g	4.15	3.25±0.12 ^g	...	3.25 ± 0.12^g	133± 8 ^g	...
08742449	5580	5580 ± 290^a	4.38	4.4 ± 0.3^a
08746834	4690	4690 ± 290^a	3.28	3.3 ± 0.3^a
08747415	5030	5030 ± 290^a	3.51	3.5 ± 0.3^a
08748251	6800	6800 ± 290^a	4.15	4.2 ± 0.3^a
08750029	...	7340± 60 ^g	7340 ± 60^g	...	3.72±0.3 ^g	...	3.7 ± 0.3^g	165± 8 ^g	...
08766619	6990	6570±120 ^b	6570 ± 120^b	3.81	3.59±0.22 ^b	...	3.59 ± 0.22^b
08827821	7390	7390 ± 290^a	3.69	3.7 ± 0.3^a
08838457	6200	6200 ± 290^a	3.85	3.9 ± 0.3^a
08869302	7280	7280 ± 290^a	4.18	4.2 ± 0.3^a
08869892
08871304	7150	7150 ± 290^a	3.43	3.4 ± 0.3^a
08881697	7730	7730 ± 290^a	3.86	3.9 ± 0.3^a
08915335	7770	7770 ± 290^a	3.48	3.5 ± 0.3^a
08933391	7630	7616±193 ^e	7616 ± 193^e	3.69	3.71±0.19 ^e	...	3.71 ± 0.19^e
08940640
08972966	7660	7660 ± 290^a	3.80	3.8 ± 0.3^a
08975515	7180	7180 ± 290^a	3.90	3.9 ± 0.3^a
09020157	6960	6880±150 ^b	6880 ± 150^b	3.97	4.12±0.21 ^b	...	4.12 ± 0.21^b
09020199	6540	6540 ± 290^a	3.98	4.0 ± 0.3^a
09052363	7610	7610 ± 290^a	3.74	3.7 ± 0.3^a
09072011
09073007
09073985	5990	5990 ± 290^a	4.37	4.4 ± 0.3^a
09077192	4750	4750 ± 290^a	4.40	4.4 ± 0.3^a
09108615	6710	6710 ± 290^a	3.81	3.8 ± 0.3^a
09111056	6800	6800 ± 290^a	3.65	3.7 ± 0.3^a
09117875
09138872	7500	7500 ± 290^a	4.03	4.0 ± 0.3^a
09143785	7600	7600 ± 290^a	4.25	4.3 ± 0.3^a
09147229	7300	7300 ± 290^a	3.57	3.6 ± 0.3^a
09156808	7070	7070 ± 290^a	3.94	3.9 ± 0.3^a
09201644
09204672	4030	4030 ± 290^a	1.82	1.8 ± 0.3^a
09204718	7150	7150 ± 290^a	3.93	3.9 ± 0.3^a
09210037
09216367	7840	7840 ± 290^a	3.65	3.7 ± 0.3^a
09222942	7000	7000 ± 290^a	3.99	4.0 ± 0.3^a
09229318	7140	7140 ± 290^a	3.65	3.7 ± 0.3^a

Table 2. continued.

KIC ID	T_{eff} (K)					$\log g$ (dex)				$v \sin i$ (km s $^{-1}$)	
	KIC ^a	Literature	Literature	Literature	Adopted*	KIC ^a	Literature	Literature	Adopted*	Spectra	Spectra
09246481	8050	8050 ± 290^a	3.79	3.8 ± 0.3^a
09264399	5060	5060 ± 290^a	4.46	4.5 ± 0.3^a
09264462	4870	4870 ± 290^a	3.31	3.3 ± 0.3^a
09267042	8130	8130 ± 290^a	3.81	3.8 ± 0.3^a
09268087
09272082
09274000	5660	5660 ± 290^a	4.46	4.5 ± 0.3^a
09291618	7610	7610 ± 290^a	3.61	3.6 ± 0.3^a
09306095	6340	6340 ± 290^a	4.63	4.6 ± 0.3^a
09324334	7250	7250 ± 290^a	4.06	4.1 ± 0.3^a
09327993	4600	4600 ± 290^a	2.37	2.4 ± 0.3^a
09336219	6520	6520 ± 290^a	4.26	4.3 ± 0.3^a
09351622	7450	7450 ± 290^a	3.53	3.5 ± 0.3^a
09353572	7190	7190 ± 290^a	3.99	4.0 ± 0.3^a
09368220	6660	6660 ± 290^a	4.10	4.1 ± 0.3^a
09386259	5810	5810 ± 290^a	4.30	4.3 ± 0.3^a
09391395	7310	7310 ± 290^a	3.96	4.0 ± 0.3^a
09395246
09408694	7480	6810±130 ^b	6810 ± 130^b	3.62	3.80±0.19 ^b	...	3.80 ± 0.19^b
09413057	8470	8630±140 ^g	8630 ± 140^g	3.87	3.62±0.07 ^g	...	3.62 ± 0.07^g	165 ± 8 ^g	...
09450940	8210	8210 ± 290^a	4.21	4.2 ± 0.3^a
09451598	6060	6060 ± 290^a	4.56	4.6 ± 0.3^a
09453075	8060	8060 ± 290^a	4.00	4.0 ± 0.3^a
09458750	5070	5070 ± 290^a	3.69	3.7 ± 0.3^a
09473000	7130	7130 ± 290^a	3.88	3.9 ± 0.3^a
09489590	7160	7160 ± 290^a	4.09	4.1 ± 0.3^a
09490042	7060	7060 ± 290^a	3.98	4.0 ± 0.3^a
09490067	6880	6880 ± 290^a	4.07	4.1 ± 0.3^a
09509296	7400	7400 ± 290^a	3.61	3.6 ± 0.3^a
09514879	5880	5880 ± 290^a	4.10	4.1 ± 0.3^a
09520434
09520864
09532644	7300	7300 ± 290^a	3.56	3.6 ± 0.3^a
09533449
09533489
09550886	7490	7490 ± 290^a	3.89	3.9 ± 0.3^a
09551281	7450	7450 ± 290^a	3.65	3.7 ± 0.3^a
09580794	7300	7300 ± 290^a	4.05	4.1 ± 0.3^a
09582720	5620	5620 ± 290^a	4.49	4.5 ± 0.3^a
09593997	7620	7620 ± 290^a	3.62	3.6 ± 0.3^a
09594100	6520	6520 ± 290^a	4.51	4.5 ± 0.3^a
09604762	7290	7290 ± 290^a	3.77	3.8 ± 0.3^a
09630640	6530	6530 ± 290^a	4.10	4.1 ± 0.3^a

Table 2. continued.

KIC ID	KIC ^a	Literature	T_{eff} (K)			KIC ^a	log g (dex)			$v \sin i$ (km s ⁻¹)	
			Literature	Literature	Adopted*		Literature	Literature	Adopted*	Spectra	Spectra
09632537	7820	7820 ± 290^a	3.83	3.8 ± 0.3^a
09640204	6440	6440 ± 290^a	4.25	4.3 ± 0.3^a
09642894	7050	7050 ± 290^a	4.09	4.1 ± 0.3^a
09643982	6580	6580 ± 290^a	4.20	4.2 ± 0.3^a
09650390	8390	8390 ± 290^a	3.68	3.7 ± 0.3^a
09651065	7390	7010±150 ^b	7010 ± 150^b	3.67	3.82±0.21 ^b	...	3.82 ± 0.21^b
09654789	6990	6990 ± 290^a	4.09	4.1 ± 0.3^a
09655055	7620	7620 ± 290^a	3.48	3.5 ± 0.3^a
09655114	7750	7400±200 ⁱ	7400 ± 200ⁱ	3.78	3.9± 0.3 ⁱ	...	3.9 ± 0.3ⁱ	150±20 ⁱ	...
09655151	7060	7060 ± 290^a	4.18	4.2 ± 0.3^a
09655177	6900	6900 ± 290^a	3.87	3.9 ± 0.3^a
09655393	7570	7570 ± 290^a	4.06	4.1 ± 0.3^a
09655422	7600	7600 ± 290^a	3.38	3.4 ± 0.3^a
09655433	8300	8300 ± 290^a
09655438	6970	6970 ± 290^a	4.09	4.1 ± 0.3^a
09655487
09655501	7740	7740 ± 290^a	3.88	3.9 ± 0.3^a
09655514	7440	7440 ± 290^a	3.61	3.6 ± 0.3^a
09655800	6780	6780 ± 290^a	4.16	4.2 ± 0.3^a
09656348	7670	7190±160 ^b	7190 ± 160^b	3.52	3.9±0.2 ^b	...	3.9 ± 0.2^b
09664869	7190	7190 ± 290^a	3.99	4.0 ± 0.3^a
09673293	8230	8230 ± 290^a	3.87	3.9 ± 0.3^a
09693282
09696853	7130	7130 ± 290^a	4.14	4.1 ± 0.3^a
09699950
09700145	7590	7590 ± 290^a	4.03	4.0 ± 0.3^a
09700322	...	6700±100 ^m	6700 ± 100^m	...	3.7± 0.1 ^m	...	3.7 ± 0.1^m	19± 1 ^m	...
09700679	5070	5070 ± 290^a	4.45	4.5 ± 0.3^a
09703601	5720	5720 ± 290^a	4.89	4.9 ± 0.3^a
09716107	7460	7460 ± 290^a	3.65	3.7 ± 0.3^a
09716350
09716947	7300	7300 ± 290^a	4.04	4.0 ± 0.3^a
09760531	6740	6740 ± 290^a	4.03	4.0 ± 0.3^a
09762713	6960	6960 ± 290^a	4.09	4.1 ± 0.3^a
09764712	6020	6020 ± 290^a	4.68	4.7 ± 0.3^a
09764965	7460	7470± 45 ^g	7470 ± 45^g	4.09	3.78±0.19 ^g	...	3.78 ± 0.19^g	85± 3 ^g	...
09773512	7960	7960 ± 290^a	3.70	3.7 ± 0.3^a
09775385	7450	7450 ± 290^a	4.05	4.5 ± 0.3^a
09775454	...	7109±159 ^e	7050±150 ⁱ	...	7050 ± 150ⁱ	...	3.91±0.21 ^e	4.0± 0.3 ⁱ	3.91 ± 0.21ⁱ	70± 5 ⁱ	...
09776474
09777532
09790479	7840	7840 ± 290^a	4.04	4.0 ± 0.3^a
09812351	7790	7847± 87 ^g	7847 ± 87^g	3.47	3.15±0.23 ^g	...	3.15 ± 0.23^g	56± 4 ^g	...

Table 2. continued.

KIC ID	T_{eff} (K)		$\log g$ (dex)				$v \sin i$ (km s $^{-1}$)				
	KIC ^a	Literature	Literature	Literature	Adopted*	KIC ^a	Literature	Literature	Adopted*	Spectra	Spectra
09813078	...	6811±138 ^b	6811 ±138^b	...	3.67±0.21 ^b	...	3.67 ±0.21^b
09818269
09836020	7480	7480 ±290^a	4.09	4.1 ±0.3^a
09845907	7940	7940 ±290^a	4.03	4.0 ±0.3^a
09851142	6800	7047±156 ^e	7047 ±156^e	3.95	3.97±0.21 ^e	...	3.97 ±0.21^e
09874181	7180	7180 ±290^a	4.08	4.1 ±0.3^a
09881909	6810	6810 ±290^a	3.86	3.9 ±0.3^a
09885882	5090	5090 ±290^a	2.63	2.6 ±0.3^a
09909300	6670	6670 ±290^a	4.19	4.2 ±0.3^a
09913481	7410	7410 ±290^a	3.53	3.5 ±0.3^a
09944208	7040	7040 ±290^a	4.29	4.3 ±0.3^a
09944730	5920	5920 ±290^a	4.18	4.2 ±0.3^a
09970568	7790	7790 ±290^a	3.64	3.6 ±0.3^a
09991621	5270	5270 ±290^a	4.35	4.4 ±0.3^a
09991766	6050	6050 ±290^a	4.25	4.3 ±0.3^a
09994789	5290	5290 ±290^a	3.85	3.9 ±0.3^a
09995464	4850	4850 ±290^a	2.64	2.6 ±0.3^a
10000056	8200	8200 ±290^a	3.96	4.0 ±0.3^a
10002897	7490	7490 ±290^a	3.74	3.7 ±0.3^a
10004510	4340	4340 ±290^a	4.60	4.6 ±0.3^a
10006158	4680	4680 ±290^a	2.39	2.4 ±0.3^a
10014548	7160	7160 ±290^a	3.92	3.9 ±0.3^a
10030943	6700	6700 ±290^a	4.30	4.3 ±0.3^a
10035772	7290	7290 ±290^a	3.48	3.5 ±0.3^a
10056217	6000	6000 ±290^a	4.28	4.3 ±0.3^a
10056297	7160	7160 ±290^a	4.03	4.0 ±0.3^a
10057129	4860	4860 ±290^a	3.17	3.2 ±0.3^a
10062593	5270	5270 ±290^a	4.93	4.9 ±0.3^a
10064111	7220	7220 ±290^a	4.05	4.1 ±0.3^a
10065244	7260	7260 ±290^a	3.98	4.0 ±0.3^a
10068892	4610	4610 ±290^a	2.29	2.3 ±0.3^a
10069934	7060	7060 ±290^a	4.01	4.0 ±0.3^a
10073601	7100	6680±130 ^b	6680 ±130^b	4.09	3.47±0.22 ^b	...	3.47 ±0.22^b
10090345	7190	7190 ±290^a	3.94	3.9 ±0.3^a
10096499	7780	8021±218 ^e	8021 ±218^e	4.13	3.91±0.16 ^e	...	3.91 ±0.16^e
10119517	6230	6450± 80 ^g	6450 ± 80^g	4.38	4.3 ±0.2 ^g	...	4.3 ±0.2^g	78± 4 ^g	...
10130777	8020	8020 ±290^a	3.71	3.7 ±0.3^a
10134600	5010	5010 ±290^a	3.06	3.1 ±0.3^a
10134800	7910	7910 ±290^a	3.71	3.7 ±0.3^a
10140513	5880	6030±100 ^b	6030 ±100^b	3.96	4.30±0.22 ^b	...	4.30 ±0.22^b
10140665	6620	6620 ±290^a	4.37	4.4 ±0.3^a
10164569	7720	7130±150 ^b	7130 ±150^b	3.66	2.90±0.22 ^b	...	2.90 ±0.22^b
10206340	5210	5760± 80 ^b	5760 ± 80^b	4.46	4.48±0.22 ^b	...	4.48 ±0.22^b

Table 2. continued.

KIC ID	T_{eff} (K)		$\log g$ (dex)				$v \sin i$ (km s $^{-1}$)				
	KIC ^a	Literature	Literature	Literature	Adopted*	KIC ^a	Literature	Literature	Adopted*	Spectra	Spectra
10208303	6380	6310±120 ^b	6310 ±120^b	4.17	4.05±0.22 ^b	...	4.05 ±0.22^b
10208345	7150	7150 ±290^a	4.01	4.0 ±0.3^a
10213987	7830	7830 ±290^a	3.94	3.9 ±0.3^a
10253943	7740	7740 ±290^a	3.70	3.7 ±0.3^a
10254547	5880	5880 ±290^a	4.84	4.8 ±0.3^a
10264728	7790	7790 ±290^a	3.85	3.9 ±0.3^a
10266959	5050	5050 ±290^a	4.40	4.4 ±0.3^a
10273246	6070	6300±120 ^b	6300 ±120^b	4.15	4.54±0.21 ^b	...	4.54 ±0.21^b
10273384	6970	6220±110 ^b	6220 ±110^b	3.96	3.79±0.25 ^b	...	3.79 ±0.25^b
10273960	6660	6460±130 ^b	6460 ±130^b	4.44	4.13±0.22 ^b	...	4.13 ±0.22^b
10274244	5210	5210 ±290^a	4.53	4.5 ±0.3^a
10281360	7530	7530 ±290^a	4.05	4.1 ±0.3^a
10289211	7900	7900 ±290^a	3.73	3.7 ±0.3^a
10338279	5400	5400 ±290^a	4.47	4.5 ±0.3^a
10339342	5950	5950 ±290^a	4.19	4.2 ±0.3^a
10340511	5850	5850 ±290^a	4.40	4.4 ±0.3^a
10341072	6300	6300 ±290^a	4.18	4.2 ±0.3^a
10355055	8110	8110 ±290^a	3.74	3.7 ±0.3^a
10361229	6980	6980 ±290^a	4.03	4.0 ±0.3^a
10383933	5100	5100 ±290^a	4.27	4.3 ±0.3^a
10385459	6920	6920 ±290^a	4.23	4.2 ±0.3^a
10389037	4710	4710 ±290^a	2.19	2.2 ±0.3^a
10394332	4920	4920 ±290^a	4.47	4.5 ±0.3^a
10448764	7400	7400 ±290^a	4.00	4.0 ±0.3^a
10450550	4970	4970 ±290^a	3.63	3.6 ±0.3^a
10450675	6420	6420 ±290^a	4.12	4.1 ±0.3^a
10451090	7580	7640± 60 ^s	7640 ± 60^s	4.13	3.74±0.19 ^s	...	3.74 ±0.19^s	44± 2 ^s	...
10451250	5650	5650 ±290^a	4.06	4.1 ±0.3^a
10453475	5200	5200 ±290^a	4.47	4.5 ±0.3^a
10467969	8850	8850 ±290^a	4.09	4.1 ±0.3^a
10471914	7290	7290 ±290^a	3.95	4.0 ±0.3^a
10484808	8140	8140 ±290^a	3.99	4.0 ±0.3^a
10526137	3180	3180 ±290^a
10526615	6080	6080 ±290^a	4.62	4.6 ±0.3^a
10533506	6510	6510 ±290^a	4.18	4.2 ±0.3^a
10533616	8320	8320 ±290^a	3.77	3.8 ±0.3^a
10534629	6070	6070 ±290^a	3.94	3.9 ±0.3^a
10536147	12 490	20 800±0 ^f	20 800±290^f	5.89	3.8 ^f	...	3.8 ±0.3^f	195±10 ^f	...
10537907	7500	7500 ±290^a	3.45	3.4 ±0.3^a
10549292	7740	7740 ±290^a	3.94	3.9 ±0.3^a
10549371	6970	6970 ±290^a	3.95	4.0 ±0.3^a
10586837	7020	7020 ±290^a	4.23	4.2 ±0.3^a
10590857	7560	7560 ±290^a	3.76	3.8 ±0.3^a

Table 2. continued.

KIC ID	T_{eff} (K)					$\log g$ (dex)				$v \sin i$ (km s $^{-1}$)	
	KIC ^a	Literature	Literature	Literature	Adopted*	KIC ^a	Literature	Literature	Adopted*	Spectra	Spectra
10604429	7620	7200 ±200 ^p	7200 ±200 ^p	3.53	3.5 ±0.5 ^p	...	3.5 ±0.3 ^a	60 ^p	...
10615125	7160	7160 ±290 ^a	3.59	3.6 ±0.3 ^a
10647493
10647611	7130	7130 ±290 ^a	3.97	4.0 ±0.3 ^a
10647860	5460	5460 ±290 ^a	4.61	4.6 ±0.3 ^a
10648728	6600	6600 ±290 ^a	4.08	4.1 ±0.3 ^a
10652134	6880	6880 ±290 ^a	4.17	4.2 ±0.3 ^a
10658302	14 810	15 900±0 ^f	15 900±290 ^f	6.08	3.9 ^f	...	3.9 ±0.3 ^f
10658802	7480	7480 ±290 ^a	4.11	4.1 ±0.3 ^a
10663892	5960	6020±100 ^b	6020±100 ^b	4.32	4.9±0.2 ^b	...	4.9 ±0.2 ^b
10664703	7630	7630 ±290 ^a	3.65	3.7 ±0.3 ^a
10664975	7950	6641±123 ^e	6641±123 ^e	3.58	3.6 ±0.3 ^a
10675762	7220	7220 ±290 ^a	3.59	3.6 ±0.3 ^a
10684587	7290	7290 ±290 ^a	3.83	3.8 ±0.3 ^a
10684673	7110	7110 ±290 ^a	3.91	3.9 ±0.3 ^a
10685653	7970	7970 ±290 ^a	3.90	3.9 ±0.3 ^a
10686752	7270	7270 ±290 ^a	3.95	4.0 ±0.3 ^a
10709716	6050	6050 ±290 ^a	4.35	4.4 ±0.3 ^a
10713398
10717871	7290	7290 ±290 ^a	3.50	3.5 ±0.3 ^a
10723718	5370	5370 ±290 ^a	4.18	4.2 ±0.3 ^a
10730618	6200	6200 ±290 ^a	4.22	4.2 ±0.3 ^a
10775968	7490	7490 ±290 ^a	3.84	3.8 ±0.3 ^a
10777541
10777903	7320	7320 ±290 ^a	3.53	3.5 ±0.3 ^a
10778640	6390	6390 ±290 ^a	4.16	4.2 ±0.3 ^a
10783150	7340	7340 ±290 ^a	3.93	3.9 ±0.3 ^a
10788451	8790	8790 ±290 ^a	4.02	4.0 ±0.3 ^a
10797526	11 710	23 600±5600 ^f	20 870±0 ^f	...	20 870±5600 ^f	4.41	3.2±0.0 ^f	...	3.2 ±0.3 ^f
10797849	6020	6020 ±290 ^a	4.20	4.2 ±0.3 ^a
10813970	7420	7420 ±290 ^a	3.61	3.6 ±0.3 ^a
10815466	8310	8310 ±290 ^a	3.86	3.9 ±0.3 ^a
10853783	7830	7830 ±290 ^a	3.88	3.9 ±0.3 ^a
10861649	5900	5900 ±290 ^a	4.18	4.2 ±0.3 ^a
10902738	4640	4640 ±290 ^a	2.47	2.5 ±0.3 ^a
10920182	5930	5930 ±290 ^a	4.24	4.2 ±0.3 ^a
10920273	5570	5570 ±290 ^a	4.09	4.1 ±0.3 ^a
10920447	7900	7900 ±290 ^a	3.98	4.0 ±0.3 ^a
10971674	5530	5530 ±290 ^a	4.31	4.3 ±0.3 ^a
10975247	7780	7780 ±290 ^a	3.9 ±0.3 ^a
10977859	8050	8190± 70 ^g	8190 ± 70 ^g	3.94	3.61±0.07 ^g	...	3.61 ±0.07 ^g	63± 3 ^g	...
10988009	7320	7320 ±290 ^a	4.00	4.0 ±0.3 ^a
11013201	7780	7200±200 ^p	7200 ±200 ^p	3.82	3.5±0.2 ^p	...	3.5 ±0.2 ^p	100 ^p	...

Table 2. continued.

KIC ID	T_{eff} (K)					$\log g$ (dex)				$v \sin i$ (km s $^{-1}$)	
	KIC ^a	Literature	Literature	Literature	Adopted*	KIC ^a	Literature	Literature	Adopted*	Spectra	Spectra
11017401	5410	5410 ± 290^a	4.39	4.4 ± 0.3^a
11020521	6670	6670 ± 290^a	4.31	4.3 ± 0.3^a
11021188	7320	7320 ± 290^a	4.15	4.2 ± 0.3^a
11027270	6850	6850 ± 290^a	3.91	3.9 ± 0.3^a
11067972	5990	5990 ± 290^a	4.46	4.5 ± 0.3^a
11069435	5590	5590 ± 290^a	4.55	4.6 ± 0.3^a
11082830	7020	7020 ± 290^a	3.96	4.0 ± 0.3^a
11090405	7710	7710 ± 290^a	3.71	3.7 ± 0.3^a
11122763	6530	6530 ± 290^a	4.28	4.3 ± 0.3^a
11125764	7980	7980 ± 290^a	3.85	3.9 ± 0.3^a
11127190	7630	7630 ± 290^a	3.72	3.7 ± 0.3^a
11128041	5670	5670 ± 290^a	4.47	4.5 ± 0.3^a
11128126	5940	5940 ± 290^a	4.32	4.3 ± 0.3^a
11129289	5990	5990 ± 290^a	4.31	4.3 ± 0.3^a
11180361	8330	8330 ± 290^a	3.55	3.6 ± 0.3^a
11182716	5390	5390 ± 290^a	4.22	4.2 ± 0.3^a
11183399	7260	7260 ± 290^a	4.03	4.0 ± 0.3^a
11183539	7470	7470 ± 290^a	3.51	3.5 ± 0.3^a
11193046	8170	8170 ± 290^a	3.70	3.7 ± 0.3^a
11197934	7860	7860 ± 290^a	3.68	3.7 ± 0.3^a
11199412	7470	7470 ± 290^a	3.70	3.7 ± 0.3^a
11230518	6140	6140 ± 290^a	4.38	4.4 ± 0.3^a
11232922
11233189
11234888	5940	5940 ± 290^a	4.33	4.3 ± 0.3^a
11235721	5740	5740 ± 290^a	4.33	4.3 ± 0.3^a
11236253	5430	5430 ± 290^a	4.45	4.5 ± 0.3^a
11240653	6460	6460 ± 290^a	4.12	4.1 ± 0.3^a
11253226	6470	6736 ± 75 ^c	6800 ± 400 ^h	6622 ± 0 ^o	6736 ± 75^c	4.18	4.2 ± 0.1 ^h	...	4.2 ± 0.1^h	19 ± 1 ^h	...
11285767	7460	7460 ± 290^a	3.65	3.7 ± 0.3^a
11288686
11290197	6340	6340 ± 290^a	4.30	4.3 ± 0.3^a
11309335	7280	7280 ± 290^a	3.86	3.9 ± 0.3^a
11340063	4900	4900 ± 290^a	3.10	3.1 ± 0.3^a
11340713
11342032
11393580	3850	3850 ± 290^a	4.45	4.5 ± 0.3^a
11394216	5140	5140 ± 290^a	4.19	4.2 ± 0.3^a
11395018	5420	5740 ± 80 ^b	5740 ± 80^b	4.47	3.65 ± 0.24 ^b	...	3.65 ± 0.24^b
11395028	5320	5720 ± 80 ^b	5320 ± 290^a	4.42	4.26 ± 0.23 ^b	...	4.26 ± 0.23^b
11395392
11402951	...	7150 ± 120 ⁱ	7250 ± 100 ^k	...	7250 ± 100^k	...	3.5 ± 0.1 ⁱ	3.5 ± 0.1 ^k	3.5 ± 0.1^k	100 ± 2 ⁱ	...
11445774	6110	6210 ± 110 ^b	6210 ± 290^b	4.33	4.64 ± 0.20 ^b	...	4.6 ± 0.2^b

Table 2. continued.

KIC ID	T_{eff} (K)					$\log g$ (dex)				$v \sin i$ (km s $^{-1}$)	
	KIC ^a	Literature	Literature	Literature	Adopted*	KIC ^a	Literature	Literature	Adopted*	Spectra	Spectra
11445913	6950	7200±120 ⁱ	7250±100 ^k	...	7250 ±100 ^k	3.89	3.5±0.2 ⁱ	3.5±0.2 ^k	3.5 ±0.2 ^k	51±1 ^k	...
11446143	4300	4300 ±290 ^a	4.47	4.5 ±0.3 ^a
11446181	5770	5770 ±290 ^a	4.38	4.4 ±0.3 ^a
11447883	6690	6800±400 ^h	6690 ±290 ^a	4.07	4.2±0.1 ^h	...	4.2 ±0.1 ^h	105±3 ^h	...
11447953	6410	6410 ±290 ^a	4.43	4.4 ±0.3 ^a
11448266	5980	6110±110 ^b	6110 ±110 ^b	4.27	4.69±0.20 ^b	...	4.7 ±0.2 ^b
11449931	5940	6130±110 ^b	6130 ±110 ^b	4.52	4.84±0.20 ^b	...	4.8 ±0.2 ^b
11454008	6870	6870 ±290 ^a	3.79	3.8 ±0.3 ^a
11494765	7050	7050 ±290 ^a	3.99	4.0 ±0.3 ^a
11497012	7660	7660 ±290 ^a	3.87	3.9 ±0.3 ^a
11498538	6290	6410±70 ^c	6450±80 ^g	6441±0 ^o	6410 ±70 ^c	4.04	3.30±0.41 ^g	...	3.3 ±0.3 ^g	40±1 ^g	45 ^o
11499354	5780	6020±100 ^b	6020 ±100 ^b	4.47	4.39±0.22 ^b	...	4.39 ±0.22 ^b
11499453	5810	5810 ±290 ^a	4.38	4.4 ±0.3 ^a
11502075	3980	3980 ±290 ^a	4.57	4.6 ±0.3 ^a
11508397	7460	7460 ±290 ^a	3.52	3.5 ±0.3 ^a
11509728	7790	7790 ±290 ^a	3.73	3.7 ±0.3 ^a
11515690	6460	6460 ±290 ^a	4.11	4.1 ±0.3 ^a
11549609	5580	5580 ±290 ^a	4.56	4.6 ±0.3 ^a
11551622	5690	5690 ±290 ^a	4.50	4.5 ±0.3 ^a
11572666	7040	7040 ±290 ^a	3.49	3.5 ±0.3 ^a
11602449	7390	7390 ±290 ^a	3.83	3.8 ±0.3 ^a
11607193	7210	7210 ±290 ^a	4.14	4.1 ±0.3 ^a
11612274	7470	7470 ±290 ^a	3.62	3.6 ±0.3 ^a
11622328
11651083
11651147	6030	6030 ±290 ^a	4.48	4.5 ±0.3 ^a
11653958	6620	6450±120 ^b	6450 ±120 ^b	4.25	4.20±0.21 ^b	...	4.20 ±0.21 ^b
11654210	6060	6200±110 ^b	6200 ±110 ^b	4.46	4.63±0.21 ^b	...	4.63 ±0.21 ^b
11657840	6120	6120 ±290 ^a	4.66	4.7 ±0.3 ^a
11661993	7200	7200 ±290 ^a	3.93	3.9 ±0.3 ^a
11671429	7360	7360 ±290 ^a	3.58	3.6 ±0.3 ^a
11700370	8290	8290 ±290 ^a	3.99	4.0 ±0.3 ^a
11700604	7630	7630 ±290 ^a	3.85	3.9 ±0.3 ^a
11706449
11706564	4550	4550 ±290 ^a	2.35	2.4 ±0.3 ^a
11707341	4210	4210 ±290 ^a	4.58	4.6 ±0.3 ^a
11708170	6640	6776±79 ^c	6918±0 ^d	6714±0 ^o	6776 ±79 ^c	4.15	4.21±0.07 ^d	...	4.21 ±0.07 ^d
11714150	8270	8270 ±290 ^a	3.87	3.9 ±0.3 ^a
11718839	8260	8260 ±290 ^a	3.78	3.8 ±0.3 ^a
11753169	7210	7210 ±290 ^a	3.94	3.9 ±0.3 ^a
11754974
11821140	8050	8050 ±290 ^a	3.85	3.9 ±0.3 ^a
11822666	8440	8440 ±290 ^a	3.87	3.9 ±0.3 ^a

Table 2. continued.

KIC ID			T_{eff} (K)			$\log g$ (dex)				$v \sin i$ (km s ⁻¹)	
	KIC ^a	Literature	Literature	Literature	Adopted*	KIC ^a	Literature	Literature	Adopted*	Spectra	Spectra
11824964	7190	7190 ± 290^a	3.97	4.0 ± 0.3^a
11874676	8220	8220 ± 290^a	4.00	4.0 ± 0.3^a
11874898	7010	6650±130 ^b	6650 ± 130^b	3.96	3.72±0.22 ^b	...	3.72 ± 0.22^b
11910256	7130	7130 ± 290^a	3.53	3.5 ± 0.3^a
11910642	7660	7660 ± 290^a	3.59	3.6 ± 0.3^a
11973705 ^o	7400	11 898±0 ^f	7300±300 ⁱ	11 150±0 ^j	11 150±290^j	4.04	4.2± 0.3 ⁱ	3.96 ^j	4.0 ± 0.3^j	120±20 ⁱ	103±10 ^j
12018834	7270	7270 ± 290^a	4.00	4.0 ± 0.3^a
12020590	8020	8020 ± 290^a	3.67	3.7 ± 0.3^a
12058428	7110	7110 ± 290^a	3.99	4.0 ± 0.3^a
12062443	7380	7380 ± 290^a	3.97	4.0 ± 0.3^a
12068180	7460	7460 ± 290^a	3.78	3.8 ± 0.3^a
12102187	7030	7030 ± 290^a	4.13	4.1 ± 0.3^a
12117689	6910	6910 ± 290^a	4.09	4.1 ± 0.3^a
12122075	7120	7120 ± 290^a	3.89	3.9 ± 0.3^a
12216817	6680	6680 ± 290^a	3.81	3.8 ± 0.3^a
12217281	7130	7130 ± 290^a	3.71	3.7 ± 0.3^a
12353648	7410	7190± 45 ^g	7190 ± 45^g	3.47	3.60±0.26 ^g	...	3.60 ± 0.26^g	189±12 ^g	...
12647070	7280	7280 ± 290^a	3.87	3.9 ± 0.3^a
12784394	7850	7850 ± 290^a	3.61	3.6 ± 0.3^a

Notes. ^o: spectroscopic binary; **Values derived from photometry:** ^(a) KIC Catalogue, Latham et al. (2005) ^(b) SPM photometry, this paper ^(c) Masana, Jordi, & Ribas (2006) ^(d) Allende Prieto & Lambert (1999) ^(e) Hauck & Mermilliod (1998); **Values derived from photometry or spectroscopy:** ^(f) Balona et al. (2011b) **Values derived from spectroscopy:** ^(g) TLS spectra, this paper ^(h) SOPHIE spectra, this paper ⁽ⁱ⁾ Catanzaro et al. (2011) ^(j) Lehmann et al. (2011) ^(k) Balona et al. (2011c) ^(l) Antoci et al., private communication ^(m) Breger et al. (2011) ⁽ⁿ⁾ Glebocki & Stawikowski (2000) ^(o) Nordström et al. (2004) ^(p) Catanzaro et al. (2010) ^(q) Molenda-Żakowicz et al. (2008) ^(r) Antoci et al. (2011);
 *: the estimated errors on the KIC values are 290 K for T_{eff} and 0.3 dex for $\log g$ (see text).

Table 3. Classification and characterization of δ Sct, γ Dor, and hybrid stars

KIC ID	Class	N	$N_{\gamma\text{Dor}}$	$N_{\delta\text{Sct}}$	N_{total}	(Freq Range) $_{\gamma\text{Dor}}$ (d^{-1})	(Freq Range) $_{\delta\text{Sct}}$ (d^{-1})	Amplitude $_{\text{high}}$ (ppm)	Freq $_{\text{high}}$ (d^{-1})	Flag
δ Sct stars										
01162150	δ Sct	136	0	136	204	...	[4.0, 35.5]	1857	16.408	...
01571717	δ Sct	98	0	98	126	...	[5.4, 56.5]	767	41.235	•
01718594	δ Sct	53	0	53	139	...	[5.4, 76.1]	1674	18.328	...
02303365	δ Sct	37	0	37	162	...	[5.0, 34.8]	7340	14.806	...
02439660	δ Sct	36	0	36	51	...	[15.9, 79.5]	829	42.967	...
02571868	δ Sct	189	0	189	345	...	[4.0, 52.7]	1766	20.550	...
02572386	δ Sct	12	0	12	59	...	[9.1, 12.1]	1091	9.481	•
02987660	δ Sct	186	0	186	537	...	[4.3, 64.0]	3610	15.049	...
03217554	δ Sct	138	0	138	446	...	[4.0, 56.1]	2407	5.604	...
03219256	δ Sct	355	0	355	532	...	[4.0, 79.7]	1431	17.857	...
03347643	δ Sct	93	0	93	164	...	[4.2, 68.2]	654	29.695	...
03425802	δ Sct	16	0	16	30	...	[24.3, 44.4]	643	31.693	...
03429637	δ Sct	18	0	18	29	...	[9.3, 19.4]	1640	10.338	...
03440495	δ Sct	8	0	8	9	...	[4.1, 21.7]	332	15.973	...
03458318	δ Sct	16	0	16	47	...	[7.0, 23.0]	1147	13.490	...
03558145	δ Sct	81	0	81	140	...	[4.0, 44.2]	2891	22.122	...
03634384	δ Sct	208	0	208	573	...	[4.4, 68.7]	1584	11.648	...
03644116	δ Sct	75	0	75	95	...	[6.5, 42.6]	1325	30.022	...
03655513	δ Sct	12	0	12	46	...	[5.2, 12.6]	2848	8.333	...
03760002	δ Sct	86	0	86	159	...	[7.3, 33.1]	2246	16.260	...
03761641	δ Sct	62	0	62	149	...	[11.6, 74.6]	506	37.307	...
03850810	δ Sct	104	0	104	422	...	[4.5, 51.1]	1936	14.462	...
03941283	δ Sct	114	0	114	173	...	[9.4, 69.1]	1067	33.270	...
03942911	δ Sct	190	0	190	295	...	[4.3, 52.9]	1220	29.490	...
04035667	δ Sct	31	0	31	78	...	[4.8, 79.0]	552	46.399	...
04048494	δ Sct	87	0	87	254	...	[9.9, 42.0]	4701	14.364	...
04077032	δ Sct	274	0	274	869	...	[4.6, 75.8]	3707	14.482	...
04168574	δ Sct	43	0	42	139	...	[4.4, 18.9]	1495	7.989	...
04252757	δ Sct	135	0	135	332	...	[5.0, 36.5]	3961	21.480	...
04269337	δ Sct	106	0	106	297	...	[5.0, 69.1]	1552	35.215	•
04383117	δ Sct	11	0	11	12	...	[22.8, 45.1]	399	26.259	...
04647763	δ Sct	142	0	142	494	...	[4.1, 74.2]	3973	23.717	...
04649476	δ Sct	88	0	88	195	...	[4.3, 46.7]	1544	20.699	...
04840675	δ Sct	49	0	49	63	...	[4.5, 47.4]	1168	22.069	...
04856630	δ Sct	124	0	124	373	...	[4.4, 48.7]	2680	19.582	...
04863077	δ Sct	160	0	160	631	...	[4.1, 40.9]	2399	20.992	...
04909697	δ Sct	321	0	321	496	...	[4.3, 73.2]	1118	19.045	...
04936524	δ Sct	30	0	29	75	...	[10.2, 54.9]	2458	28.039	...
05080290	δ Sct	4	0	4	11	...	[4.0, 21.5]	332	21.543	...
05209712	δ Sct	85	0	85	165	...	[5.4, 65.2]	931	14.048	...
05272673	δ Sct	71	0	71	184	...	[4.5, 32.1]	9479	16.809	...
05391416	δ Sct	120	0	120	401	...	[4.0, 61.9]	2740	9.621	...

Table 3. continued.

KIC ID	Class	N	N _{γDor}	N _{δSct}	N _{total}	(Freq Range) _{γDor} (d ⁻¹)	(Freq Range) _{δSct} (d ⁻¹)	Amplitude _{high} (ppm)	Freq _{high} (d ⁻¹)	Flag
05428254	δ Sct	168	0	168	285	...	[4.2, 66.2]	2775	19.161	...
05474427	δ Sct	129	0	129	283	...	[4.1, 31.1]	5363	14.816	...
05603049	δ Sct	118	0	118	209	...	[4.0, 48.5]	2163	24.345	...
05632093	δ Sct	53	0	53	153	...	[4.5, 75.8]	623	47.616	...
05709664	δ Sct	25	0	24	46	...	[4.2, 29.0]	823	19.440	...
05768203	δ Sct	3	0	3	5	...	[7.8, 17.0]	1269	7.808	...
05774557	δ Sct	60	0	60	133	...	[4.7, 35.4]	3426	13.855	...
05785707	δ Sct	99	0	99	200	...	[4.4, 71.3]	1036	41.279	...
06123324	δ Sct	103	0	103	468	...	[4.1, 51.0]	12596	3.235	...
06586052	δ Sct	78	0	78	219	...	[4.1, 49.2]	4161	20.880	...
06590403	δ Sct	99	0	99	410	...	[4.1, 51.3]	17926	5.007	...
06606229	δ Sct	35	0	35	85	...	[4.2, 49.7]	4403	6.417	...
06629106	δ Sct	25	0	25	95	...	[4.5, 27.0]	2608	16.943	...
06668729	δ Sct	228	0	228	463	...	[4.1, 48.9]	2003	21.164	...
06790335	δ Sct	447	0	447	1080	...	[4.0, 51.7]	3374	20.265	...
06804821	δ Sct	20	0	20	26	...	[12.8, 23.3]	730	14.518	...
06865077	δ Sct	53	0	53	215	...	[5.3, 73.1]	2102	24.163	...
06937758	δ Sct	73	0	73	257	...	[4.4, 67.2]	4883	20.077	...
06939291	δ Sct	21	0	21	36	...	[7.5, 27.6]	725	17.876	...
06947064	δ Sct	6	0	6	13	...	[20.6, 23.0]	2104	22.791	...
06965789	δ Sct	291	0	291	942	...	[4.0, 73.2]	3135	16.321	•
07106205	δ Sct	18	0	18	53	...	[8.0, 19.5]	4901	13.395	...
07212040	δ Sct	99	0	99	121	...	[9.7, 62.1]	860	25.848	...
07217483	δ Sct	34	0	34	87	...	[4.2, 35.1]	4795	13.932	...
07265427	δ Sct	190	0	190	391	...	[4.4, 51.4]	1943	24.137	...
07287118	δ Sct	118	0	118	178	...	[6.5, 49.8]	2241	30.830	...
07352425	δ Sct	113	0	113	222	...	[4.3, 33.5]	1847	11.820	...
07450284	δ Sct	136	0	136	298	...	[4.0, 49.1]	3167	19.726	...
07548479	δ Sct	67	0	67	93	...	[5.9, 67.2]	1451	21.709	...
07583939	δ Sct	501	0	501	806	...	[4.2, 78.6]	1330	23.165	...
07697795	δ Sct	114	0	114	383	...	[4.2, 35.7]	2523	17.487	...
07699056	δ Sct	305	0	305	651	...	[4.1, 75.2]	2406	12.977	...
07773133	δ Sct	155	0	155	531	...	[4.6, 33.5]	23529	5.826	...
07777435	δ Sct	43	0	43	55	...	[6.0, 45.9]	1866	20.216	...
07834612	δ Sct	197	0	197	627	...	[4.1, 47.5]	4822	8.529	...
07842286	δ Sct	122	0	122	441	...	[4.4, 78.5]	2785	26.424	...
07842621	δ Sct	29	0	29	48	...	[4.4, 42.9]	688	29.791	...
07900367	δ Sct	30	0	30	79	...	[4.6, 41.2]	3857	13.247	...
08103917	δ Sct	39	0	39	69	...	[4.0, 38.1]	1799	17.747	...
08245366	δ Sct	101	0	101	367	...	[4.0, 49.1]	27451	11.938	...
08248630	δ Sct	184	0	184	311	...	[4.0, 37.2]	1652	19.486	...
08264546	δ Sct	38	0	36	82	...	[4.0, 38.4]	1180	24.985	...
08330778	δ Sct	5	0	5	9	...	[4.9, 26.4]	131	26.427	...

Table 3. continued.

KIC ID	Class	N	N _{γDor}	N _{δSct}	N _{total}	(Freq Range) _{γDor} (d ⁻¹)	(Freq Range) _{δSct} (d ⁻¹)	Amplitude _{high} (ppm)	Freq _{high} (d ⁻¹)	Flag
08352420	δ Sct	14	0	14	63	...	[6.9, 19.3]	5 376	9.271	...
08415752	δ Sct	49	0	49	60	...	[7.3, 66.3]	365	37.764	...
08429756	δ Sct	53	0	53	67	...	[22.1, 61.9]	590	27.746	...
08446738	δ Sct	37	0	37	60	...	[8.0, 67.3]	985	38.249	...
08459354	δ Sct	285	0	284	988	...	[4.1, 51.6]	3 867	19.468	...
08499639	δ Sct	64	0	64	117	...	[4.0, 21.3]	1 117	13.160	...
08516686	δ Sct	41	0	41	44	...	[21.1, 60.0]	142	43.752	...
08525286	δ Sct	97	0	97	235	...	[4.3, 53.4]	2 189	34.056	•
08560996	δ Sct	25	0	25	27	...	[16.9, 51.7]	824	20.944	...
08565229	δ Sct	118	0	118	405	...	[8.1, 46.8]	3 902	22.543	...
08579615	δ Sct	34	0	34	68	...	[4.1, 31.9]	987	8.130	...
08608260	δ Sct	192	0	192	325	...	[4.1, 35.7]	1 332	13.191	...
08623953	δ Sct	107	0	107	342	...	[6.6, 54.5]	11 516	27.257	...
08655712	δ Sct	253	0	253	494	...	[4.0, 35.2]	2 141	14.436	...
08695156	δ Sct	56	0	56	237	...	[4.3, 54.7]	3 358	5.777	...
08717065	δ Sct	74	0	73	206	...	[4.5, 61.5]	811	24.547	...
08747415	δ Sct	4	0	4	6	...	[11.0, 12.5]	39	11.030	...
08750029	δ Sct	3	0	3	7	...	[4.4, 22.4]	484	22.439	...
08827821	δ Sct	89	0	89	172	...	[12.9, 50.1]	1 689	17.713	...
08869892	δ Sct	34	0	34	129	...	[4.2, 18.6]	5 539	7.699	...
08881697	δ Sct	93	0	93	339	...	[5.5, 76.3]	1 835	16.557	...
08933391	δ Sct	7	0	7	7	...	[6.7, 14.5]	193	6.708	...
09020199	δ Sct	53	0	53	180	...	[4.0, 57.3]	5 855	7.477	...
09108615	δ Sct	10	0	10	21	...	[6.6, 49.2]	497	6.617	...
09111056	δ Sct	208	0	208	775	...	[4.0, 56.2]	12 668	5.655	...
09138872	δ Sct	98	0	97	273	...	[4.2, 49.2]	2 268	19.697	...
09143785	δ Sct	90	0	90	392	...	[5.8, 77.6]	2 386	11.798	...
09156808	δ Sct	69	0	69	116	...	[6.4, 48.5]	2 204	21.279	...
09201644	δ Sct	207	0	207	448	...	[4.3, 42.5]	2 067	14.723	...
09210037	δ Sct	101	0	101	288	...	[4.6, 34.8]	7 634	9.282	...
09229318	δ Sct	263	0	263	851	...	[4.0, 44.1]	5 249	6.246	...
09246481	δ Sct	57	0	57	124	...	[4.1, 62.3]	402	33.845	...
09267042	δ Sct	185	0	185	475	...	[4.1, 69.9]	7 895	24.664	...
09291618	δ Sct	100	0	100	522	...	[4.1, 32.9]	3 352	10.321	...
09306095	δ Sct	232	0	232	1254	...	[4.2, 71.6]	56 655	10.173	...
09324334	δ Sct	142	0	142	356	...	[4.1, 39.2]	8 675	10.272	...
09353572	δ Sct	12	0	12	16	...	[6.5, 49.0]	1 780	13.392	...
09368220	δ Sct	179	0	179	505	...	[4.2, 62.5]	8 093	5.392	...
09395246	δ Sct	63	0	63	199	...	[4.6, 58.3]	4 588	7.697	...
09408694	δ Sct	278	0	278	844	...	[4.3, 80.0]	155 660	5.661	...
09450940	δ Sct	99	0	99	219	...	[6.0, 76.0]	3 959	29.997	...
09453075	δ Sct	21	0	21	60	...	[4.6, 34.9]	2 389	19.313	...
09489590	δ Sct	75	0	75	113	...	[7.3, 46.7]	1 549	15.788	...

Table 3. continued.

KIC ID	Class	N	N _{γDor}	N _{δSct}	N _{total}	(Freq Range) _{γDor} (d ⁻¹)	(Freq Range) _{δSct} (d ⁻¹)	Amplitude _{high} (ppm)	Freq _{high} (d ⁻¹)	Flag
09533449	δ Sct	64	0	64	180	...	[4.1, 49.3]	3 170	12.519	...
09551281	δ Sct	170	0	170	335	...	[4.4, 41.8]	1 593	21.480	...
09580794	δ Sct	84	0	84	393	...	[4.1, 50.5]	2 886	10.188	...
09642894	δ Sct	28	0	28	100	...	[5.1, 29.1]	7 796	14.678	...
09655055	δ Sct	64	0	64	182	...	[4.2, 25.1]	2 269	7.842	...
09655114	δ Sct	268	0	268	508	...	[4.5, 77.3]	3 633	20.569	...
09655177	δ Sct	103	0	101	420	...	[4.7, 27.6]	8 012	8.510	...
09655393	δ Sct	229	0	229	498	...	[4.7, 64.6]	2 682	28.159	...
09655422	δ Sct	137	0	137	385	...	[4.0, 50.2]	5 689	5.128	•
09655514	δ Sct	165	0	165	305	...	[4.7, 64.1]	3 336	15.177	...
09673293	δ Sct	20	0	20	23	...	[24.2, 48.8]	192	29.120	...
09693282	δ Sct	324	0	324	1047	...	[4.1, 63.6]	4 391	8.683	...
09699950	δ Sct	64	0	64	142	...	[13.8, 49.1]	5 219	17.011	...
09700145	δ Sct	72	0	72	230	...	[4.0, 35.2]	4 431	13.062	•
09700322	δ Sct	28	0	28	75	...	[9.8, 24.1]	27 944	12.569	...
09762713	δ Sct	38	0	38	80	...	[4.4, 26.8]	3 687	13.859	...
09773512	δ Sct	15	0	13	41	...	[9.2, 14.9]	2 242	9.207	...
09776474	δ Sct	57	0	57	93	...	[4.4, 68.6]	1 173	16.266	...
09812351	δ Sct	170	0	170	480	...	[4.8, 79.8]	4 279	18.581	...
09818269	δ Sct	27	0	26	85	...	[9.4, 76.2]	1 666	19.175	...
09836020	δ Sct	28	0	28	41	...	[13.7, 22.3]	1 062	17.715	...
09845907	δ Sct	127	0	124	570	...	[4.9, 77.0]	33 209	17.597	...
09874181	δ Sct	71	0	71	114	...	[5.6, 31.7]	1 116	20.316	...
10000056	δ Sct	88	0	88	387	...	[4.4, 65.9]	8 606	20.141	...
10002897	δ Sct	33	0	33	181	...	[4.5, 49.0]	4 046	15.393	...
10056297	δ Sct	63	0	63	323	...	[4.6, 39.9]	32 902	9.560	...
10134800	δ Sct	84	0	81	319	...	[4.1, 49.1]	2 894	27.058	...
10213987	δ Sct	9	0	9	20	...	[7.2, 20.6]	1 156	17.059	•
10253943	δ Sct	246	0	246	805	...	[4.2, 78.8]	6 959	25.206	...
10273384	δ Sct	81	0	81	238	...	[6.4, 25.6]	18 859	8.223	...
10289211	δ Sct	267	0	267	645	...	[4.4, 49.9]	2 067	19.812	...
10355055	δ Sct	45	0	45	140	...	[5.7, 52.6]	3 433	22.084	...
10448764	δ Sct	92	0	92	484	...	[4.1, 33.6]	10 776	9.591	...
10451090	δ Sct	79	0	79	157	...	[10.5, 64.8]	1 411	38.376	...
10484808	δ Sct	59	0	59	86	...	[10.5, 80.0]	886	27.118	...
10533616	δ Sct	4	0	4	5	...	[31.9, 50.6]	34	31.853	...
10549292	δ Sct	82	0	82	92	...	[4.9, 48.3]	957	18.081	...
10549371	δ Sct	15	0	15	44	...	[7.1, 15.8]	3 996	13.880	...
10590857	δ Sct	87	0	87	343	...	[4.4, 48.5]	2 217	20.924	...
10604429	δ Sct	90	0	90	147	...	[4.0, 38.7]	873	18.407	...
10615125	δ Sct	109	0	109	385	...	[4.1, 39.2]	5 064	9.661	...
10658802	δ Sct	62	0	62	312	...	[4.4, 37.1]	2 998	8.159	...
10664703	δ Sct	228	0	228	506	...	[4.0, 47.3]	4 047	5.558	...

Table 3. continued.

KIC ID	Class	N	N _{γDor}	N _{δSct}	N _{total}	(Freq Range) _{γDor} (d ⁻¹)	(Freq Range) _{δSct} (d ⁻¹)	Amplitude _{high} (ppm)	Freq _{high} (d ⁻¹)	Flag
10684587	δ Sct	306	0	306	760	...	[4.0, 48.9]	7 128	12.837	...
10684673	δ Sct	9	0	9	28	...	[5.8, 10.4]	7 430	10.387	...
10686752	δ Sct	62	0	62	87	...	[12.7, 58.8]	628	40.473	...
10713398	δ Sct	80	0	80	383	...	[5.1, 48.1]	3 106	15.348	...
10717871	δ Sct	234	0	234	693	...	[4.2, 39.7]	3 778	12.217	...
10775968	δ Sct	11	0	11	17	...	[4.5, 24.7]	432	21.549	...
10777903	δ Sct	277	0	277	966	...	[4.1, 38.0]	4 486	16.791	...
10788451	δ Sct	122	0	122	301	...	[4.0, 43.1]	3 603	23.160	...
10813970	δ Sct	183	0	183	648	...	[4.1, 49.8]	5 261	9.606	...
10815466	δ Sct	267	0	267	721	...	[4.1, 79.0]	2 188	36.712	...
10853783	δ Sct	102	0	102	136	...	[4.0, 50.7]	1 708	28.955	...
10920447	δ Sct	89	0	89	132	...	[4.0, 62.9]	1 622	31.523	...
10977859	δ Sct	67	0	67	120	...	[4.1, 63.6]	2 014	59.969	...
10988009	δ Sct	169	0	165	613	...	[4.1, 48.8]	5 483	12.957	...
11013201	δ Sct	26	0	26	56	...	[5.5, 57.8]	522	33.416	...
11021188	δ Sct	70	0	70	77	...	[4.5, 55.5]	1 360	23.831	...
11090405	δ Sct	54	0	54	89	...	[4.1, 37.5]	992	14.371	...
11125764	δ Sct	35	0	35	95	...	[19.2, 65.5]	1 868	38.327	...
11127190	δ Sct	48	0	47	156	...	[13.7, 59.3]	3 559	18.731	...
11183539	δ Sct	213	0	213	440	...	[4.1, 48.8]	2 265	22.664	...
11340713	δ Sct	26	0	26	113	...	[4.2, 23.6]	11 333	10.150	...
11395392	δ Sct	90	0	90	413	...	[4.8, 46.2]	6 577	25.188	...
11402951	δ Sct	97	0	97	161	...	[5.3, 49.1]	884	23.846	...
11497012	δ Sct	85	0	85	258	...	[4.0, 41.1]	1 660	24.105	...
11661993	δ Sct	147	0	147	440	...	[4.3, 49.5]	3 473	14.035	...
11671429	δ Sct	312	0	312	624	...	[4.1, 49.4]	1 425	15.970	...
11700370	δ Sct	30	0	30	30	...	[5.2, 72.0]	101	28.678	...
11754974	δ Sct	87	0	84	396	...	[4.3, 69.9]	57 658	16.345	...
11821140	δ Sct	32	0	32	70	...	[18.4, 57.4]	235	24.877	...
11874676	δ Sct	73	0	73	241	...	[4.9, 67.5]	1 798	13.577	...
12020590	δ Sct	19	0	19	34	...	[18.8, 37.4]	393	22.215	...
12068180	δ Sct	298	0	298	722	...	[4.1, 49.3]	2 226	20.302	...
12353648	δ Sct	48	0	44	277	...	[4.3, 24.0]	3 928	7.818	...
12647070	δ Sct	33	0	33	52	...	[9.8, 39.2]	1 110	13.356	...
12784394	δ Sct	3	0	3	11	...	[29.4, 47.9]	107	42.652	...
Hybrid stars										
02168333	hybrid	68	13	53	278	[0.2, 5.0]	[5.5, 49.1]	1 452	21.718	...
02694337	hybrid	52	27	22	123	[0.2, 4.9]	[5.4, 34.6]	506	24.500	...
02707479	hybrid	188	58	124	674	[0.2, 5.0]	[5.1, 51.1]	2 267	15.158	...
02853280	hybrid	53	28	23	102	[0.2, 5.0]	[5.0, 35.1]	988	13.000	...
02975832	hybrid	15	10	4	128	[0.3, 3.5]	[5.7, 16.5]	733	2.034	•
03097912	hybrid	21	15	4	56	[0.2, 4.6]	[5.2, 20.0]	212	1.466	•
03119604	hybrid	171	12	157	196	[0.2, 4.6]	[5.0, 76.9]	554	41.151	...

Table 3. continued.

KIC ID	Class	N	$N_{\gamma\text{Dor}}$	$N_{\delta\text{Sct}}$	N_{total}	(Freq Range) $_{\gamma\text{Dor}}$ (d^{-1})	(Freq Range) $_{\delta\text{Sct}}$ (d^{-1})	Amplitude $_{\text{high}}$ (ppm)	Freq $_{\text{high}}$ (d^{-1})	Flag
03231406	hybrid	362	62	292	793	[0.2, 5.0]	[5.0, 65.0]	1761	17.438	...
03240556	hybrid	191	40	151	329	[0.3, 5.0]	[5.0, 63.6]	867	25.220	...
03245420	hybrid	42	10	32	224	[0.8, 3.9]	[5.0, 45.8]	2733	14.097	...
03337002	hybrid	162	92	64	529	[0.2, 4.9]	[5.0, 52.8]	4594	4.558	...
03437940	hybrid	347	106	224	957	[0.2, 5.0]	[5.1, 63.2]	4886	10.476	...
03453494	hybrid	176	47	129	358	[0.3, 5.0]	[5.0, 62.9]	487	7.499	...
03851151	hybrid	7	3	1	22	[0.2, 1.3]	[26.5, 26.5]	42	26.487	...
03970729	hybrid	156	44	105	332	[0.2, 5.0]	[5.6, 28.2]	1394	18.828	...
04044353	hybrid	59	13	44	153	[0.6, 4.8]	[5.1, 54.5]	553	2.390	...
04170631	hybrid	495	74	412	138	[0.2, 5.0]	[5.1, 59.5]	6264	8.314	...
04180199	hybrid	91	30	61	404	[0.5, 4.9]	[5.2, 51.2]	790	3.284	...
04281581	hybrid	77	51	21	282	[0.2, 4.6]	[5.2, 54.3]	478	0.882	...
04476836	hybrid	9	5	3	52	[0.5, 5.0]	[5.5, 10.9]	969	9.859	...
04480321	hybrid	142	54	86	504	[0.2, 5.0]	[5.1, 61.2]	2323	0.710	...
04488840	hybrid	178	42	129	517	[0.3, 5.0]	[5.0, 51.3]	1277	15.803	...
04550962	hybrid	179	93	83	603	[0.2, 5.0]	[5.3, 54.1]	2912	2.259	...
04556345	hybrid	137	19	116	186	[0.3, 4.2]	[13.1, 64.5]	653	26.640	...
04671225	hybrid	74	39	30	191	[0.2, 5.0]	[5.1, 46.3]	1271	8.880	...
04768677	hybrid	13	3	7	47	[0.2, 4.7]	[6.2, 52.2]	124	22.904	...
04919818	hybrid	45	34	10	74	[0.4, 5.0]	[5.0, 32.4]	342	2.871	...
04920125	hybrid	28	20	8	92	[0.4, 4.8]	[5.6, 29.3]	390	23.884	...
04989900	hybrid	42	24	16	210	[0.2, 4.8]	[5.0, 38.9]	718	2.189	...
05038228	hybrid	203	72	125	616	[0.2, 5.0]	[5.1, 49.7]	2261	0.904	...
05219533	hybrid	35	22	11	112	[0.3, 4.6]	[5.4, 29.9]	437	10.285	...
05356349	hybrid	41	14	22	60	[0.2, 5.0]	[5.1, 51.5]	205	9.826	...
05437206	hybrid	120	32	82	258	[0.2, 4.7]	[5.2, 49.7]	1637	13.011	...
05446068	hybrid	63	33	24	217	[0.3, 4.9]	[5.3, 52.1]	558	0.287	...
05473171	hybrid	112	46	64	391	[0.3, 4.8]	[5.1, 54.5]	3578	7.574	...
05476864	hybrid	85	26	54	374	[0.2, 3.4]	[5.1, 19.2]	1862	1.667	•
05641711	hybrid	119	46	68	294	[0.3, 4.8]	[5.0, 51.6]	758	21.111	...
05722346	hybrid	179	72	99	507	[0.2, 4.9]	[5.0, 50.4]	3002	11.325	•
05724440	hybrid	425	70	343	663	[0.2, 5.0]	[5.1, 79.7]	1918	19.251	...
05810113	hybrid	41	17	22	92	[0.2, 3.5]	[5.8, 20.6]	652	0.333	...
05857714	hybrid	210	41	166	850	[0.2, 3.7]	[5.0, 55.0]	22930	12.227	...
05940273	hybrid	170	80	81	463	[0.2, 5.0]	[5.0, 51.0]	1571	3.016	...
05965837	hybrid	93	29	60	354	[0.7, 4.5]	[5.0, 49.2]	7243	3.392	...
06032730	hybrid	87	26	57	144	[0.2, 5.0]	[5.0, 78.1]	1140	16.267	...
06067817	hybrid	133	27	103	296	[0.2, 4.9]	[5.1, 79.7]	1374	34.408	...
06141372	hybrid	19	5	14	21	[0.3, 4.8]	[5.1, 31.9]	338	18.991	•
06142919	hybrid	59	37	19	115	[0.3, 4.9]	[5.4, 49.2]	986	16.316	...
06187665	hybrid	184	60	121	659	[0.2, 5.0]	[5.0, 35.5]	3826	11.729	...
06199731	hybrid	42	18	21	215	[0.4, 4.9]	[5.1, 22.5]	2183	7.643	...
06268890	hybrid	359	73	284	152	[0.2, 4.8]	[5.1, 55.1]	15399	6.866	...

Table 3. continued.

KIC ID	Class	N	$N_{\gamma\text{Dor}}$	$N_{\delta\text{Sct}}$	N_{total}	(Freq Range) $_{\gamma\text{Dor}}$ (d ⁻¹)	(Freq Range) $_{\delta\text{Sct}}$ (d ⁻¹)	Amplitude $_{\text{high}}$ (ppm)	Freq $_{\text{high}}$ (d ⁻¹)	Flag
06289468	hybrid	62	17	40	103	[0.5, 4.9]	[5.1, 40.4]	432	13.652	...
06381306	hybrid	64	43	16	123	[0.2, 4.9]	[5.3, 53.3]	234	5.814	...
06432054	hybrid	356	68	279	829	[0.2, 5.0]	[5.0, 74.9]	2901	10.571	...
06443122	hybrid	154	63	84	537	[0.2, 5.0]	[5.0, 55.3]	1466	2.425	...
06446951	hybrid	288	30	256	509	[0.4, 4.8]	[5.1, 52.9]	1509	14.872	...
06509175	hybrid	112	42	68	449	[0.6, 5.0]	[5.1, 53.7]	4431	3.954	...
06587551	hybrid	44	4	39	79	[0.2, 3.6]	[5.5, 60.6]	192	17.422	...
06614168	hybrid	143	40	99	392	[0.2, 4.8]	[5.0, 57.7]	2002	8.356	...
06670742	hybrid	194	57	134	530	[0.4, 5.0]	[5.1, 70.3]	1411	12.789	...
06694649	hybrid	120	39	78	248	[0.3, 4.9]	[5.0, 57.7]	1027	12.771	...
06756386	hybrid	63	9	52	237	[0.3, 4.8]	[5.1, 72.6]	1001	8.964	...
06756481	hybrid	114	42	71	256	[0.2, 5.0]	[5.1, 74.0]	540	5.766	...
06761539	hybrid	212	56	154	627	[0.2, 4.9]	[5.1, 59.1]	1975	17.826	...
06776331	hybrid	405	51	351	789	[0.2, 5.0]	[5.3, 48.7]	1697	13.789	...
06922690	hybrid	183	46	128	478	[0.3, 4.9]	[5.0, 49.4]	1475	15.257	...
06951642	hybrid	75	34	40	295	[0.2, 4.6]	[5.5, 50.8]	2838	0.721	...
07109598	hybrid	152	33	116	291	[0.3, 4.8]	[5.1, 54.7]	908	18.597	...
07119530	hybrid	106	78	19	481	[0.2, 5.0]	[5.0, 15.2]	2443	4.193	...
07122746	hybrid	54	7	47	191	[1.1, 4.9]	[5.1, 48.8]	735	30.154	...
07204237	hybrid	269	54	214	537	[0.2, 4.9]	[5.0, 63.4]	2926	17.993	...
07211759	hybrid	163	37	125	587	[0.3, 4.9]	[5.1, 79.4]	736	7.318	...
07300387	hybrid	329	64	254	852	[0.2, 4.9]	[5.2, 50.5]	3469	10.293	...
07350486	hybrid	22	17	4	58	[0.3, 4.7]	[5.3, 17.1]	130	1.330	...
07352776	hybrid	105	32	65	382	[0.2, 5.0]	[6.1, 36.5]	1764	2.374	...
07502559	hybrid	64	38	20	145	[0.5, 4.7]	[5.2, 31.9]	1383	4.522	...
07533694	hybrid	14	6	5	59	[0.3, 4.9]	[5.6, 49.5]	1621	11.243	...
07553237	hybrid	46	34	10	132	[0.2, 4.9]	[5.4, 15.6]	2184	14.713	...
07668791	hybrid	23	4	17	30	[0.2, 4.9]	[5.0, 31.1]	98	20.643	...
07702705	hybrid	196	63	130	575	[0.3, 4.9]	[5.1, 53.3]	878	2.038	...
07732458	hybrid	20	10	4	26	[0.2, 4.9]	[5.0, 32.1]	359	13.184	...
07748238	hybrid	53	30	17	144	[0.4, 4.9]	[5.0, 49.1]	552	2.292	...
07756853	hybrid	6	1	5	6	[0.2, 3.1]	[5.0, 27.0]	98	21.141	...
07770282	hybrid	70	53	10	195	[0.2, 4.7]	[28.5, 51.3]	2136	1.004	...
07771991	hybrid	12	6	4	25	[0.8, 4.1]	[5.3, 21.4]	70	2.055	...
07827131	hybrid	39	17	19	175	[0.3, 4.7]	[5.0, 39.4]	939	10.044	...
07831302	hybrid	76	22	51	184	[0.2, 3.6]	[5.5, 48.8]	1051	18.750	•
07848288	hybrid	247	62	178	370	[0.2, 4.9]	[5.0, 66.9]	840	25.238	•
07959867	hybrid	73	23	43	303	[0.2, 4.5]	[5.6, 39.3]	1081	7.713	...
07977996	hybrid	118	27	84	220	[0.2, 4.9]	[5.1, 58.2]	1224	11.030	...
08029546	hybrid	79	38	38	359	[0.2, 4.7]	[5.7, 27.4]	996	2.034	...
08054146	hybrid	38	11	24	80	[0.3, 3.2]	[5.5, 76.0]	185	66.295	...
08149341	hybrid	183	27	149	350	[0.2, 4.9]	[5.1, 50.5]	1681	27.016	...
08197788	hybrid	128	52	75	410	[0.3, 4.8]	[5.1, 47.3]	3441	14.998	...

Table 3. continued.

KIC ID	Class	N	$N_{\gamma\text{Dor}}$	$N_{\delta\text{Sct}}$	N_{total}	(Freq Range) $_{\gamma\text{Dor}}$ (d ⁻¹)	(Freq Range) $_{\delta\text{Sct}}$ (d ⁻¹)	Amplitude _{high} (ppm)	Freq _{high} (d ⁻¹)	Flag
08264404	hybrid	97	32	57	414	[0.2, 4.8]	[5.1, 52.3]	5380	9.396	...
08264583	hybrid	50	34	14	175	[0.3, 4.8]	[5.1, 54.0]	519	0.968	...
08264674	hybrid	54	33	16	215	[0.2, 5.0]	[5.2, 18.1]	400	6.598	...
08264698	hybrid	140	49	89	465	[0.3, 4.8]	[5.2, 47.9]	1848	13.801	•
08397426	hybrid	46	22	24	197	[0.3, 4.9]	[5.1, 14.1]	1241	5.576	...
08454553	hybrid	59	26	26	255	[0.2, 5.0]	[5.0, 22.7]	2014	2.920	...
08460993	hybrid	258	70	186	630	[0.2, 5.0]	[5.0, 56.6]	1085	18.067	...
08507325	hybrid	79	41	36	146	[0.2, 4.9]	[5.1, 49.2]	213	11.679	...
08516008	hybrid	126	52	71	229	[0.3, 5.0]	[5.0, 49.1]	886	13.376	...
08590553	hybrid	70	22	47	146	[0.3, 4.9]	[5.5, 53.3]	1002	24.285	...
08738244	hybrid	116	39	71	185	[0.2, 5.0]	[5.0, 49.6]	346	14.621	...
08915335	hybrid	71	27	42	162	[0.2, 4.2]	[5.1, 33.5]	1429	8.828	...
08940640	hybrid	232	64	164	866	[0.3, 4.9]	[5.4, 52.7]	10783	17.839	...
08972966	hybrid	286	47	237	641	[0.2, 5.0]	[5.1, 50.5]	2946	19.225	...
08975515	hybrid	25	14	7	61	[0.3, 4.7]	[5.3, 25.8]	293	13.972	...
09052363	hybrid	13	4	7	16	[0.2, 1.5]	[19.1, 48.0]	44	41.966	...
09072011	hybrid	133	27	101	445	[0.2, 4.9]	[5.3, 55.9]	6138	6.116	...
09073007	hybrid	104	50	50	347	[0.2, 5.0]	[5.0, 29.5]	5031	11.471	...
09222942	hybrid	94	62	24	259	[0.2, 5.0]	[5.2, 50.3]	671	2.162	...
09351622	hybrid	48	21	17	127	[0.2, 4.8]	[5.2, 13.4]	1152	6.020	...
09391395	hybrid	28	24	2	97	[0.2, 4.5]	[5.3, 15.4]	465	1.949	...
09413057	hybrid	137	35	101	277	[0.2, 4.9]	[5.1, 51.8]	497	13.546	...
09473000	hybrid	11	6	4	43	[0.2, 5.0]	[5.6, 17.4]	997	8.699	...
09509296	hybrid	96	42	53	389	[0.2, 4.9]	[5.3, 51.0]	1406	17.677	...
09532644	hybrid	64	33	28	273	[0.4, 5.0]	[5.4, 35.5]	1520	20.487	...
09533489	hybrid	17	7	8	37	[1.5, 4.4]	[6.4, 37.6]	333	4.008	...
09550886	hybrid	109	24	80	255	[0.4, 5.0]	[5.6, 68.6]	3063	50.126	...
09604762	hybrid	10	3	4	12	[0.9, 3.7]	[5.2, 24.3]	126	18.151	...
09650390	hybrid	122	56	57	313	[0.4, 4.9]	[5.1, 51.7]	797	1.071	...
09651065	hybrid	107	20	84	345	[0.2, 4.8]	[5.5, 47.6]	2259	19.478	...
09655438	hybrid	22	7	11	43	[0.2, 4.6]	[5.4, 31.9]	389	12.992	...
09655501	hybrid	138	24	110	173	[0.2, 4.4]	[5.0, 53.7]	530	27.723	...
09656348	hybrid	29	18	2	137	[0.2, 4.8]	[5.5, 21.9]	806	2.818	...
09664869	hybrid	88	49	33	320	[0.2, 5.0]	[5.4, 41.5]	1389	1.622	...
09700679	hybrid	50	35	11	114	[0.2, 5.0]	[5.1, 34.7]	95	0.262	...
09716947	hybrid	63	19	39	302	[0.2, 4.8]	[5.4, 16.8]	833	6.215	...
09764965	hybrid	24	8	10	72	[0.3, 5.0]	[5.1, 34.6]	961	27.178	...
09775385	hybrid	22	13	7	58	[0.7, 4.0]	[5.1, 25.9]	189	1.788	...
09775454	hybrid	18	10	2	73	[0.2, 4.6]	[14.7, 14.9]	316	4.161	...
09790479	hybrid	9	5	3	25	[1.4, 4.4]	[5.5, 20.0]	246	1.618	...
09813078	hybrid	73	29	37	352	[0.3, 3.9]	[7.4, 39.5]	3871	17.588	...
09970568	hybrid	150	64	83	395	[0.2, 5.0]	[5.0, 55.5]	945	3.408	...
10014548	hybrid	162	42	114	314	[0.2, 5.0]	[5.0, 57.8]	775	1.528	...

Table 3. continued.

KIC ID	Class	N	N _{γDor}	N _{δSct}	N _{total}	(Freq Range) _{γDor} (d ⁻¹)	(Freq Range) _{δSct} (d ⁻¹)	Amplitude _{high} (ppm)	Freq _{high} (d ⁻¹)	Flag
10035772	hybrid	125	38	83	427	[0.2, 4.9]	[5.4, 65.8]	1947	26.891	...
10065244	hybrid	115	43	57	448	[0.2, 5.0]	[5.0, 49.1]	10097	11.930	...
10130777	hybrid	361	55	305	908	[0.4, 4.9]	[5.1, 63.7]	2101	33.821	...
10164569	hybrid	53	25	24	145	[0.2, 4.9]	[5.0, 53.5]	466	15.396	...
10208345	hybrid	74	41	27	212	[0.3, 4.9]	[5.1, 20.5]	861	3.452	...
10264728	hybrid	101	37	61	436	[0.2, 4.6]	[5.4, 53.5]	875	3.379	...
10361229	hybrid	25	20	5	137	[0.5, 4.9]	[5.6, 29.3]	813	2.653	...
10471914	hybrid	308	46	254	534	[0.2, 4.9]	[5.2, 57.0]	2156	15.070	...
10537907	hybrid	110	22	83	510	[0.2, 4.5]	[5.1, 45.3]	4741	11.555	...
10647493	hybrid	78	28	47	378	[0.2, 4.6]	[5.1, 56.1]	5536	17.101	...
10647611	hybrid	69	22	42	317	[0.5, 4.6]	[5.1, 51.2]	4527	15.723	...
10664975	hybrid	9	5	3	21	[1.3, 4.4]	[6.1, 19.9]	383	2.575	...
10675762	hybrid	68	23	40	300	[0.3, 4.7]	[5.0, 50.4]	3118	15.914	...
10685653	hybrid	47	24	21	149	[0.2, 5.0]	[5.4, 43.9]	565	19.411	...
10783150	hybrid	77	63	6	613	[0.3, 5.0]	[5.1, 17.0]	3896	1.560	...
10975247	hybrid	8	5	3	8	[0.3, 4.8]	[7.1, 19.5]	86	13.943	...
11180361	hybrid	36	11	25	72	[0.2, 5.0]	[5.0, 60.0]	334	3.752	...
11193046	hybrid	112	62	48	303	[0.2, 4.9]	[5.0, 54.7]	704	1.275	...
11197934	hybrid	213	81	121	397	[0.3, 5.0]	[5.1, 60.4]	720	1.939	...
11285767	hybrid	133	40	86	416	[0.2, 5.0]	[5.0, 59.7]	6496	21.061	...
11288686	hybrid	62	22	33	316	[0.2, 4.6]	[5.3, 41.1]	4053	18.487	...
11309335	hybrid	146	22	122	272	[0.3, 4.8]	[5.0, 59.7]	1191	23.435	...
11445913	hybrid	167	18	144	328	[0.2, 4.2]	[7.2, 50.4]	1654	31.558	...
11508397	hybrid	92	42	48	145	[0.2, 4.9]	[5.1, 48.2]	340	11.367	...
11572666	hybrid	44	17	22	164	[0.2, 4.9]	[5.0, 48.9]	976	18.279	...
11602449	hybrid	84	36	40	310	[0.5, 4.9]	[6.4, 49.7]	1392	10.579	...
11607193	hybrid	102	73	14	396	[0.2, 4.9]	[5.0, 16.5]	716	1.817	...
11700604	hybrid	20	14	4	66	[0.3, 5.0]	[5.0, 27.0]	515	27.013	...
11714150	hybrid	13	9	1	28	[0.3, 4.1]	[6.0, 11.0]	307	0.756	...
11718839	hybrid	167	49	115	235	[0.3, 4.9]	[5.1, 42.4]	696	16.441	...
11822666	hybrid	51	31	20	73	[0.4, 5.0]	[5.0, 35.7]	298	2.050	...
11824964	hybrid	21	11	5	38	[0.4, 4.5]	[5.0, 34.6]	125	2.160	...
12117689	hybrid	23	16	5	74	[0.3, 4.6]	[5.1, 25.0]	1229	3.218	...
12122075	hybrid	80	54	20	215	[0.3, 5.0]	[5.0, 31.9]	1260	1.116	•
12216817	hybrid	143	55	84	609	[0.2, 5.0]	[5.2, 52.6]	22007	8.121	...
γ Dor stars										
01432149	γ Dor	8	8	0	56	[0.6, 3.5]	...	322	3.451	...
01571152	γ Dor	57	57	0	189	[0.3, 5.8]	...	1061	0.394	...
02020966	γ Dor	13	13	0	31	[0.3, 3.2]	...	798	1.735	...
02166218	γ Dor	17	17	0	42	[0.3, 3.2]	...	149	1.798	...
02300165	γ Dor	47	47	0	219	[0.5, 5.5]	...	2500	1.679	...
02558273	γ Dor	25	25	0	65	[0.3, 3.3]	...	334	2.015	...
02568519	γ Dor	6	6	0	21	[0.2, 4.1]	...	150	0.848	...

Table 3. continued.

KIC ID	Class	N	N _{γDor}	N _{δSct}	N _{total}	(Freq Range) _{γDor} (d ⁻¹)	(Freq Range) _{δSct} (d ⁻¹)	Amplitude _{high} (ppm)	Freq _{high} (d ⁻¹)	Flag
02575161	γ Dor	8	8	0	38	[0.6, 2.5]	...	329	2.245	...
02720582	γ Dor	34	34	0	70	[0.3, 5.6]	...	467	0.551	...
02835795	γ Dor	8	8	0	64	[0.4, 2.4]	...	865	0.359	...
03215800	γ Dor	16	16	0	51	[0.2, 3.7]	...	1696	1.506	...
03218637	γ Dor	83	83	0	237	[0.2, 6.0]	...	4526	3.849	...
03222364	γ Dor	23	23	0	93	[0.4, 3.7]	...	496	2.482	...
03327681	γ Dor	14	14	0	36	[0.3, 1.5]	...	301	1.011	...
03331147	γ Dor	24	24	0	115	[0.3, 5.8]	...	4684	1.427	...
03424493	γ Dor	54	54	0	204	[0.2, 5.9]	...	7606	2.709	...
03449625	γ Dor	18	18	0	77	[0.3, 3.3]	...	1035	0.942	...
03539153	γ Dor	109	109	0	373	[0.2, 6.0]	...	4512	2.035	...
03655608	γ Dor	9	9	0	14	[0.5, 2.6]	...	77	0.636	...
03663141	γ Dor	4	4	0	34	[2.3, 5.0]	...	135	2.788	...
03758717	γ Dor	13	13	0	63	[0.6, 3.2]	...	259	0.871	...
03868032	γ Dor	8	8	0	39	[0.3, 1.7]	...	249	0.398	...
03966357	γ Dor	87	87	0	349	[0.2, 5.3]	...	3706	1.595	...
04069477	γ Dor	77	77	0	250	[0.2, 5.7]	...	3305	1.408	...
04164363	γ Dor	73	73	0	300	[0.2, 5.9]	...	8312	1.381	•
04677684	γ Dor	37	37	0	132	[0.3, 5.6]	...	890	4.496	...
04758316	γ Dor	126	126	0	416	[0.2, 5.9]	...	4489	0.991	...
05024455	γ Dor	18	18	0	102	[0.5, 4.4]	...	1556	1.341	•
05105754	γ Dor	156	156	0	544	[0.2, 5.8]	...	10511	1.687	...
05113797	γ Dor	26	26	0	114	[0.2, 5.1]	...	431	2.836	...
05164767	γ Dor	11	11	0	32	[0.2, 2.1]	...	109	0.958	...
05180796	γ Dor	25	25	0	88	[0.3, 4.3]	...	503	1.890	...
05294571	γ Dor	66	66	0	176	[0.4, 4.9]	...	1138	1.494	...
05371747	γ Dor	62	62	0	216	[0.2, 5.9]	...	1379	1.128	...
05630362	γ Dor	69	69	0	210	[0.2, 5.8]	...	6821	4.856	...
05724048	γ Dor	25	25	0	62	[0.2, 4.3]	...	269	2.131	...
05772411	γ Dor	18	18	0	27	[0.3, 3.5]	...	83	0.843	...
05880360	γ Dor	36	36	0	139	[0.2, 5.8]	...	787	1.601	...
05954264	γ Dor	27	27	0	66	[1.2, 4.0]	...	1442	1.840	...
06301745	γ Dor	17	17	0	74	[0.3, 5.8]	...	1023	0.393	...
06462033	γ Dor	46	46	0	137	[0.2, 4.5]	...	740	1.435	...
06500578	γ Dor	50	50	0	126	[0.2, 6.0]	...	782	1.500	...
06519869	γ Dor	142	142	0	513	[0.2, 5.8]	...	5215	1.353	...
06923424	γ Dor	57	57	0	144	[0.3, 5.7]	...	1948	2.735	...
07007103	γ Dor	80	80	0	267	[0.2, 5.9]	...	1780	1.540	...
07106648	γ Dor	38	38	0	103	[0.2, 6.0]	...	1335	2.355	...
07215607	γ Dor	21	21	0	33	[0.3, 4.9]	...	291	2.231	...
07220356	γ Dor	23	23	0	42	[0.4, 4.4]	...	74	1.261	...
07304385	γ Dor	147	147	0	774	[0.2, 5.4]	...	23271	1.269	...
07436266	γ Dor	45	45	0	182	[0.2, 4.4]	...	1703	1.714	...

Table 3. continued.

KIC ID	Class	N	N _{γDor}	N _{δSct}	N _{total}	(Freq Range) _{γDor} (d ⁻¹)	(Freq Range) _{δSct} (d ⁻¹)	Amplitude _{high} (ppm)	Freq _{high} (d ⁻¹)	Flag
07694191	γ Dor	16	16	0	17	[0.5, 5.3]	...	92	2.658	...
07742739	γ Dor	57	57	0	282	[0.2, 5.9]	...	2292	2.057	...
07767565	γ Dor	26	26	0	127	[0.4, 4.9]	...	532	1.994	...
07798339	γ Dor	8	0	0	4	[0.2, 4.9]	...	38	0.450	...
07890526	γ Dor	20	20	0	75	[0.2, 5.4]	...	391	1.353	...
07908633	γ Dor	11	11	0	18	[0.2, 3.0]	...	121	2.795	...
08104589	γ Dor	18	18	0	39	[0.2, 2.1]	...	129	0.538	...
08123127	γ Dor	141	141	0	320	[0.2, 6.0]	...	1991	0.774	...
08144674	γ Dor	18	18	0	39	[0.2, 5.2]	...	52	0.494	...
08197761	γ Dor	56	56	0	274	[0.2, 5.3]	...	6407	1.097	...
08222685	γ Dor	35	35	0	104	[0.2, 4.0]	...	4330	2.010	...
08230025	γ Dor	50	50	0	232	[0.2, 5.9]	...	878	3.659	...
08264061	γ Dor	70	70	0	321	[0.2, 5.9]	...	5350	1.400	...
08264075	γ Dor	34	34	0	157	[0.2, 5.9]	...	2238	1.201	...
08264274	γ Dor	34	34	0	135	[0.2, 5.3]	...	2102	1.483	•
08264588	γ Dor	43	43	0	189	[0.2, 5.9]	...	5540	5.002	...
08264617	γ Dor	126	126	0	463	[0.3, 5.8]	...	29753	1.242	•
08330056	γ Dor	32	32	0	104	[0.2, 5.5]	...	974	2.537	•
08355130	γ Dor	165	165	0	636	[0.2, 5.8]	...	10314	1.375	...
08489712	γ Dor	46	46	0	128	[0.2, 6.0]	...	257	0.555	...
08651452	γ Dor	91	91	0	356	[0.2, 5.8]	...	10285	2.434	...
08766619	γ Dor	39	39	0	158	[0.3, 5.6]	...	1122	2.047	•
08838457	γ Dor	39	39	0	107	[0.2, 5.9]	...	743	2.256	...
08869302	γ Dor	114	114	0	772	[0.2, 4.0]	...	5990	0.647	...
08871304	γ Dor	136	136	0	546	[0.2, 5.6]	...	3742	0.970	...
09020157	γ Dor	29	29	0	118	[0.3, 2.8]	...	1323	1.234	...
09117875	γ Dor	5	5	0	8	[0.6, 1.4]	...	133	0.667	...
09147229	γ Dor	98	98	0	311	[0.2, 5.4]	...	4172	1.984	...
09490042	γ Dor	107	107	0	280	[0.2, 5.8]	...	675	1.621	...
09490067	γ Dor	68	68	0	150	[0.2, 5.9]	...	686	2.240	...
09594100	γ Dor	33	33	0	181	[0.2, 5.9]	...	1987	1.052	...
09654789	γ Dor	75	75	0	313	[0.2, 5.7]	...	5913	0.992	...
09655151	γ Dor	32	32	0	197	[0.9, 6.0]	...	2328	1.418	•
09655800	γ Dor	64	64	0	268	[0.2, 4.1]	...	4462	1.944	...
09716107	γ Dor	30	30	0	161	[0.7, 6.0]	...	1755	2.152	•
09909300	γ Dor	94	94	0	372	[0.2, 5.8]	...	7073	1.496	...
10069934	γ Dor	125	125	0	333	[0.2, 6.0]	...	4669	1.082	...
10073601	γ Dor	21	21	0	46	[0.2, 2.2]	...	90	1.220	...
10096499	γ Dor	18	18	0	83	[0.2, 6.0]	...	484	2.668	...
10281360	γ Dor	23	23	0	110	[0.8, 5.6]	...	490	1.961	...
10385459	γ Dor	94	94	0	428	[0.2, 5.8]	...	11426	2.596	...
10586837	γ Dor	48	48	0	189	[0.2, 5.9]	...	1317	1.569	...
10652134	γ Dor	78	78	0	546	[0.2, 3.5]	...	4757	0.766	...

Table 3. continued.

KIC ID	Class	N	N _{γDor}	N _{δSct}	N _{total}	(Freq Range) _{γDor} (d ⁻¹)	(Freq Range) _{δSct} (d ⁻¹)	Amplitude _{high} (ppm)	Freq _{high} (d ⁻¹)	Flag
11199412	γ Dor	12	12	0	53	[0.4, 5.7]	...	2856	0.685	...
11447883	γ Dor	61	61	0	209	[0.2, 3.0]	...	1871	1.367	...
11612274	γ Dor	29	29	0	107	[0.2, 5.4]	...	2638	2.540	...
11874898	γ Dor	17	17	0	100	[0.2, 5.2]	...	1971	0.989	...
12018834	γ Dor	103	103	0	309	[0.3, 5.7]	...	2834	1.762	...
12058428	γ Dor	68	68	0	261	[0.2, 5.9]	...	2812	1.598	...
12102187	γ Dor	69	69	0	246	[0.2, 6.0]	...	4821	0.929	...

Table 4. Classification of the stars that do not belong to the δ Sct, γ Dor or hybrid groups

KIC ID	Class	Flag	KIC ID	Class	Flag	KIC ID	Class	Flag
Stars with no clear periodic signal in the δ Sct and γ Dor regions								
02163434	...	•	09386259	10920182	solar-like	...
02311130	...	•	09458750	...	•	10920273	solar-like	...
02578251	09514879	11067972	solar-like	...
02970244	09520434	solar-like	...	11069435	solar-like	...
02997802	09593997	11122763	solar-like	...
03111451	09703601	solar-like	...	11128041
03119825	09764712	solar-like	...	11128126	solar-like	...
03220783	09991621	solar-like	...	11129289	solar-like	...
03427365	09991766	solar-like	...	11182716	solar-like	...
03733735	09994789	solar-like	...	11230518	solar-like	...
03759814	10056217	solar-like	...	11232922	solar-like	...
03760826	10062593	11233189	solar-like	...
04588487	10090345	11234888	solar-like	...
04850899	10140665	solar-like	...	11235721	solar-like	...
05024150	solar-like	•	10208303	solar-like	...	11236253	solar-like	...
05024454	solar-like	•	10254547	solar-like	...	11253226
05024456	...	•	10266959	solar-like	•	11290197	solar-like	...
05112932	solar-like	•	10273246	solar-like	...	11393580	solar-like	...
05199464	solar-like	•	10273960	solar-like	...	11394216	solar-like	...
05201088	...	•	10339342	solar-like	...	11395018	solar-like	...
05980337	10340511	solar-like	...	11395028	solar-like	...
07338125	10341072	solar-like	...	11446143	solar-like	...
07662076	10383933	solar-like	...	11446181	solar-like	...
07669848	solar-like	...	10450550	solar-like	...	11448266	solar-like	...
08143903	solar-like	...	10450675	solar-like	...	11449931
08159135	10451250	solar-like	•	11454008
08218419	solar-like	...	10453475	11499354	solar-like	...
08223987	solar-like	...	10467969	solar-like	...	11502075	solar-like	...
08293302	10526137	11509728
08323104	10526615	solar-like	•	11549609	solar-like	...
08355837	10533506	solar-like	...	11551622	solar-like	•
08460025	...	•	10534629	solar-like	...	11651083	solar-like	...
08482540	10647860	solar-like	...	11651147	solar-like	...
08488065	10663892	solar-like	...	11653958	solar-like	...
09073985	solar-like	...	10709716	solar-like	...	11654210	solar-like	...
09204672	10723718	solar-like	...	11657840	solar-like	•
09264399	10730618	solar-like	...	11706449	solar-like	•
09264462	solar-like	...	10777541	solar-like	•	11707341	solar-like	...
09272082	10778640	solar-like	•	11910256
09274000	10861649	solar-like	...	11910642
09336219
Binaries								
01294756	binary+ δ Sct	...	06678614	EB+ δ Sct	...	09760531	binary	...

Table 4. continued.

KIC ID	Class	Flag	KIC ID	Class	Flag	KIC ID	Class	Flag
02162283	EB+ δ Sct	...	07385478	EB+ γ Dor	...	09851142	EB+ γ Dor	...
02557430	EB+ γ Dor	...	07596250	EB+ γ Dor	...	09913481	EB+ γ Dor	...
02584908	EB	...	08043961	EB+ δ Sct	...	09944730	binary	...
02718596	binary	...	08145477	EB	...	10119517	EB	...
03230227	EB+ γ Dor	...	08223568	binary	...	10206340	EB+ γ Dor	...
04150611	EB+hybrid	...	08330092	EB+ δ Sct	...	10274244	EB+ γ Dor	...
04570326	EB+ δ Sct	...	08479107	EB	•	10971674	EB	...
05088308	EB+ γ Dor	...	08545456	EB	...	11082830	binary	...
05197256	EB+ δ Sct	...	09204718	binary+ δ Sct	...	11180361	EB	...
05296877	EB	...	09216367	EB+ γ Dor	...	11342032	binary	...
05513861	EB	...	09451598	EB	...	11447953	EB	...
05988140	binary+ δ Sct	...	09630640	binary+ δ Sct	...	11973705	binary+SPB+ δ Sct	...
Stellar activity/rotational modulation								
01573064	rotation/activity	...	08283796	rotation/activity	...	10140513	rotation/activity	...
01995489	rotation/activity	...	08330463	rotation/activity	•	10338279	rotation/activity	...
02423932	rotation/activity	...	08703413	rotation/activity	...	10394332	rotation/activity	...
02569639	rotation/activity	...	08742449	rotation/activity	•	10648728	rotation/activity	...
02583658	rotation/activity	...	08748251	rotation/activity	...	10797849	rotation/activity	...
03348390	rotation/activity	...	09077192	rotation/activity	...	11017401	rotation/activity	•
03528578	rotation/activity	...	09268087	rotation/activity	...	11020521	rotation/activity	...
03643717	rotation/activity	...	09582720	rotation/activity	...	11027270	rotation/activity	...
04075519	rotation/activity	...	09632537	rotation/activity	...	11183399	rotation/activity	...
04160876	rotation/activity	...	09640204	rotation/activity	...	11240653	rotation/activity	...
04857678	rotation/activity	...	09643982	rotation/activity	...	11445774	rotation/activity	...
05200084	rotation/activity	•	09655487	rotation/activity	•	11494765	rotation/activity	...
05436432	rotation/activity	...	09696853	rotation/activity	...	11498538	rotation/activity	...
05476495	rotation/activity	...	09716350	rotation/activity	...	11499453	rotation/activity	...
06279848	rotation/activity	...	09777532	rotation/activity	...	11515690	rotation/activity	...
06440930	rotation/activity	...	09881909	rotation/activity	...	11622328	rotation/activity	...
06448112	rotation/activity	...	09944208	rotation/activity	...	11708170	rotation/activity	...
07985370	rotation/activity	...	10004510	rotation/activity	...	12062443	rotation/activity	...
08211500	rotation/activity	...	10064111	rotation/activity	...	12217281	rotation/activity	...
B type stars								
05217733	Bstar SPB	...	10030943	Bstar candidate β Cep	...	10658302	Bstar SPB	...
08583770	Bstar	...	10536147	Bstar SPB	...	10797526	Bstar SPB	...
08714886	Bstar SPB
Candidate red giants								
02306469	red giant	...	02995525	red giant	...	08746834	red giant	•
02306716	red giant	...	03248627	red giant	...	09327993	red giant	...
02310479	red giant	...	03354022	red giant	...	09520864	red giant	...
02443055	red giant	...	03355066	red giant	...	09885882	red giant	...
02444598	red giant	...	03427144	red giant	...	09995464	red giant	...
02556297	red giant	...	03449373	red giant	...	10006158	red giant	...
02556387	red giant	...	03458097	red giant	...	10057129	red giant	...

Table 4. continued.

KIC ID	Class	Flag	KIC ID	Class	Flag	KIC ID	Class	Flag
02557115	red giant	...	03525951	red giant	...	10068892	red giant	...
02584202	red giant	...	03546061	red giant	...	10134600	red giant	...
02834796	red giant	...	03629080	red giant	...	10389037	red giant	...
02855687	red giant	...	03633693	red giant	...	10902738	red giant	...
02860123	red giant	...	03836911	red giant	...	11340063	red giant	...
02969151	red giant	...	04144300	red giant	...	11706564	red giant	...
02972401	red giant	...	05024750	red giant	...	11753169	red giant	●
02989746	red giant	...	05112786	red giant
Cepheid								
07548061	Cepheid
Contaminated stars								
03457434	contaminated	●	04937257	contaminated	●	09655433	contaminated	●
04048488	contaminated	●	05724810	contaminated	●